Lodz University of Technology
Faculty of Mechanical Engineering
Division of Dynamics

The effect of horizontal oscillations of the beam on the collective dynamics of n pendula hanging from this beam.

A THESIS
SUBMITTED FOR THE DEGREE OF
DOCTOR OF PHILOSOPHY

Author:
Piotr Kołuda

Supervisor:
dr hab. inż. Przemysław Perlikowski, professor TUL
Auxiliary Supervisor:
dr inż. Łukasz Borkowski

Łódź 24th October 2014

Acknowledgement

This research has been performed at Lodz University of Technology at Division of Dynamics and has been supported by the Foundation for Polish Science, Team Programme under project TEAM/2010/5/5.

I would like to thank Professor Tomasz Kapitaniak for the possibility of participation in the project „TEAM" and his invaluable help. I am also grateful to my supervisor Professor Przemysław Perlikowski, who has supported me in my research and helped me during four years of my doctoral studies. At the end, I would like to thank my wife, she always has been by my side. She has supported me in difficult moments and she has given me the motivation to work harder.

Piotr Kołuda

Lodz, May, 2014

Abstract

This PhD thesis is devoted to analysis of synchronous states which exist in a system consists of horizontally moving beam with n self-excited double pendula suspended to it. The results obtained during four years of study have been published in three articles in journals form JCR list. The main difference in analysis is in forcing of pendula. In the first and the second paper the pendula are exited by van der Pol's type of damping, while in the third one by clock's escapement mechanism. Those papers create a series which give an overview of dynamics of the considered system.

In the first article "Synchronization of two self-excited double pendula" the analysed model is consists of beam with two suspended double pendula. The excitation is provided by the van der Pol's type of damping and is placed in the pivot of upper pendula, hence the system is described by a continuous ordinary differential equations. For assumed model, with two double pendula, four synchronous states exist, i.e, all pendula in phase, all in anti-phase and two mixed solutions (upper pendula in phase and lower in anti-phase and vice verse). The numerical calculations are performed using continuation toolbox Auto07p. The path-following allows to analyse, in detail, the existence, stability and bifurcations along branches of period solutions. The starting points of path-following are periodic solutions obtained for identical pendula. Bifurcations parameters are as follow: the masses of pendula and beam and their influence on system's dynamics is investigated. Finally, the ranges of stability of synchronous states in two parameters' space are calculated.

The second paper "Dynamics of n coupled double pendula suspended to the moving beam" extents analysis showed in the previous article. The model consists of n double pendula coupled via the beam. The main aim is to compute a number of synchronous states for arbitrary number of double pendula. The analytical condition which enables calculation of exiting synchronous states is derived using energy balance method. Because of its trigonometric form the solutions can be obtained only numerically for limited number of coupled systems. The detail investigations are performed for the system consists of 3,4 and 5 double pendula. In considered systems pendula synchronize in clusters. In each cluster the number of pendula is a prime number. Based on Goldbach's conjectures, which showed that any number can be expressed as prime number, one can obtain the synchronous states for any number of coupled systems. At the end of our paper the stability of synchronous states is discussed.

In the last article "Synchronization configurations of two coupled double pendula" the analysed model consists of beam with two suspended double pendula. The excitation is provided by the clock escapement mechanism which is placed between lower and upper pendula. Contrary to the previous model, equations governed system's dynamics are discontinuous ordinary differential equations. The

analytical investigations are performed using energy balance method. In the system with clock escapement mechanism, as well as for model with the van der Pol's type of damping, four synchronous states are identified. The numerical calculations performed for identical pendula confirm the existence of synchronous states. Bifurcation diagrams are computed for stable periodic solutions and show their stability as a function of system's parameters. Finally, the influence of mismatch in system's parameters is investigated. The dynamics of considered system is comparable, to system with the van der Pol's type of damping and both excitation terms can be treated as interchangeable.

Appended papers

Paper 1 P. Koluda, P. Perlikowski, K. Czolczynski, and T. Kapitaniak. Synchronization of two self-excited double pendula. European Physical Journal: Special Topics, 223(4):613629, 2014.

We consider the synchronization of two self-excited by van der Pol's type of damping double pendula. We show that such pendula hanging on the same beam can have four different synchronous configurations. Our approximate analytical analysis allows us to derive the synchronization conditions and explain the observed types of synchronization. We consider an energy balance in the system and describe how the energy is transferred between the pendula via the oscillating beam, allowing thus the pendula synchronization. Changes and stability ranges of the obtained solutions with increasing and decreasing masses of the pendula are shown using path-following.

Paper 2 P. Koluda, P. Brzeski, and P. Perlikowski. Dynamics of n coupled double pendula suspended to the moving beam. International Journal of Structural Stability and Dynamics, 14(8):1440028, 2014.

We consider the synchronization of n self-excited by van der Pol's type of damping double pendula. For such pendula hanging on the same beam, different synchronous configurations can be obtained (in-phase and anti-phase states). An approximate analytical analysis allows to derive the synchronization condition and explain the observed types of synchronization for any number of coupled double pendula. The energy balance method is used to show how the energy between the pendula is transferred via the oscillating beam allowing their synchronization. We compute periodic solutions for $n = 2, 3, 4, 5$ coupled double pendula, based on analytical predictions. For all obtained periodic solutions, we investigate how the stability properties change with the varying natural frequency of the beam.

Paper 3 P. Koluda, P. Perlikowski, K. Czolczynski, and T. Kapitaniak. Synchronization configurations of two coupled double pendula. Communications in Nonlinear Science and Numerical Simulation, 19(4):977990, 2014.

We consider the synchronization of two self-excited by clock's escapement mechanism double pendula hanging from a horizontal beam which can roll on the parallel surface. We show that such pendula can obtain four different robust synchronous configurations. Our approximate analytical analysis allows to derive the synchronization conditions and explains the observed types of synchronizations. We consider the energy balance in the system and show how the energy is transferred between the pendula via the oscillating beam allowing the pendula' synchronization.

Contents

1 Introduction

The synchronization phenomena was written up in XVII-th century by the Dutch scientist Christian Huygens [1]. When he was sick, he observed that two pendulum clocks hanged on the same wall can synchronize their motions in anti-phase. Recently, a large progress in understanding of this phenomena has been made and synchronizability of two and more single pendula is well understood [2, 3, 4, 5, 6, 7, 8, 9].

This PhD thesis is devoted to description of dynamics of double pendula coupled via the beam. The double pendulum can be considered as a full model of mechanical clock because the additional pendulum corresponds to the motion of clock's case. The first investigations on dynamics of the double pendulum can be found in the paper by Rott [10], where an analytical investigation of the Hamiltonian system is presented for different ratios between natural frequencies of the pendula. The next results obtained by Miles [11] describe dynamics of double pendulum under parametric excitation around the $2:1$ resonance. A mode interaction in the double pendulum, including a detailed bifurcation analysis near two multiple bifurcation points and a transition to quasi-periodic motion and chaos around the $2:1$ parametric resonance, are presented in Refs. [12, 13, 5]. Similarly as for $2:1$, the $1:1$ resonance leads to dynamics that include multiple bifurcation points, symmetry breaking points and cascades of period doubling bifurcations [5]. In Strzalko et. al. [14] the rotations of the set of two pairs of double pendula mounted on the platform which oscillates vertically is investigated experimentally and numerically. The rotating pendula can be $1:1$ and $1:2$ synchronized with the oscillations of the platform. Those states are extremely sensitive to perturbation (fifteen possible configurations are described). Double pendula can be also considered as an example of many physical systems commonly met in engineering, e.g., a model of bridge-pedestrian interactions [15], golf or hockey swing interactions with arms [16], human body [17] or trunk [18] models. Generally speaking, such systems are globally coupled multidimensional networks, so one can expect a coexistence of multiple attractors of different types (periodic, quasiperiodic and chaotic), see Refs. [2, 9, 19, 20].

As aforementioned, in the literature there are numerous analytical description of double pendulum motion under parametric excitation. Nevertheless, there is lack of studies of interaction between two or more coupled systems. In this PhD thesis two models of double pendula system are taken under consideration, both of them are self-excited. In the first model the double pendula are excited by van der Pol's type of damping [21, 22] and in the second one by clock escapement mechanism [23].

2 The Doctoral Thesis and Main Objective

Thesis:

The proper selection of parameters of coupled double pendulums increase their synchronizability.

Main Objective:

The main objective of the thesis is description of synchronizability of double pendulums hanged on the beam. For identical pendulums the synchronous states will be identified with an analytical method. The stability of obtained synchronous states will be calculated numerically using path-following. Then, investigations of synchronous states will be extended for pendulums with non-identical masses. All obtained results will be summed up in a catalogue which presents the possible periodic solutions of coupled double pendulums.

3 Thesis Organization

The PhD thesis is organized as follow. The description of analysed models is shown in Section 4. In Section 4.1 the overview of dynamics of system with van der Pol's type of damping is given. The systems consist of 2, 3, 4, 5 and arbitrary number of coupled double pendula are considered. Section 4.2 contains the description of the model with clock escapement mechanism and presents the interactions between two coupled double pendula. The brief conclusion of obtained results is given in Section 5. In Section 6 three published papers are presented. Section 7 contains the doctoral thesis, main objective and summary in polish.

4 Analyzed Models

4.1 System with the van der Pol's type of damping.

The analysed system is shown in Fig. 1. It consists of a rigid beam and two double pendula suspended on it. The beam of the mass M can move along the horizontal direction, its movement is described by the coordinate x_b.The beam is connected to a linear spring and a linear damper, k_x and c_x.

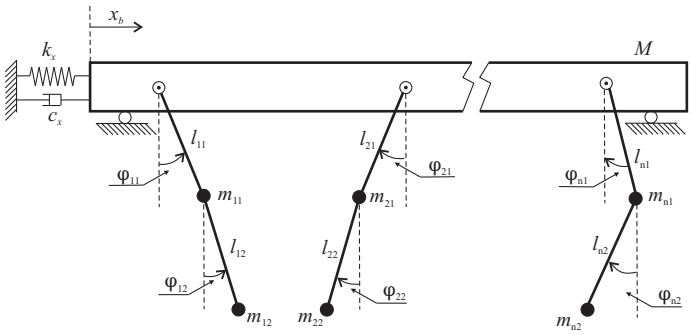

Fig. 1: The model of the analyzed systems.

Each double pendulum consists of two light beams of the length l_{i1} and the masses m_{i1} (i-th upper pendulum) and the length l_{i2} and m_{i2} (i-th lower pendulum), where $i = 1, 2$, mounted at its ends. We consider double pendula with the same lengths $l_{i1} = l_{i2} = l$ but different masses m_{i1} and m_{i2} (to maintain generality in the derivation of equations, we use indexes for lengths of the pendula). The motion of each double pendulum is described by the angles φ_{i1} (upper pendulum) and φ_{i2} (lower pendulum). The upper pendula are self-excited by the van der Pol type of damping (not shown in Fig. (1)) given by the momentum (torque) $c_{vdp}\dot{\varphi}_{1i}(1-\mu\varphi_{1i}^2)$, where c_{vdp} and μ are constant. Van der Pol damping results in the generation of a stable limit cycle. The lower pendula are damped with a viscous damper with the coefficient c_{i2}. After introduction of dimensionless time $\tau = t\omega$, equations of motion of the considered system are as follows:

$$\ddot{y}_b + \sum_{i=1}^{n} \mathbf{A}_{i1}(\ddot{\psi}_{i1}\cos\psi_{i1} - \dot{\psi}_{i1}^2\sin\psi_{i1}) + \sum_{i=1}^{n} \mathbf{A}_{i2}(\ddot{\psi}_{i2}\cos\psi_{i2} - \dot{\psi}_{i2}^2\sin\psi_{i2}) + \tag{1}$$

$$+\mathbf{K}y_b + \mathbf{C}\dot{y}_b = 0$$

$$\delta_{i1}\ddot{y}_b\cos\psi_{i1} + \mathbf{L}_{i1}\ddot{\psi}_{i1} + \mathbf{L}_{i3}\ddot{\psi}_{i2}\cos(\psi_{i1}-\psi_{i2}) = \tag{2}$$

$$-\mathbf{L}_{i3}\dot{\psi}_{i2}^2\sin(\psi_{i1}-\psi_{i2}) - \mathbf{G}_{i1}\sin(\psi_{i1}) - \mathbf{C}_{vdp}(1-\mu\psi_{i1}^2)\dot{\psi}_{i1} - \mathbf{C}_{i2}(\dot{\psi}_{i2}-\dot{\psi}_{i1})$$

$$\delta_{i2}\ddot{y}_b\cos\psi_{i2} + \mathbf{L}_{i3}\ddot{\psi}_{i1}\cos(\psi_{i1}-\psi_{i2}) + \mathbf{L}_{i2}\ddot{\psi}_{i2} = \tag{3}$$

$$\mathbf{L}_{i3}\dot{\psi}_{i1}^2\sin(\psi_{i1}-\psi_{i2}) - \mathbf{G}_{i2}\sin(\psi_{i2}) + \mathbf{C}_{i2}(\dot{\psi}_{i2}-\dot{\psi}_{i1})$$

where $i = 1, ..., n$, $y = \frac{x}{l_b}$, $\dot{y} = \frac{\dot{x}}{l_b\omega}$, $\ddot{y} = \frac{\ddot{x}}{l_b\omega^2}$, $\psi = \varphi$, $\dot{\psi} = \frac{\dot{\varphi}}{\omega}$, $\ddot{\psi} = \frac{\ddot{\varphi}}{\omega^2}$, $\mathbf{M} = M + \sum_{i=1}^{n}\sum_{j=1}^{2} m_{ij}$, $\mathbf{A}_{i1} = \frac{(m_{i1}+m_{i2})l_{i1}}{\mathbf{M}l_b}$, $\mathbf{A}_{i2} = \frac{m_{i2}l_{i2}}{\mathbf{M}l_b}$, $\mathbf{K} = \frac{k_x}{\mathbf{M}\omega^2}$, $\mathbf{C} = \frac{c_x}{\mathbf{M}\omega}$, $\delta_{i1} = \frac{(m_{i1}+m_{i2})l_{i1}}{\mathbf{M}l_{12}}$, $\delta_{i2} = \frac{m_{i2}l_{i2}}{\mathbf{M}l_{12}}$, $\mathbf{L}_{i1} = \frac{(m_{i1}+m_{i2})l_{i1}^2}{l_{12}l_b\mathbf{M}}$, $\mathbf{L}_{i2} = \frac{m_{i2}l_{i2}^2}{l_{12}l_b\mathbf{M}}$, $\mathbf{L}_{i3} = \frac{m_{i2}l_{i2}l_{i1}}{l_b\mathbf{M}l_{12}}$, $\mathbf{G}_{i1} = \frac{(m_{i1}+m_{i2})l_{i1}g}{l_{12}\omega^2 l_b\mathbf{M}}$, $\mathbf{G}_{i2} = \frac{m_{i2}l_{i2}g}{l_{12}\omega^2 l_b\mathbf{M}}$, $\mathbf{C}_{vdp} = \frac{c_{vdp}}{\omega l_b\mathbf{M}l_{12}}$, $\mathbf{C}_{i2} = \frac{c_{i2}}{l_{12}\omega_0 l_b\mathbf{M}}$ are dimensionless parameters.

As aforementioned pendula are identical, their oscillations have small amplitudes and perform periodic motion. The motion of each pendulum is given by: $\psi_{ij} = \Phi_{ij}\sin(\omega_0\tau + \beta_{ij})$, where β_{ij} $(i,\ j = 1,\ 2)$ are phase differences between the pendula and ω_0 is frequency of harmonic motion.

This assumptions let us find synchronization condition using analytical energy balance method. Equations of the energy balance have following form:

$$W_{beam}^{DRIVE} - W_{beam}^{DAMP} = 0 \tag{4}$$

$$W_{i1}^{SYN\ P} - W_{i1}^{SYN} + W_{i1}^{SELF} + W_{i1}^{DAMP} = 0 \tag{5}$$

$$W_{i2}^{SYN\ P} - W_{i2}^{SYN} + W_{i2}^{DAMP} = 0 \tag{6}$$

for $i = 1, ..., n$. The first component of Equation (4) represents the work performed by horizontal components of the force with which the double pendula act on the beam causing its motion (W_{beam}^{DRIVE}) and second component energy which is dissipated by the linear damper c_x (W_{beam}^{DAMP}). Equation (5) describes energy balance of the upper pendulums. The first component represents the energy which is transferred to the beam ($W_{i1}^{SYN\ P}$), while the second one describes the energy which is transferred to lower pendulum (W_{i1}^{SYN}). The third describes the energy which is supplied to the system by the van der Pol's type of damping (W_{i1}^{SELF}) and last one represents the energy which is dissipated (W_{i1}^{DAMP}) by pendulum's damping. The last equation (6) describes the energy balance in the lower pendulums. The first component corresponds to the energy which is transferred to the upper pendulum ($W_{i2}^{SYN\ P}$). The second component represents energy which is transferred to the beam (W_{i2}^{SYN}) via upper pendulum. The last one describes energy which is dissipated by the viscous damper (W_{i2}^{DAMP}).

When energies $W_{i1}^{SYN\ P}$ and $W_{i2}^{SYN\ P}$vanish the synchronization between lower and upper pendulums is observed. Such situation occurs when phase difference angels have following values:

$$\beta_{i1} = \beta_{i2} \vee (\beta_{i1} = 0 \wedge \beta_{i2} = \pi).$$

As it is easy to see there are two modes of synchronization between lower and upper pendulums. The first one is synchronization in phase, when both pendulums move in the same direction. The second mode is anti-phase synchronization, this type of synchronization occurs when lower and upper

pendulums are oscillating in opposite directions. In each equation of energy balance describing motion of pendulums (5-6) are components represent the transfer of energy to the beam, directly or via the upper pendula. Ona can say that pendula act with synchronization momentum on the beam (upper pendula directly and lower pendula via upper ones). In synchronous state the work done by this momentum during one period of motion is equal to zero, hence $W_{ij}^{SYN} = 0$ $(i = 1, ..., n,\ j = 1, 2)$. This condition can be written in the following form:

$$W_{kl}^{SYN} = \xi \delta_{kl} \Phi_{kl} \left[\sum_{i=1}^{n} \sum_{j=1}^{2} \Theta_{ij} M_{ij} \sin(\beta_{ij} - \beta_{kl}) \right] = 0 \quad k = 1, ..., n,\ l = 1, 2, \tag{7}$$

where:$\xi = \frac{-\omega_0^5 \pi}{M l_b (\mathbf{K} - \omega_0^2)}$, $M_{i1} = (m_{i1} + m_{i2}) l_{i1}$, $M_{i2} = m_{i2} l_{i2}$, $\Theta_{ij} = \Phi_{ij}(1 + 0.25\Phi_{ij}^2)$, $i = 1, ...n$, $j = 1, 2$. As it easy to see those equations give us trigonometrical relations between phase angles β_{ij} and enable to calculate all possible synchronous states. The derivation assumes that in synchronous state beam is at rest. The only exception is the case where upper and lower pendula are synchronized in phase (the upper and lower pendulum can be either in phase or in anti-phase to each other).

Synchronization of two double pendula

For system consists of two double pendula equations 7 have the following form:

$$\begin{aligned}
&\Theta_{12} M_{12} \sin(\beta_{12} - \beta_{11}) + \Theta_{21} M_{21} \sin(\beta_{21} - \beta_{11}) + \Theta_{22} M_{22} \sin(\beta_{22} - \beta_{11}) = 0 \\
&\Theta_{11} M_{11} \sin(\beta_{11} - \beta_{12}) + \Theta_{21} M_{21} \sin(\beta_{21} - \beta_{12}) + \Theta_{22} M_{22} \sin(\beta_{22} - \beta_{12}) = 0 \\
&\Theta_{11} M_{11} \sin(\beta_{11} - \beta_{21}) + \Theta_{12} M_{12} \sin(\beta_{12} - \beta_{21}) + \Theta_{22} M_{22} \sin(\beta_{22} - \beta_{21}) = 0 \\
&\Theta_{11} M_{11} \sin(\beta_{11} - \beta_{22}) + \Theta_{12} M_{12} \sin(\beta_{12} - \beta_{22}) + \Theta_{21} M_{21} \sin(\beta_{21} - \beta_{22}) = 0
\end{aligned} \tag{8}$$

Equations 8 are fulfilled for β_{ij}, which are combinations of 0 and π. Assuming that $\beta_{11} = 0$, one can identify the following pendulum configurations which are presented in Fig. 2(a-d). The first type is the configuration shown in Fig. 2(a). Both upper and lower pendula are phase synchronized, i.e., $\psi_{11} = \psi_{21}$ and $\psi_{12} = \psi_{22}$ ($\beta_{11} = \beta_{12} = \beta_{21} = \beta_{22} = 0$ or $\beta_{11} = \beta_{21} = 0,\ \beta_{12} = \beta_{22} = \pi$). The upper and lower pendula are respectively in phase and anti-phase synchronized i.e., $\psi_{11} = \psi_{21}$ and $\psi_{12} = -\psi_{22}$ in the configuration of Fig. 2(b) ($\beta_{11} = \beta_{12} = \beta_{21} = 0$, $\beta_{22} = \pi$ or $\beta_{11} = \beta_{12} = \beta_{22} = 0$, $\beta_{21} = \pi$). Fig. 2(c) presents the case when both upper and lower pendula are synchronized in anti-phase i.e., $\psi_{11} = -\psi_{21}$ and $\psi_{12} = -\psi_{22}$ ($\beta_{11} = \beta_{12} = 0$, $\beta_{21} = \beta_{22} = \pi$ or $\beta_{11} = \beta_{22} = 0$, $\beta_{12} = \beta_{21} = \pi$). Finally in Fig. 2(d) we present the case when upper pendula are in anti-phase and lower pendula in phase $\psi_{11} = -\psi_{21}$

and $\psi_{12} = \psi_{22}$ ($\beta_{11} = \beta_{12} = \beta_{22} = 0$, $\beta_{21} = \pi$ or $\beta_{11} = 0$, $\beta_{21} = \beta_{12} = \beta_{22} = \pi$).

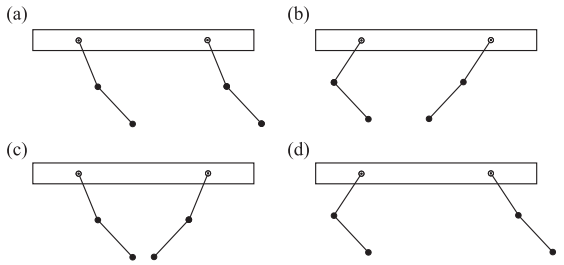

Fig. 2: Synchronous states of system ((1)-(3)): (a) upper and lower pendula in phase: $\beta_{11} = \beta_{21} = \beta_{12} = \beta_{22}$; (b) upper pendula in phase, lower pendula in anti-phase: $\beta_{11} = \beta_{21} = 0$, and $\beta_{12} = \beta_{22} = \pi$; (c) upper and lower pendulums in anti-phase: $\beta_{11} = \beta_{12} = 0$ and $\beta_{21} = \beta_{22} = \pi$; (d) upper pendulums in anti-phase, lower pendulums in phase: $\beta_{11} = \beta_{22} = 0$ and $\beta_{12} = \beta_{21} = \pi$.

Synchronization of system consists of 3, 4, 5 **double pendula**

In this section we show an analytical condition for synchronous solutions of n coupled double pendula. The derivation of synchronization condition is shown in the Appendix A of Koluda et. al. [22]. To simplify form of this condition we assume that pendula have identical masses and lengths, i.e, $m_{i1} = m_{i2}$ and $l_{i1} = l_{i2}$ (for $i = 1, \ldots, n$) and we use trigonometric identity: $\sin(\alpha_1 - \alpha_2) = \sin\alpha_1 \cos\alpha_2 - \cos\alpha_1 \sin\alpha_2$. For n coupled double pendula the synchronization condition has the following form:

$$\begin{aligned}
\cos\beta_{11}(\textstyle\sum_{k=1}^{k=n}\sin\beta_{k1} - \sin\beta_{11}) - \sin\beta_{11}(\sum_{k=1}^{k=n}\cos\beta_{k1} - \cos\beta_{11}) &= 0 \\
\cos\beta_{21}(\textstyle\sum_{k=1}^{k=n}\sin\beta_{k1} - \sin\beta_{21}) - \sin\beta_{21}(\sum_{k=1}^{k=n}\cos\beta_{k1} - \cos\beta_{21}) &= 0 \\
\vdots \qquad\qquad & \vdots \\
\cos\beta_{n1}(\textstyle\sum_{k=1}^{k=n}\sin\beta_{k1} - \sin\beta_{n1}) - \sin\beta_{n1}(\sum_{k=1}^{k=n}\cos\beta_{k1} - \cos\beta_{n1}) &= 0
\end{aligned} \tag{9}$$

for $i = 3, ..., n$.

The solutions f Eqs 9 for $n = 3$ double pendula are as follows: $\beta_{11} = 0 \wedge \beta_{21} = \frac{2\pi}{3} \wedge \beta_{31} = \frac{4\pi}{3}$ or $\beta_{11} = \beta_{21} = \beta_{31}$. Hence, four different configurations are presented in Fig. 3 (in each state pendula in double pendulum can either in phase or anti-phase synchronization) For $n = 4$ we also observe four possible synchronous states with following phase shifts: $\beta_{11} = \beta_{21} = 0 \wedge \beta_{31} = \beta_{41} = \pi$ or $\beta_{11} = \beta_{21} = \beta_{31} = \beta_{41}$ and we show them in Fig.4. Finally, for $n = 5$ the synchronization condition takes the form: $\beta_{11} = 0 \wedge \sin\beta_{21} + \sin\beta_{31} + \sin\beta_{41} + \sin\beta_{51} = 0$. That implies the flowing solutions: $\beta_{21} = 0 \wedge \beta_{31} = 0 \wedge \beta_{41} = 0 \wedge \beta_{51} = 0$ or $\beta_{11} = 0 \wedge \beta_{21} = \frac{2}{5}\pi \wedge \beta_{31} = \frac{4}{5}\pi \wedge \beta_{41} = \frac{6}{5}\pi \wedge \beta_{51} = \frac{8}{5}\pi$ or combinations when two double pendula are in anti-phase synchronization and three are shifted by $2\pi/3$ (see phase shifted state of three coupled double pendula). All described configurations are

presented in Fig. 5.

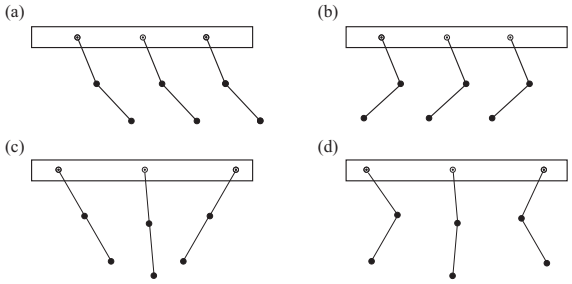

Fig. 3: Possible synchronous states for $n = 3$ double pendula: (a,b) upper and lower pendulums in phase $\beta_{11} = \beta_{21} = \beta_{31}$, $\beta_{12} = \beta_{22} = \beta_{32}$; (c,d) upper and lower pendula shifted by $\frac{2\pi}{3}$:$\beta_{11} = 0 \wedge \beta_{21} = \frac{2\pi}{3} \wedge \beta_{31} = \frac{4\pi}{3}$ and $\beta_{12} = 0 \wedge \beta_{22} = \frac{2\pi}{3} \wedge \beta_{32} = \frac{4\pi}{3}$.

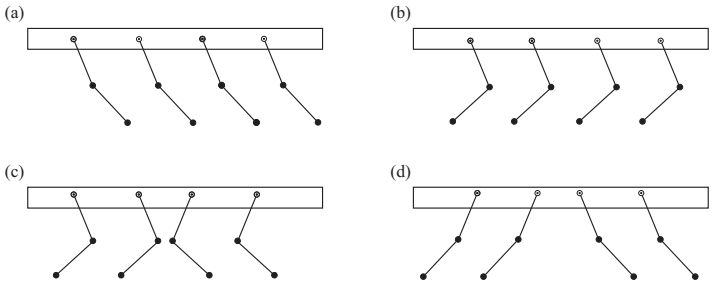

Fig. 4: Possible synchronous states for $n = 4$ double pendula: (a,b) upper and lower pendula in phase: $\beta_{11} = \beta_{21} = \beta_{31} = \beta_{41}$ and $\beta_{12} = \beta_{22} = \beta_{32} = \beta_{42}$; (c,d) upper and lower pendula in anti-phase in pairs: $\beta_{11} = -\beta_{31}$,$\beta_{21} = -\beta_{41}$ and $\beta_{12} = -\beta_{32}$, $\beta_{22} = -\beta_{42}$.

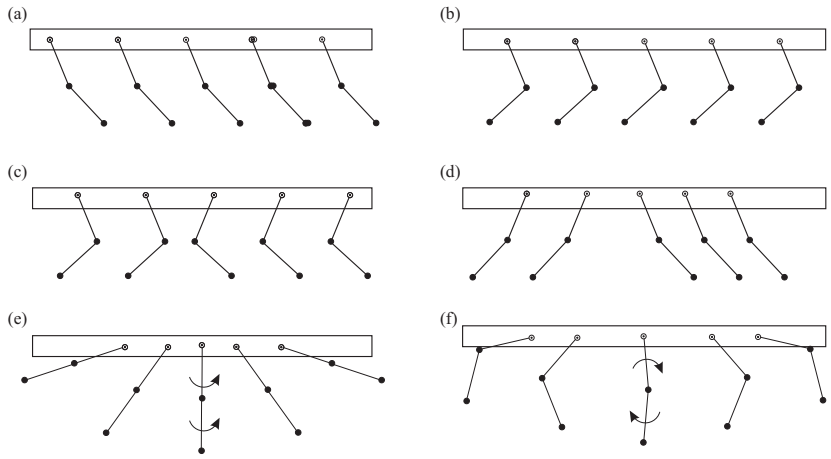

Fig. 5: Possible synchronous states for $n = 5$ double pendula: (a,b) upper and lower pendula in phase: $\beta_{11} = \beta_{21} = \beta_{31} = \beta_{41} = \beta_{51}$ and $\beta_{12} = \beta_{22} = \beta_{32} = \beta_{42} = \beta_{52}$; (c,d) upper and lower pendula synchronized in phase in two anti-phase clusters; (e,f) upper and lower pendula shifted by $\frac{2\pi}{5}$: $\beta_{11} = 0 \bigwedge \beta_{21} = \frac{2\pi}{5} \bigwedge \beta_{31} = \frac{4\pi}{5} \bigwedge \beta_{41} = \frac{6\pi}{5} \bigwedge \beta_{51} = \frac{8\pi}{5}$ and $\beta_{12} = 0 \bigwedge \beta_{22} = \frac{2\pi}{5} \bigwedge \beta_{32} = \frac{4\pi}{5} \bigwedge \beta_{42} = \frac{6\pi}{5} \bigwedge \beta_{52} = \frac{8\pi}{5}$.

Synchronous states for n double pendula

According to detailed analysis of synchronization in system of $n = 2, 3, 4, 5$ coupled double pendula we can generalize obtained results for an arbitrary number n of systems. Despite the value of n we can observe the state where all double pendula are synchronized in phase which means that all upper and similarly all lower pendula are completely synchronized. They act on the beam causing its oscillations. Considering other possible configurations we have to recall our assumptions which are used to derive the analytical condition of synchronization: the beam is at rest and double pendula perform harmonic motion. The minimum number of double pendula in cluster is two because for two and more double pendula in cluster, forces acting on beam vanish. As clusters are not acting on one another via the beam, the phase shift between clusters can be an arbitrary number from 0 to 2π. The number of double pendula in each cluster is a prime number because any other number can be expressed as a sum of prime numbers [24]. The phase shift between double pendula in cluster is $2\pi/n_1$, where n_1 is a number of double pendula in the cluster (n_1 is a prime number). For example for $n = 11$ we can observe the following numbers of double pendula in clusters: (3, 2, 2, 2, 2) or (3, 3, 3, 2) or (5, 3, 3) or (5, 2, 2, 2) or (7, 2, 2) or (11). Note that (9, 2) is not a possible solution - the cluster of nine double pendula can be created from three clusters with three pendula shifted by $2\pi/3$. The formula which let us calculate the number of possible configurations is complex, hence it is better to base on an algorithm (see Appendix B in [22]) which give us explicit results. The number of possible clusters grows much faster than the number n of double pendula (the tendency is close to exponential), e.g, for $n = 10$ (5 clusters), $n = 30$ (98 clusters), $n = 60$ (2198 clusters), $n = 90$ (38257 clusters), $n = 120$ (145627 clusters). Additionally, when number of double pendula is a prime number we have a case where double pendula are equally distributed with phase shift $2\pi/n$, so for our example with $n = 11$ double pendula we observe a seventh possible configuration. For all mentioned above types of synchronization in each double pendulum the upper and lower pendulum can be synchronized in phase or anti-phase, hence the number of possible synchronous states is two times bigger than the number of possible clusters.

4.2 System with clock escapement mechanism.

The analyzed system is shown in Fig. 6. It consists of the rigid beam and two double pendula suspended on it. The beam of mass M can move in horizontal direction, its movement is described by coordinate X. The beam is connected to the refuge by a linear spring with stiffness coefficient K_X and linear damper with damping coefficient C_X. Each double pendulum consist of two light beams of length L_{ci}, L_{si} and two masses M_{ci} and M_{si}, where $i = 1, 2$, mounted at beam's ends. The lower pendulums are

mounted to the upper ones at the distance L_{ai}. The motion of each double pendulum is described by angles φ_{ci} (the lower pendula) and φ_{si} (the upper pendula). The oscillations of the double pendula are damped by the viscous dampers C_{si} and C_{ci} (not shown in Fig. 6). The lower pendula of each double pendulum are excited by the clock escapement mechanism represented by momentum M_{Di}. This mechanism acts in two successive steps (the first step is followed by the second one and the second one by the first one). In the first step if $0 < (\varphi_{ci} - \varphi_{si}) < \gamma_N$ then $M_{Di} > M_{Ni}$ and when $(\varphi_{ci} - \varphi_{si}) < 0$ or $\gamma_N < (\varphi_{ci} - \varphi_{si})$ then $M_{Di} = 0$, where γ_N and M_{Ni} are constant values which characterize the mechanism. For the second stage one has for $-\gamma_N < (\varphi_{ci} - \varphi_{si}) < 0$ $M_{Di} = -M_{Ni}$ and$M_{Di} = 0$ for $0 < (\varphi_{ci} - \varphi_{si})$ or $-\gamma_N > (\varphi_{ci} - \varphi_{si})$. Considering a mass M_{c1}, length $L_{c1}$of the first lower pendulum and gravitational acceleration g as a reference parameters and take dimensionless time $\tau = \alpha t$, where $\alpha = \sqrt{\frac{g}{L_{c1}}}$, equations of system's motion take form:

$$m_{ci}l_{ci}^2\ddot{\varphi}_{ci} + m_{ci}l_{at}l_{ci}\ddot{\varphi}_{si}\cos(\varphi_{ci} - \varphi_{si}) + m_{ci}l_{ci}l_{ai}\dot{\varphi}_{si}^2\sin(\varphi_{ci} - \varphi_{si}) + m_{ci}l_{ci}\ddot{x}\cos\varphi_{ci} + c_{\varphi ci}\left(\dot{\varphi}_{ci} - \dot{\varphi}_{si}\right) \quad (10)$$
$$+m_{ci}m_{ci}\sin\varphi_{ci} = N_{Di}$$

$$m_{ci}l_{ci}^2\ddot{\varphi_{ci}} + m_{ci}l_{ai}^2\ddot{\varphi}_{si} + m_{ci}l_{ai}l_{ci}\ddot{\varphi}_{ci}\cos(\varphi_{ci} - \varphi_{si}) + m_{ci}l_{ci}l_{ai}\dot{\varphi}_{si}^2\sin(\varphi_{ci} - \varphi_{si}) + m_{si}l_{si}\ddot{x}\cos\varphi_{si} + c_{\varphi si}\dot{\varphi}_{si} \quad (11)$$

$$-c_{\varphi ci}\left(\dot{\varphi}_{ci} - \dot{\varphi}_{si}\right) + m_{si}l_{si}\sin\varphi_{si} = -N_{Di}$$

$$\left(m_B + \sum_{i=1}^{2}(m_{ci} + m_{Si})\right)\ddot{x} + c_x\dot{x} + k_x x = \sum_{i=1}^{2}(m_{si}l_{si} + m_{ci}l_{ai})\left(-\ddot{\varphi}_{si}\cos\varphi_{si} + \dot{\varphi}_{si}^2\sin\varphi_{si}\right) \quad (12)$$
$$+\sum_{i=1}^{2}m_{ci}l_{ci}\left(-\ddot{\varphi}_{ci}\cos\varphi_{ci} + \dot{\varphi}_{ci}^2\sin\varphi_{ci}\right)$$

where: $i = 1,\ 2$, $m_{ci} = \frac{M_{ci}}{M_{c1}}$, $m_{si} = \frac{M_{si}}{M_{c1}}$, $m_b = \frac{M_B}{M_{c1}}$, $l_{ci} = \frac{L_{ci}}{L_{c1}}$, $l_{si} = \frac{L_{si}}{L_{c1}}$, $x = \frac{X}{L_{ci}}$, $c_{\varphi ci} = \frac{C_{\varphi ci}\sqrt{L_{c1}}}{M_{c1}L_{c1}^2\sqrt{g}}$, $c_{\varphi si} = \frac{C_{\varphi si}\sqrt{L_{c1}}}{M_{c1}L_{c1}^2\sqrt{g}}$, $c_x = \frac{C_X\sqrt{L_{c1}}}{M_{c1}\sqrt{g}}$, $k_x = \frac{K_X L_{c1}}{M_{c1}g}$, $N_{Di} = \frac{M_{Di}}{M_{c1}L_{c1}g}$ and symbols $\dot{}$ and $\ddot{}$ denote respectively $\frac{d}{d\tau}$ and $\frac{d^2}{d\tau^2}$.

For obtined equations we can perform similar analisys are for system with van der Pol's type of damping. Let us assume that motion of system is periodic and oscillations of the double pendula can be approximated by harmonic functions: $\varphi_{ci} = \Phi_{ci}\sin(\tau + \beta_{ci})$ and $\varphi_{si} = \Phi_{si}\sin(\tau + \beta_{si})$ where β_{si} and β_{ci} are phase shift angels between pendula.

hence based on energy balance method we can determine the energy which is transferred to the beam from pendula, the energy which is transferred between lower and upper pendula and the energy which drive pendula during one period of motion. The equations of energy balance have the following form:

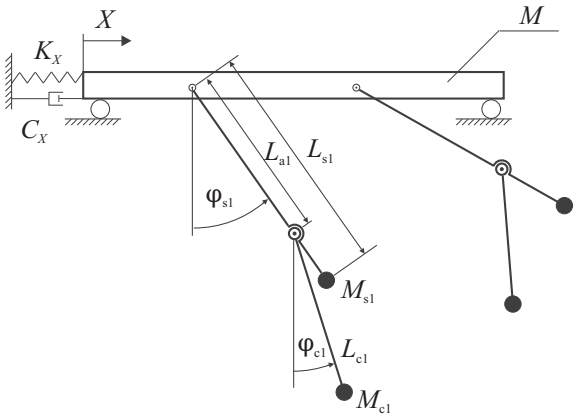

Fig. 6: The model of two double pendula suspended to a beam.

$$W_{ci}^{INERT} + W_{ci}^{SYN} + W_{csi}^{DAMP} = W_{ci}^{DRIVE} \tag{13}$$

$$W_{si}^{INERT} + W_{si}^{SYN} + W_{si}^{DAMP} + W_{sci}^{DAMP} = W_{si}^{DRIVE} \tag{14}$$

$$W_{b}^{DAMP} = W_{b}^{SYN}. \tag{15}$$

Eq. 13 corresponds to energy balance of $i-th$ lower pendulum, Eq. 14 to energy balance of $i-th$ upper pendulum and finally the Eq. 15 to the energy balance of the beam. In Eqs 13and 14 components W^{SYN} represent synchronization energy. The sum $W_{ci}^{SYN} + W_{si}^{SYN} = W_{i}^{SYN}$ $(i = 1, 2)$ is total synchronization energy of $i-th$ double pendulum which is transferred to the beam. The synchronization occurs when W_{i}^{SYN} vanished. Assuming that lenghs and masses of pendula are equal the solution of Eqs 13-15 let us derive the synchronization condition of double pendula in the following form:

$$\begin{aligned} \sin(\beta_{si} - \beta_{ck}) &= 0 \\ \sin(\beta_{ci} - \beta_{ck}) &= 0 \\ \sin(\beta_{si} - \beta_{sk}) &= 0 \\ \sin(\beta_{ci} - \beta_{sk}) &= 0 \end{aligned} \tag{16}$$

where $i = 1, 2$ and $k = 1, 2$. Assuming that $\beta_{c1} = 0$ (one phase angle can be arbitrarily taken). System of equations 16 is fulfilled when phase angles $\beta_{c1}, \beta_{c2}, \beta_{s1}, \beta_{s2}$ are combinations of 0 or π. The possible synchronization states are shown in Fig.7.

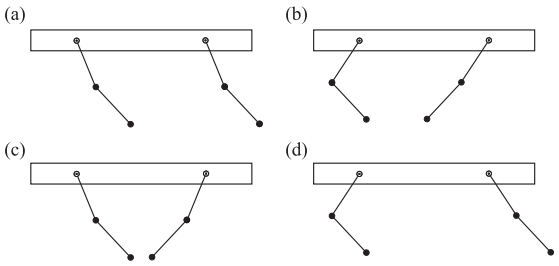

Fig. 7: Possible states of synchronizations: (a) all pendula are in phase $\beta_{s1} = \beta_{s2} = \beta_{c1} = \beta_{c2} = 0$, i.e,. both pendulum move identically; (b) upper pendula are in phase $\beta_{s1} = \beta_{s2} = \pi$, $\beta_{c1} = \beta_{c2} = 0$, i.e., both pendula move identically, lower and upper pendulum are in anti-phase; (c) both pendulums move in opposite directions $\beta_{s1} = \beta_{c1} = 0$, $\beta_{s2} = \beta_{c2} = \pi$; (d) upper pendula are in anti-phase, the lower and the upper pendula are in anti-phase $\beta_{s1} = \beta_{c2} = \pi$, $\beta_{s2} = \beta_{c1} = 0$.

5 Conclusions

The aim of this study was to derive a mathematical model of the systems, calculate periodic solutions, identify the different types of synchronous states and investigate the influence of system's parameters on the stability of synchronization.

In first paper for identical pendula, four different synchronous configurations are possible. The appearance of those states can be explained by the energy expressions which also show why other synchronous states are not possible. Nevertheless, not all synchronous states are stable for the given parameters of the beam. When the pendula are nonidentical, i.e., have different masses, we observe synchronous states for which the phase difference between the pendula vary in range from 0 to π. All obtained solutions destabilize in the Neimark-Sacker or saddle-node bifurcations, which results in an appearance of unsynchronized quasiperiodic oscillations or a jump to another attractor.

In second article we derive the analytical condition which enable calculation of the possible periodic solutions for any number of double pendula. The number of possible configurations grows with the number of coupled pendula. We examine how stability of each considered periodic solution changes with varying natural frequency of the beam. In the considered system, the typical bifurcation that stabilizes/destabilizes periodic solutions is a Neimark-Sacker bifurcation. The proper choice of beam's mass parameter one can ensure that only selected solutions are stable.

The last paper let us conclude that two double pendula self-exited by the escapement mechanism hanging from the horizontally movable beam can synchronize in four configurations. When the pendula are nonidentical, i.e., have different lengths (and periods of oscillations) for small parameters' mismatch we observe the synchronous states for which the phase difference between the pendula is close to 0 or π but for larger differences unsynchronized quasiperiodic oscillation dominates.

References

[1] C. Huygens, Letter to de sluse, in: Oeuveres completes de christian huygens (letters; no. 133 of 24 february 1665, no. 1335 of 26 february 1665, no. 1345 of 6 march 1665), societe hollandaise dessciences, martinus nijhor, la haye: 1665.

[2] A. Pikovsky, M. Rosenblum, J. Kurths, Synchronization. A Universal Concept in Nonlinear Sciences, Cambridge University Press, 2001.

[3] M. Bennett, M. Schatz, H. Rockwood, K. Wiesenfeld, Huygens's clocks, Proceedings: Mathematics, Physical and Engineering Sciences 458 (2002) 563–579.

[4] J. Pantaleone, Synchronization of metronomes, American Journal of Physics 70 (10) (2002) 992–1000.

[5] M. Senator, Synchronization of two coupled escapement-driven pendulum clocks, Journal of Sound and Vibration 291 (3-5) (2006) 566–603.

[6] K. Czolczynski, P. Perlikowski, A. Stefanski, T. Kapitaniak, Huygens'odd sympathy experiment revisited, International Journal of Bifurcation and Chaos 21 (07) (2011) 2047–2056.

[7] K. Czołczyński, P. Perlikowski, A. Stefański, T. Kapitaniak, Why two clocks synchronize: Energy balance of the synchronized clocks, Chaos: An Interdisciplinary Journal of Nonlinear Science 21 (2) (2011) 023129.

[8] K. Wiesenfeld, D. Borrero-Echeverry, Huygens (and others) revisited, Chaos: An Interdisciplinary Journal of Nonlinear Science 21 (4) (2011) 047515.

[9] M. Kapitaniak, K. Czolczynski, P. Perlikowski, A. Stefanski, T. Kapitaniak, Synchronization of clocks, Physics Reports 517 (1) (2012) 1–69.

[10] N. Rott, A multiple pendulum for the demonstration of non-linear coupling, Zeitschrift für angewandte Mathematik und Physik ZAMP 21 (4) (1970) 570–582.

[11] J. Miles, Parametric excitation of an internally resonant double pendulum, Zeitschrift für angewandte Mathematik und Physik ZAMP 36 (3) (1985) 337–345.

[12] A. Skeldon, T. Mullin, Mode interaction in a double pendulum, Physics Letters A 166 (3) (1992) 224–229.

[13] A. Skeldon, Dynamics of a parametrically excited double pendulum, Physica D: Nonlinear Phenomena 75 (4) (1994) 541–558.

[14] J. Strzalko, J. Grabski, J. Wojewoda, M. Wiercigroch, T. Kapitaniak, Synchronous rotation of the set of double pendula: Experimental observations, Chaos: An Interdisciplinary Journal of Nonlinear Science 22 (4) (2012) 047503.

[15] T. Morbiato, R. Vitaliani, A. Saetta, Numerical analysis of a synchronization phenomenon: pedestrian–structure interaction, Computers & Structures 89 (17) (2011) 1649–1663.

[16] A. P. Willmott, J. Dapena, The planarity of the stickface motion in the field hockey hit, Journal of sports sciences 30 (4) (2012) 369–377.

[17] Y. Suzuki, T. Nomura, M. Casadio, P. Morasso, Intermittent control with ankle, hip, and mixed strategies during quiet standing: a theoretical proposal based on a double inverted pendulum model, Journal of theoretical biology 310 (2012) 55–79.

[18] K. Granata, S. Wilson, Trunk posture and spinal stability, Clinical Biomechanics 16 (8) (2001) 650–659.

[19] P. Perlikowski, M. Kapitaniak, K. Czolczynski, A. Stefanski, T. Kapitaniak, Chaos in coupled clocks, International Journal of Bifurcation and Chaos 22 (12).

[20] M. Kapitaniak, M. Lazarek, M. Nielaczny, K. Czolczynski, P. Perlikowski, T. Kapitaniak, Synchronization extends the life time of the desired behavior of globally coupled systems, Scientific reports 4.

[21] P. Koluda, P. Perlikowski, K. Czolczynski, T. Kapitaniak, Synchronization of two self-excited double pendula, European Physical Journal: Special Topics 223 (4) (2014) 613–629.

[22] P. Koluda, P. Brzeski, P. Perlikowski, Dynamics of n coupled double pendula suspended to the moving beam, International Journal of Structural Stability and Dynamics 14(8) (2014) 1440028–1 – 1440028–24.

[23] P. Koluda, P. Perlikowski, K. Czolczynski, T. Kapitaniak, Synchronization configurations of two coupled double pendula, Communications in Nonlinear Science and Numerical Simulation 19 (4) (2014) 977–990.

[24] R. Vaughan, On the number of partitions into primes, The Ramanujan Journal 15 (1) (2008) 109–121.

6 Articles

6.1 Article 1

Eur. Phys. J. Special Topics **223**, 613–629 (2014)

DOI: 10.1140/epjst/e2014-02129-7

THE EUROPEAN PHYSICAL JOURNAL SPECIAL TOPICS

Review

Synchronization of two self-excited double pendula

P. Koluda[1], P. Perlikowski[1,a], Krzysztof Czolczynski[1], and T. Kapitaniak[1]

Division of Dynamics, Faculty of Mechanical Engineering, Lodz University of Technology, 90-924 Lodz, Stefanowskiego 1/15, Poland

Received 3 March 2014 / Received in final form 18 March 2014
Published online XX April 2014

Abstract. We consider the synchronization of two self-excited double pendula. We show that such pendula hanging on the same beam can have four different synchronous configurations. Our approximate analytical analysis allows us to derive the synchronization conditions and explain the observed types of synchronization. We consider an energy balance in the system and describe how the energy is transferred between the pendula via the oscillating beam, allowing thus the pendula synchronization. Changes and stability ranges of the obtained solutions with increasing and decreasing masses of the pendula are shown using path-following.

1 Introduction

Synchronization is commonly observed to occur among oscillators [1–5]. It is a process where two or more systems interact with one another and come to oscillate together. Groups of oscillators are observed to synchronize in a diverse variety of systems, despite inevitable differences between oscillators. The history of synchronization goes back to the 17th century. In 1673 the Dutch scientist Ch. Huygens observed weak synchronization of two pendulum clocks [6]. Recently, the phenomenon of synchronization of clocks hanging on a common movable beam [7] has been the subject of research conducted by numerous authors [6,8–18]. These studies explain the phenomenon of synchronization of a number of single pendula.

In our work we consider an interaction between two double pendula. One of the first investigations on dynamics of the double pendulum can be found in the paper by Rott [19], where an analytical investigation of the Hamiltonian system for different ratios between natural frequencies of pendula is presented. The next results obtained by Miles [20] show dynamics of the double pendulum under parametric excitation around the 2 : 1 resonance. A mode interaction in the double pendulum, including a detailed bifurcation analysis near two multiple bifurcation points and a transition to quasi-periodic motion and chaos around the 2 : 1 parametric resonance, is presented in [21–23]. Similarly as for 2 : 1, the 1 : 1 resonance leads to dynamics including multiple bifurcation points, symmetry breaking and cascades of period doubling bifurcations

[a] e-mail: przemyslaw.perlikowski@p.lodz.pl

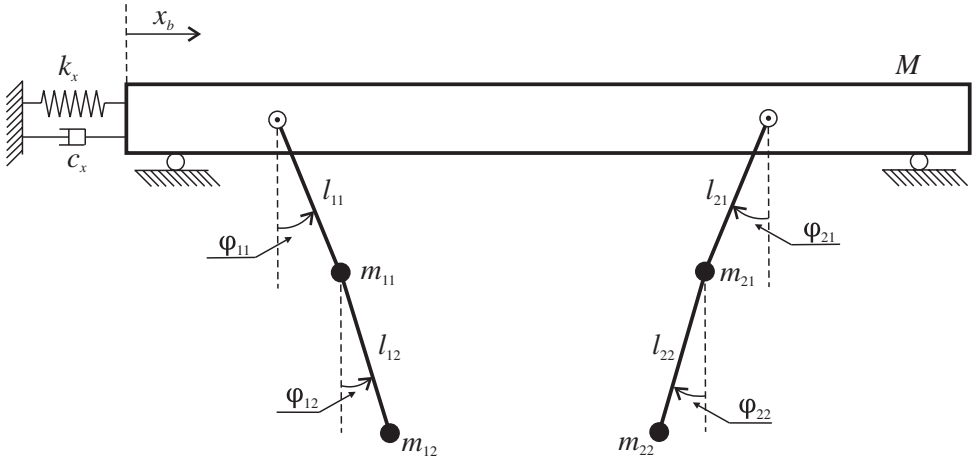

Fig. 1. Model of the system – two double pendula are mounted to the beam which can move horizontally. Each double pendulum consists of an upper pendulum of the length l_{i1} and the mass m_{i1} and a lower pendulum of the length l_{i2} and the mass m_{i2} $(i = 1, 2)$. The upper pendula are self-excited.

[23]. Double pendula can be also considered as an example of many physical systems commonly met in engineering, e.g., a model of bridge-pedestrian interactions [24], golf or hockey swing interactions with arms [25], human body [26] or trunk [27] models.

In this paper we consider the synchronization of two self-excited double pendula. The oscillations of each double pendulum are self-excited by the van der Pol type of damping associated with the upper parts (upper pendula) of each double pendulum. We show that two such double pendula hanging on the same beam can synchronize both in phase and in anti-phase. We give an evidence that the observed synchronous states are robust as they exist for a wide range of system parameters and are preserved for the parameter mismatch. The performed approximate analytical analysis allows us to derive the synchronization conditions and explain the observed types of synchronization. The energy balance in the system allows us to show how the energy is transferred between the pendula via the oscillating beam.

This paper is organized as follows: Sect. 2 describes the considered model of the coupled double pendula, in Sect. 3 we derive an energy balance of the synchronized pendula, whereas Sect. 4 presents the results of our numerical simulations and describes the observed synchronization states and their ranges of stability. Finally, we summarize our results in Sect. 5.

2 Model

The analyzed system is shown in Fig. 1. It consists of a rigid beam and two double pendula suspended on it. The beam of the mass M can move along the horizontal direction, its movement is described by the coordinate x_b.The beam is connected to a linear spring and a linear damper, k_x and c_x.

Each double pendulum consists of two light beams of the length l_{i1} and the masses m_{i1} (i-th upper pendulum) and the length l_{i2} and m_{i2} (i-th lower pendulum), where $i = 1, 2$, mounted at its ends. We consider double pendula with the same lengths $l_{11} = l_{21} = l_{12} = l_{22} = l$ but different masses m_{i1} and m_{i2} (to maintain generality in the derivation of equations, we use indexes for lengths of the pendula). The motion of each double pendulum is described by the angles φ_{i1} (upper pendulum) and φ_{i2}

(lower pendulum). The upper pendula are self-excited by the van der Pol type of damping (not shown in Fig. 1) given by the momentum (torque) $c_{vdp}\dot{\varphi}_{1i}(1-\mu\varphi_{1i}^2)$, where c_{vdp} and μ are constant. Van der Pol damping results in the generation of a stable limit cycle [1]. The lower pendula are damped with a viscous damper with the coefficient c_{i2}. The equations of motion of the considered system are as follows:

$$\begin{aligned}
&(M+\sum_{i=1}^{2}\sum_{j=1}^{2}m_{ij})\ddot{x}_b+\sum_{i=1}^{2}(m_{i1}+m_{i2})l_{i1}(\ddot{\varphi}_{i1}\cos\varphi_{i1}-\dot{\varphi}_{i1}^2\sin\varphi_{i1})\\
&+\sum_{i=1}^{2}m_{i2}l_{i2}(\ddot{\varphi}_{i2}\cos\varphi_{i2}-\dot{\varphi}_{i2}^2\sin\varphi_{i2})+k_x x_b+c_x\dot{x}_b=0\\
&(m_{i1}+m_{i2})l_{i1}\ddot{x}_b\cos\varphi_{i1}+(m_{i1}+m_{i2})l_{i1}^2\ddot{\varphi}_{i1}+m_{i2}l_{i1}l_{i2}\ddot{\varphi}_{i2}\cos(\varphi_{i1}-\varphi_{i2})\\
&+m_{i2}l_{i1}l_{i2}\dot{\varphi}_{i2}^2\sin(\varphi_{i1}-\varphi_{i2})+(m_{i1}+m_{i2})l_{i1}g\sin(\varphi_{i1})\\
&+c_{vdp}(1-\mu\varphi_{i1}^2)\dot{\varphi}_{i1}+c_{i2}(\dot{\varphi}_{i2}-\dot{\varphi}_{i1})=0\\
&m_{i2}l_{i2}\ddot{x}_b\cos\varphi_{i2}+m_{i2}l_{i1}l_{i2}\ddot{\varphi}_{i1}\cos(\varphi_{i1}-\varphi_{i2})+m_{i2}l_{i2}^2\ddot{\varphi}_{i2}\\
&-m_{i2}l_{i1}l_{i2}\dot{\varphi}_{i1}^2\sin(\varphi_{i1}-\varphi_{i2})+m_{i2}l_{i2}g\sin(\varphi_{i2})-c_{i2}(\dot{\varphi}_{i2}-\dot{\varphi}_{i1})=0.
\end{aligned}\tag{1}$$

Introducing the dimensionless time $\tau=\omega t$, where $\omega^2=\frac{g}{l_{11}}$ is the natural frequency of the upper pendula, we can rewrite Eq. (1) in the dimensionless form as:

$$\begin{aligned}
&\ddot{y}_b+\sum_{i=1}^{2}\mathbf{A}_{i1}(\ddot{\psi}_{i1}\cos\psi_{i1}-\dot{\psi}_{i1}^2\sin\psi_{i1})+\sum_{i=1}^{2}\mathbf{A}_{i2}(\ddot{\psi}_{i2}\cos\psi_{i2}-\dot{\psi}_{i2}^2\sin\psi_{i2})\\
&+\mathbf{K}y_b+\mathbf{C}\dot{y}_b=0
\end{aligned}\tag{2}$$

$$\begin{aligned}
&\delta_{i1}\ddot{y}_b\cos\psi_{i1}+\mathbf{L}_{i1}\ddot{\psi}_{i1}+\mathbf{L}_{i3}\ddot{\psi}_{i2}\cos(\psi_{i1}-\psi_{i2})=\\
&-\mathbf{L}_{i3}\dot{\psi}_{i2}^2\sin(\psi_{i1}-\psi_{i2})-\mathbf{G}_{i1}\sin(\psi_{i1})-\mathbf{C}_{vdp}(1-\mu\psi_{i1}^2)\dot{\psi}_{i1}-\mathbf{C}_{i2}(\dot{\psi}_{i2}-\dot{\psi}_{i1})
\end{aligned}\tag{3}$$

$$\begin{aligned}
&\delta_{i2}\ddot{y}_b\cos\psi_{i2}+\mathbf{L}_{i3}\ddot{\psi}_{i1}\cos(\psi_{i1}-\psi_{i2})+\mathbf{L}_{i2}\ddot{\psi}_{i2}=\\
&\mathbf{L}_{i3}\dot{\psi}_{i1}^2\sin(\psi_{i1}-\psi_{i2})-\mathbf{G}_{i2}\sin(\psi_{i2})+\mathbf{C}_{i2}(\dot{\psi}_{i2}-\dot{\psi}_{i1})
\end{aligned}\tag{4}$$

where $\mathbf{A}_{i1}=\frac{(m_{i1}+m_{i2})l_{i1}}{Ml_b}$, $\mathbf{A}_{i2}=\frac{m_{i2}l_{i2}}{Ml_b}$, $\mathbf{K}=\frac{k_x}{M\omega^2}$, $\mathbf{C}=\frac{c_x}{M\omega}$, $\delta_{i1}=\frac{(m_{i1}+m_{i2})l_{i1}}{Ml_{12}}$, $\delta_{i2}=\frac{m_{i2}l_{i2}}{Ml_{12}}$, $\mathbf{L}_{i1}=\frac{(m_{i1}+m_{i2})l_{i1}^2}{l_{12}l_bM}$, $\mathbf{L}_{i2}=\frac{m_{i2}l_{i2}^2}{l_{12}l_bM}$, $\mathbf{L}_{i3}=\frac{m_{i2}l_{i2}l_{i1}}{l_bMl_{12}}$, $\mathbf{G}_{i1}=\frac{(m_{i1}+m_{i2})l_{i1}g}{l_{12}\omega^2l_bM}$, $\mathbf{G}_{i2}=\frac{m_{i2}l_{i2}g}{l_{12}\omega^2l_bM}$, $\mathbf{C}_{vdp}=\frac{c_{vdp}}{\omega l_bMl_{12}}$, $\mathbf{C}_{i2}=\frac{c_{i2}}{l_{12}\omega l_bM}$.

3 Analytical conditions for synchronization

3.1 Force with which the pendula act on the beam

In this section we derive an approximate analytical condition for the pendulum synchronization in the considered system. Assuming that the double pendula are identical and perform periodic oscillations with the frequency ω_0 and low amplitudes, one can describe displacements, velocities and accelerations of the upper and lower pendula in the following way:

$$\psi_{ij}=\Phi_{ij}\sin(\omega_0\tau+\beta_{ij}),\tag{5}$$

$$\dot{\psi}_{ij} = \omega_0 \Phi_{ij} \cos(\omega_0 \tau + \beta_{ij}), \tag{6}$$

$$\ddot{\psi}_{ij} = -\omega_0^2 \Phi_{ij} \sin(\omega_0 \tau + \beta_{ij}), \tag{7}$$

where β_{ij} $(i, j = 1, 2)$ are phase differences between the pendula.

Equation (2) allows an estimation of the resultant force with which the pendula act on the beam:

$$F = -\sum_{i=1}^{2} \mathbf{A}_{i1}(\ddot{\psi}_{i1} \cos\psi_{i1} - \dot{\psi}_{i1}^2 \sin\psi_{i1}) - \sum_{i=1}^{2} \mathbf{A}_{i2}(\ddot{\psi}_{i2} \cos\psi_{i2} - \dot{\psi}_{i2}^2 \sin\psi_{i2}). \tag{8}$$

Substituting Eqs. (5–7) into Eq. (8) and considering the relation $\cos^2\alpha \sin\alpha = 0.25 \sin\alpha + 0.25 \sin 3\alpha$, one obtains:

$$\begin{aligned} F = {} & \mathbf{A}_{11}[\omega_0^2 \Phi_{11}(1 + 0.25\Phi_{11}^2) \sin(\omega_0\tau + \beta_{11}) + \omega_0^2 \Phi_{11}^3 0.25 \sin(3\omega_0\tau + 3\beta_{11})] \\ & + \mathbf{A}_{12}[\omega_0^2 \Phi_{12}(1 + 0.25\Phi_{12}^2) \sin(\omega_0\tau + \beta_{12}) + \omega_0^2 \Phi_{12}^3 0.25 \sin(3\omega_0\tau + 3\beta_{12})] \\ & + \mathbf{A}_{21}[\omega_0^2 \Phi_{21}(1 + 0.25\Phi_{21}^2) \sin(\omega_0\tau + \beta_{21}) + \omega_0^2 \Phi_{21}^3 0.25 \sin(3\omega_0\tau + 3\beta_{21})] \\ & + \mathbf{A}_{22}[\omega_0^2 \Phi_{22}(1 + 0.25\Phi_{22}^2) \sin(\omega_0\tau + \beta_{22}) + \omega_0^2 \Phi_{22}^3 0.25 \sin(3\omega_0\tau + 3\beta_{22})]. \end{aligned} \tag{9}$$

Equation (9) is the right-hand side of equation of the beam motion (2), hence we have:

$$\ddot{y}_b + \mathbf{K} y_b + \mathbf{C} \dot{y}_b = F. \tag{10}$$

Assuming that the damping coefficient $\mathbf{C}$ is small, one gets:

$$\begin{aligned} y_b &= \sum_{i=1}^{2}\sum_{j=1}^{2} \mathbf{X}_{1ij}\mathbf{A}_{ij} \sin(\omega_0\tau + \beta_{ij}) + \sum_{i=1}^{2}\sum_{j=1}^{2} \mathbf{X}_{3ij}\mathbf{A}_{ij} \sin(3\omega_0\tau + 3\beta_{ij}), \\ \ddot{y}_b &= \sum_{i=1}^{2}\sum_{j=1}^{2} \mathbf{A}_{1ij}\mathbf{A}_{ij} \sin(\omega_0\tau + \beta_{ij}) + \sum_{i=1}^{2}\sum_{j=1}^{2} 9\mathbf{A}_{3ij}\mathbf{A}_{ij} \sin(3\omega_0\tau + 3\beta_{ij}), \end{aligned} \tag{11}$$

where:

$$\begin{aligned} X_{1ij} &= \frac{\omega_0^2 \Phi_{ij}(1 + 0.25\Phi_{ij}^2)}{\mathbf{K} - \omega_0^2}, \quad X_{3ij} = \frac{0.25\omega_0^2 \Phi_{ij}^3}{\mathbf{K} - 9\omega_0^2}, \\ \mathbf{A}_{1ij} &= \frac{-\omega_0^4 \Phi_{ij}(1 + 0.25\Phi_{ij}^2)}{\mathbf{K} - \omega_0^2}, \quad \mathbf{A}_{3ij} = \frac{-0.25\omega_0^4 \Phi_{ij}^3}{\mathbf{K} - 9\omega_0^2}. \end{aligned} \tag{12}$$

Equations (11) represent the displacement and the acceleration of the beam M, respectively.

3.2 Energy balance of the system

Multiplying Eq. (2) by the velocity of the beam $\dot{y}_b$, we obtain:

$$\begin{aligned} \ddot{y}_b \dot{y}_b + \mathbf{K} y_b \dot{y}_b = {} & -\mathbf{C}\dot{y}_b^2 - \sum_{i=1}^{2} \mathbf{A}_{i1}(\ddot{\psi}_{i1}\dot{y}_b \cos\psi_{i1} - \dot{\psi}_{i1}^2 \dot{y}_b \sin\psi_{i1}) \\ & - \sum_{i=1}^{2} \mathbf{A}_{i2}(\ddot{\psi}_{i2}\dot{y}_b \cos\psi_{i2} - \dot{\psi}_{i2}^2 \dot{y}_b \sin\psi_{i2}). \end{aligned} \tag{13}$$

Assuming that the motion of the pendulum is periodic with the period T ($T = 2\pi/\omega_0$) and integrating Eq. (13), we obtain the following energy balance:

$$\int_0^T \ddot{y}_b \dot{y}_b d\tau + \int_0^T \mathbf{K} y_b \dot{y}_b d\tau = -\int_0^T \mathbf{C} \dot{y}_b^2 d\tau - \int_0^T \sum_{j=1}^{2} \left(\sum_{i=1}^{2} \mathbf{A}_{ij} (\ddot{\psi}_{ij} \cos\psi_{ij} - \dot{\psi}_{ij}^2 \sin\psi_{ij}) \right) \dot{y}_b d\tau. \tag{14}$$

The left-hand side of Eq. (14) represents an increase in the total energy of the beam which for the periodic oscillations is equal to zero:

$$\int_0^T \ddot{y}_b \dot{y}_b d\tau + \int_0^T \mathbf{K} y_b \dot{y}_b d\tau = 0. \tag{15}$$

The first component of the right-hand side of Eq. (14) represents the energy dissipated by the linear damper $\mathbf{C}$:

$$W_{beam}^{DAMP} = \int_0^T \mathbf{C} \dot{y}_b^2 d\tau, \tag{16}$$

whereas the second component represents the work performed by horizontal components of the force with which the double pendula act on the beam causing its motion:

$$W_{beam}^{DRIVE} = -\int_0^T \sum_{j=1}^{2} \left(\sum_{i=1}^{2} \mathbf{A}_{ij} (\ddot{\psi}_{ij} \cos\psi_{ij} - \dot{\psi}_{ij}^2 \sin\psi_{ij}) \right) \dot{y}_b d\tau. \tag{17}$$

Substituting Eqs. (16) and (17) into Eq. (14), we get:

$$W_{beam}^{DRIVE} - W_{beam}^{DAMP} = 0. \tag{18}$$

Multiplying the equation of the upper pendulum (Eq. (3)) by the velocity $\dot{\psi}_{i1}$, we obtain:

$$\begin{aligned} &\delta_{i1} \ddot{y}_b \dot{\psi}_{i1} \cos\psi_{i1} + \mathbf{L}_{i1} \ddot{\psi}_{i1} \dot{\psi}_{i1} + \mathbf{L}_{i3} \ddot{\psi}_{i2} \dot{\psi}_{i1} \cos(\psi_{i1} - \psi_{i2}) = -\mathbf{L}_{i3} \dot{\psi}_{i1} \dot{\psi}_{i2}^2 \sin(\psi_{i1} - \psi_{i2}) \\ &-\mathbf{G}_{i1} \dot{\psi}_{i1} \sin(\psi_{i1}) - \mathbf{C}_{vdp} (1 - \mu \psi_{i1}^2) \dot{\psi}_{i1}^2 + \mathbf{C}_{i2} (\dot{\psi}_{i2} - \dot{\psi}_{i1}) \dot{\psi}_{i1}. \end{aligned} \tag{19}$$

Assuming that the oscillations of the pendula are periodic with the period T and integrating Eq. (19), one obtains the following energy balance:

$$\begin{aligned} &\int_0^T \mathbf{L}_{i1} \ddot{\psi}_{i1} \dot{\psi}_{i1} d\tau + \int_0^T \mathbf{G}_{i1} \dot{\psi}_{i1} \sin\psi_{i1} d\tau = -\int_0^T \delta_{i1} \ddot{y}_b \dot{\psi}_{i1} \cos\psi_{i1} d\tau \\ &\quad - \int_0^T \mathbf{L}_{i3} (\dot{\psi}_{i1} \dot{\psi}_{i2}^2 \sin(\psi_{i1} - \psi_{i2}) + \ddot{\psi}_{i2} \dot{\psi}_{i1} \cos(\psi_{i1} - \psi_{i2})) d\tau \\ &- \int_0^T \mathbf{C}_{vdp} \dot{\psi}_{i1}^2 d\tau + \int_0^T \mathbf{C}_{vdp} \mu \psi_{i1}^2 \dot{\psi}_{i1}^2 d\tau + \int_0^T \mathbf{C}_{i2} \dot{\psi}_{i2} \dot{\psi}_{i1} d\tau - \int_0^T \mathbf{C}_{i2} \dot{\psi}_{i1}^2 d\tau. \end{aligned} \tag{20}$$

The left side of Eq. (20) represents the total energy of the upper pendula, which in the case of periodic oscillations is equal to zero:

$$\int_0^T \mathbf{L}_{i1} \ddot{\psi}_{i1} \dot{\psi}_{i1} d\tau + \int_0^T \mathbf{G}_{i1} \dot{\psi}_{i1} \sin\psi_{i1} d\tau = 0. \tag{21}$$

The first component of the right side of Eq. (20) represents the energy which is transferred to the beam:

$$W_{i1}^{SYN} = \int_0^T \delta_{i1} \ddot{y}_b \dot{\psi}_{i1} \cos\psi_{i1} d\tau. \tag{22}$$

The second component describes the energy which is transferred to the lower pendulum:

$$W_{i1}^{SYN\ P} = -\int_0^T \mathbf{L}_{i3}(\dot{\psi}_{i1}\dot{\psi}_{i2}^2 \sin(\psi_{i1}-\psi_{i2}) + \ddot{\psi}_{i2}\dot{\psi}_{i1}\cos(\psi_{i1}-\psi_{i2}))d\tau, \tag{23}$$

and the third component describes the energy which is supplied to the system by the van der Pol damper in one-period oscillations:

$$W_{i1}^{DAMP} = -\int_0^T (\mathbf{C}_{vdp} + \mathbf{C}_{i2})\dot{\psi}_{i1}^2 - \mathbf{C}_{i2}\dot{\psi}_{i2}\dot{\psi}_{i1} d\tau. \tag{24}$$

Finally, the last component represents the energy dissipated by the van der Pol damper:

$$W_{i1}^{SELF} = -\int_0^T \mu \mathbf{C}_{vdp} \psi_{i1}^2 \dot{\psi}_{i1}^2 d\tau, \tag{25}$$

Substituting Eqs. (22–25) into Eq. (20), we obtain the following relation:

$$W_{i1}^{SYN\ P} - W_{i1}^{SYN} + W_{i1}^{SELF} + W_{i1}^{DAMP} = 0,$$

Multiplying the equation of the lower pendulum (Eq. (4)) by the velocity $\dot{\psi}_{i2}$, one gets:

$$\delta_{i2}\ddot{y}_b\dot{\psi}_{i2}\cos\psi_{i2} + \mathbf{L}_{i3}\ddot{\psi}_{i1}\dot{\psi}_{i2}\cos(\psi_{i1}-\psi_{i2}) + \mathbf{L}_{i2}\dot{\psi}_{i2}\ddot{\psi}_{i2} = \tag{26}$$

$$\mathbf{L}_{i3}\dot{\psi}_{i1}^2\dot{\psi}_{i2}\sin(\psi_{i1}-\psi_{i2}) - \mathbf{G}_{i2}\dot{\psi}_{i2}\sin(\psi_{i2}) - \mathbf{C}_{i2}(\dot{\psi}_{i2}-\dot{\psi}_{i1})\dot{\psi}_{i2}.$$

Assuming that the oscillations of the pendulum are periodic with the period T, the integration of Eq. (26) gives the following energy balance:

$$\int_0^T \mathbf{L}_{i2}\dot{\psi}_{i2}\ddot{\psi}_{i2}d\tau + \int_0^T \mathbf{G}_{i2}\dot{\psi}_{i2}\sin(\psi_{i2})d\tau = -\int_0^T \beta_{i2}\ddot{y}_b\dot{\psi}_{i2}\cos\psi_{i2}d\tau$$
$$-\int_0^T \mathbf{L}_{i3}(\dot{\psi}_{i1}^2\dot{\psi}_{i2}\sin(\psi_{i1}-\psi_{i2}) - \ddot{\psi}_{i1}\dot{\psi}_{i2}\cos(\psi_{i1}-\psi_{i2}))d\tau$$
$$-\int_0^T \mathbf{C}_{i2}\dot{\psi}_{i2}^2 d\tau + \int_0^T \mathbf{C}_{i2}\dot{\psi}_{i1}\dot{\psi}_{i2}d\tau. \tag{27}$$

The left side of Eq. (27) represents the total energy of the lower pendulum, which in the case of periodic oscillations is equal to zero:

$$\int_0^T \mathbf{L}_{i2}\dot{\psi}_{i2}\ddot{\psi}_{i2}d\tau + \int_0^T \mathbf{G}_{i2}\dot{\psi}_{i2}\sin(\psi_{i2})d\tau = 0. \tag{28}$$

The first component of the right side of Eq. (27) represents the energy which is transferred to the beam via the upper pendulum or to the next pendulum via the upper pendulum and the beam:

$$W_{i2}^{SYN} = \int_0^T \delta_{i2}\ddot{y}_b\dot{\psi}_{i2}\cos\psi_{i2}d\tau. \tag{29}$$

The second component describes the energy which is transferred to the upper pendulum:

$$W_{i2}^{SYN\ P} = -\int_0^T \mathbf{L}_{i3}(\dot{\psi}_{i1}^2\dot{\psi}_{i2}\sin(\psi_{i1}-\psi_{i2}) - \ddot{\psi}_{i1}\dot{\psi}_{i2}\cos(\psi_{i1}-\psi_{i2}))d\tau. \tag{30}$$

and the last component represents the energy dissipated by the damper:

$$W_{i2}^{DAMP} = -\int_0^T \mathbf{C}_{i2}(\dot{\psi}_{i2}-\dot{\psi_{i1}})\dot{\psi_{i2}}d\tau \tag{31}$$

Substituting Eqs. (29–31) into Eq. (27), one obtains the following relation:

$$W_{i2}^{SYN\ P} - W_{i2}^{SYN} + W_{i2}^{DAMP} = 0.$$

3.3 Energy transfer between the upper and lower pendula

The energy transferred from the upper to lower pendulum is given by:

$$W_{i1}^{SYN\ P} = -\int_0^T \mathbf{L}_{i3}(\ddot{\psi}_{i2}\cos(\psi_{i1}-\psi_{i2}) + \dot{\psi}_{i2}^2\sin(\psi_{i1}-\psi_{i2}))\dot{\psi}_{i1}d\tau, \tag{32}$$

and the energy transferred from the lower to upper pendulum is:

$$W_{i2}^{SYN\ P} = -\int_0^T \mathbf{L}_{i3}(\ddot{\psi}_{i1}\cos(\psi_{i1}-\psi_{i2}) - \dot{\psi}_{i1}^2\sin(\psi_{i1}-\psi_{i2}))\dot{\psi}_{i2}d\tau. \tag{33}$$

Taking into account Eqs. (5–7), Eq. (33) takes the form:

$$\begin{aligned} W_{i1}^{SYN\ P} = -\mathbf{L}_{i3}\int_0^T & (-\omega_0^2\Phi_{i2}\sin(\omega_0 t+\beta_{i2})\cos(\Phi_{i1}\sin(\omega_0 t+\beta_{i1}) - \Phi_{i2}\sin(\omega_0 t+\beta_{i2})) \\ & +\omega_0^2\Phi_{i2}^2\cos^2(\omega_0 t+\beta_{i2})\sin(\Phi_{i1}\sin(\omega_0 t+\beta_{i1}) \\ & -\Phi_{i2}\sin(\omega_0 t+\beta_{i2})))\omega_0\Phi_{i1}\cos(\omega_0 t+\beta_{i1})d\tau \\ = \mathbf{L}_{i3}\pi\omega_0^2\Phi_{i1}\Phi_{i2}&\sin(\beta_{i2}-\beta_{i1}), \end{aligned} \tag{34}$$

and

$$W_{i2}^{SYN\ P} = \mathbf{L}_{i3}\pi\omega_0^2\Phi_{i1}\Phi_{i2}\sin(\beta_{i1}-\beta_{i2}) = -W_{i1}^{SYN\ P}, \tag{35}$$

The synchronization between the lower and upper pendula occurs when:

$$W_{i1}^{SYN\ P} = 0 \quad \Rightarrow \quad \sin(\beta_{i1}-\beta_{i2}) = 0. \tag{36}$$

Condition (36) is fulfilled when:

$$\beta_{i1} = \beta_{i2} \vee (\beta_{i1} = 0 \wedge \beta_{i2} = \pi). \tag{37}$$

In the first case, the oscillations of the upper and lower pendula are in-phase, i.e., the pendula move in the same directions, whereas in the second case they are in anti-phase, i.e., the pendula move in the opposite directions. For low oscillations, limit conditions (37) define two normal modes of oscillations [1].

3.4 Synchronization of the double pendula

In each equation of the pendulum motion, there is a component influencing the beam motion

$$M_{ij}^{SYN} = \delta_{ij}\ddot{y}_b \cos\psi_{ij}, \tag{38}$$

which is called the synchronization momentum (torque). The work done by this momentum during one period is equal to zero.

$$W_{ij}^{SYN} = \int_0^T \delta_{ij}\ddot{y}_b \cos\psi_{ij}\dot{\psi}_{ij} d\tau = 0. \tag{39}$$

Substituting Eqs. (5, 6) and (11) into (39) and performing the linearization, we arrive at:

$$\begin{aligned}
W_{11}^{SYN} &= \int_0^T \delta_{11}\left(\sum_{i=1}^{2}\sum_{j=1}^{2}\mathbf{A}_{1ij}\mathbf{A}_{ij}\sin(\omega_0 t+\beta_{ij}) + \sum_{i=1}^{2}\sum_{j=1}^{2}\mathbf{A}_{3ij}\mathbf{A}_{ij}\sin(3\omega_0 t+3\beta_{ij})\right) \\
&\quad \times\omega_0\Phi_{11}\cos(\omega_0 t+\beta_{11})d\tau = \\
&= \delta_{11}\omega_0\pi\Phi_{11}\sum_{i=1}^{2}\sum_{j=1}^{2}\mathbf{A}_{1ij}\mathbf{A}_{ij}\sin(\beta_{ij}-\beta_{11}) = \\
&= \xi\delta_{11}\Phi_{11}\left[\sum_{i=1}^{2}\sum_{j=1}^{2}\Theta_{ij}M_{ij}\sin(\beta_{ij}-\beta_{11})\right] = 0, \\
W_{12}^{SYN} &= \xi\delta_{12}\Phi_{12}\left[\sum_{i=1}^{2}\sum_{j=1}^{2}\Theta_{ij}M_{ij}\sin(\beta_{ij}-\beta_{12})\right] = 0, \\
W_{21}^{SYN} &= \xi\delta_{21}\Phi_{21}\left[\sum_{i=1}^{2}\sum_{j=1}^{2}\Theta_{ij}M_{ij}\sin(\beta_{ij}-\beta_{21})\right] = 0, \\
W_{22}^{SYN} &= \xi\delta_{22}\Phi_{22}\left[\sum_{i=1}^{2}\sum_{j=1}^{2}\Theta_{ij}M_{ij}\sin(\beta_{ij}-\beta_{22})\right] = 0,
\end{aligned} \tag{40}$$

where:

$$\xi = \frac{-\omega_0^5\pi}{Ml_b(\mathbf{K}-\omega_0^2)}, \quad M_{i1} = (m_{i1}+m_{i2})l_{i1}, \quad M_{i2} = m_{i2}l_{i2}, \quad \Theta_{ij} = \Phi_{ij}(1+0.25\Phi_{ij}^2). \tag{41}$$

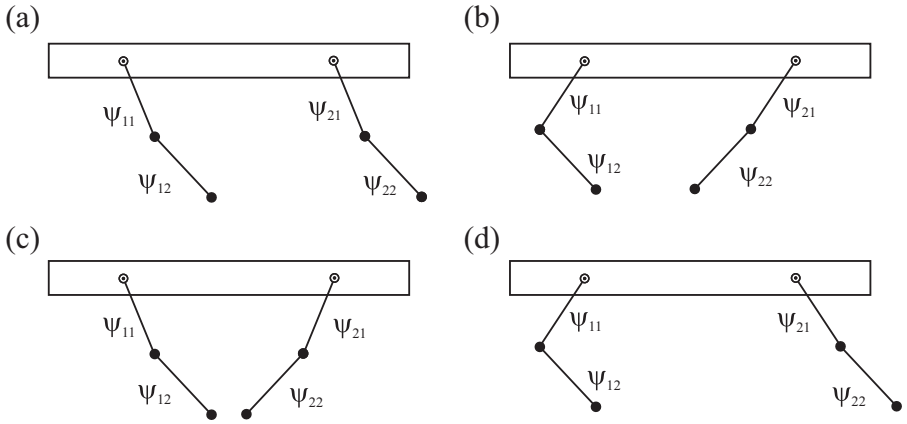

Fig. 2. Synchronous states of the system (1): (a) upper and lower pendula in phase: $\psi_{11} = \psi_{21}$ and $\psi_{12} = \psi_{22}$, (b) upper pendula in phase, lower pendula in anti-phase: $\psi_{11} = \psi_{21}$ and $\psi_{12} = -\psi_{22}$, (c) upper and lower pendula in anti-phase: $\psi_{11} = -\psi_{21}$ and $\psi_{12} = -\psi_{22}$ (d) upper pendula in anti-phase, lower pendula in phase: $\psi_{11} = -\psi_{21}$ and $\psi_{12} = \psi_{22}$.

Equations (40) allow the calculation of the phase angles β_{ij} for which the synchronization of periodic oscillations of the pendula occurs. The synchronization occurs when the following equations are fulfilled:

$$\begin{aligned}
&\Theta_{12}M_{12}\sin(\beta_{12}-\beta_{11}) + \Theta_{21}M_{21}\sin(\beta_{21}-\beta_{11}) + \Theta_{22}M_{22}\sin(\beta_{22}-\beta_{11}) = 0,\\
&\Theta_{11}M_{11}\sin(\beta_{11}-\beta_{12}) + \Theta_{21}M_{21}\sin(\beta_{21}-\beta_{12}) + \Theta_{22}M_{22}\sin(\beta_{22}-\beta_{12}) = 0,\\
&\Theta_{11}M_{11}\sin(\beta_{11}-\beta_{21}) + \Theta_{12}M_{12}\sin(\beta_{12}-\beta_{21}) + \Theta_{22}M_{22}\sin(\beta_{22}-\beta_{21}) = 0,\\
&\Theta_{11}M_{11}\sin(\beta_{11}-\beta_{22}) + \Theta_{12}M_{12}\sin(\beta_{12}-\beta_{22}) + \Theta_{21}M_{21}\sin(\beta_{21}-\beta_{22}) = 0.
\end{aligned} \tag{42}$$

Equations (42) are fulfilled for β_{ij}, which are combinations of 0 and π. Assuming that $\beta_{11} = 0$, one can identify the following pendulum configurations which are presented in Fig. 2(a–d). The first type is the configuration shown in Fig. 2(a). Both the upper and lower pendula are phase synchronized, i.e., $\psi_{11} = \psi_{21}$ and $\psi_{12} = \psi_{22}$ ($\beta_{11} = \beta_{12} = \beta_{21} = \beta_{22} = 0$ or $\beta_{11} = \beta_{21} = 0$, $\beta_{12} = \beta_{22} = \pi$). The upper and lower pendula are synchronized in phase and anti-phase, respectively, i.e., $\psi_{11} = \psi_{21}$ and $\psi_{12} = -\psi_{22}$ in the configuration from Fig. 2(b) ($\beta_{11} = \beta_{12} = \beta_{21} = 0$, $\beta_{22} = \pi$ or $\beta_{11} = \beta_{12} = \beta_{22} = 0$, $\beta_{21} = \pi$). Figure 2(c) presents the case when both the upper and lower pendula are synchronized in anti-phase, i.e., $\psi_{11} = -\psi_{21}$ and $\psi_{12} = -\psi_{22}$ ($\beta_{11} = \beta_{12} = 0$, $\beta_{21} = \beta_{22} = \pi$ or $\beta_{11} = \beta_{22} = 0$, $\beta_{12} = \beta_{21} = \pi$). Finally, in Fig. 2(d), we present the case when the upper pendula are in anti-phase and the lower pendula are in phase $\psi_{11} = -\psi_{21}$ and $\psi_{12} = \psi_{22}$ ($\beta_{11} = \beta_{12} = \beta_{22} = 0$, $\beta_{21} = \pi$ or $\beta_{11} = 0$, $\beta_{21} = \beta_{12} = \beta_{22} = \pi$).

4 Numerical investigations

In our numerical calculations, we use the Auto 07p [29] continuation toolbox to obtain periodic solutions. To start path-following, we integrate Eqs. (2–4) with the fourth-order Runge-Kutta method. We consider the following parameter values: $m_{11} = m_{12} = m_{21} = m_{22} = 1.0\,[\mathrm{kg}]$, $M = 10.0\,[\mathrm{kg}]$, $l_{11} = l_{12} = l_{21} = l_{22} = 0.2485\,[\mathrm{m}]$, $k_x = 4.0\,[\mathrm{N/m}]$, $c_x = 1.53\,[\mathrm{Ns/m}]$, $c_{vdp} = -0.1\,[\mathrm{Ns/m}]$, $\mu = 60.0\,[\mathrm{m}^{-2}]$, $c_{i2} = 0.0016\,[\mathrm{Ns/m}]$, which yield the following dimensionless coefficients $\mathbf{A}_{i1} = 0.0354986$,

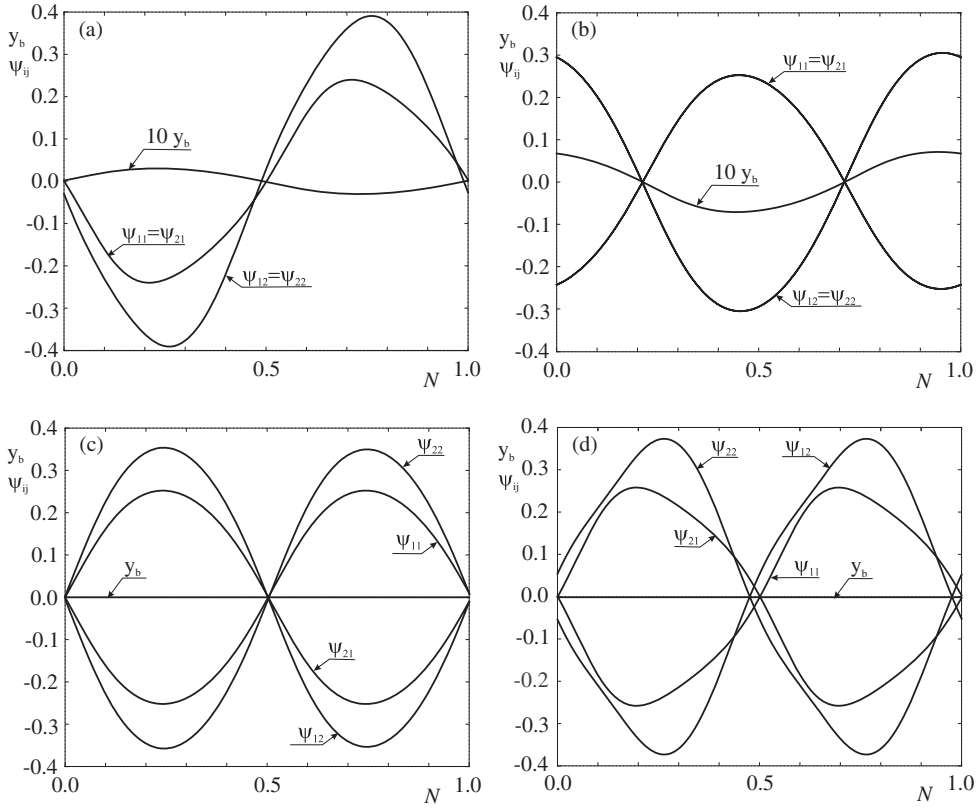

Fig. 3. Pendulum and beam displacements for one period of motion ($N = 1$) for four different periodic solutions in the case of identical masses of the pendula: $m_{11} = m_{12} = m_{21} = m_{22} = 1.0\,[\mathrm{kg}]$. The displacement y_b of the beam M is shown 10 times magnified. (a) pendulum configuration from Fig. 2(a) with the period $T = 7.233$, (b) pendulum configuration from Fig. 2(a) with the period $T = 3.362$, (c) pendulum configuration from Fig. 2(c) with the period $T = 3.748$, and (d) pendulum configuration from Fig. 2(c) with the period $T = 8.266$.

$\mathbf{A}_{i2} = 0.01774933$, $\delta_{i1} = 0.142857$, $\delta_{i2} = 0.0714286$, $\mathbf{L}_{i1} = 0.035986$, $\mathbf{L}_{i2} = 0.0177493$, $\mathbf{L}_{i3} = 0.0177493$, $\mathbf{G}_{i1} = 0.0354986$, $\mathbf{G}_{i2} = 0.0177493$, $\mathbf{C}_{vdp} = -0.00457491$, $\mathbf{C}_{i2} = 0.0000714286$, $\mathbf{C} = 0.0173934$, $\mathbf{K} = 0.00723723$. Our bifurcation parameters are masses of the pendula and the beam. To hold an intuitive physical interpretation, we change dimensional masses, but all the calculation are performed for dimensionless equations.

4.1 Periodic solutions to the pendula with identical masses

Depending on the initial conditions, we observe four different synchronous states of system (2–4) as shown in Fig. 3(a–d). The in-phase motion is represented by two periodic solutions: the first type is characterized by a lack of phase differences in the pendulum angular positions: $\beta_{11} = \beta_{21} = \beta_{12} = \beta_{22}$ (see Fig. 3(a)), whereas the second one - by a phase difference between the upper and lower pendula in each double pendulum: $\beta_{11} = \beta_{21}$, $\beta_{12} = \beta_{22}$ and $\beta_{i1} - \beta_{i2} = \pi$, $i = 1, 2$ (see Fig. 3(b)). In both cases, the displacements of the upper and lower pendula of each double pendulum are identical, i.e., $\psi_{11} = \psi_{21}$, $\psi_{12} = \psi_{22}$. The beam motion is in anti-phase

to the upper pendula and in-phase (Fig. 3(a)) or anti-phase (Fig. 3(b)) to the lower ones. These two configurations correspond to the analytically predicted synchronous state presented in Fig. 2(a). The second type, the anti-phase motion, for which the beam is not moving, is shown in Fig. 3(c,d). We can also distinguish two types of this periodic solution, both characterized by the following phase differences of the pendulum displacements: $\beta_{11} - \beta_{21} = \pi$ and $\beta_{12} - \beta_{22} = \pi$, but different phase shifts between the pendula in each double pendulum: $\beta_{i1} - \beta_{i2} = \pi$, $i = 1, 2$ (see Fig. 3(c)) and $\beta_{i1} - \beta_{i2} = 0$, $i = 1, 2$ (see Fig. 3(d)). The beam M is at rest, because reaction forces acting on the beam are vanishing. These pendulum configurations correspond to the theoretically predicted synchronous state presented in Fig. 2(c). Note that for this type of the synchronous state, amplitudes of pendulum oscillations can be estimated analytically. Substituting $\beta_{11} = \beta_{12} = 0$ and $\beta_{21} = \beta_{22} = \pi$ in Eqs. (42), one can derive an analytical formula for amplitudes of pendulum oscillations. The amplitudes of the upper pendula can be approximated by:

$$\Phi_{11} = \Phi_{21} = 2\sqrt{\frac{1}{\mu}}. \tag{43}$$

The approximate values of the amplitudes of oscillations of the lower pendula can be calculated from the following condition:

$$\begin{aligned}\frac{1}{4}\omega_0\pi(4\mathbf{C}_{i2}(\Phi_{i1}^2 + \Phi_{i2}^2) + \mathbf{C}_{vdp}\Phi_{i1}^2(4 - \mu\Phi_{i1}^2) - 8\mathbf{C}_{i2}\Phi_{i1}\Phi_{i2}\cos(\beta_{i1} - \beta_{i2}) \\ +\Phi_{i1}\Phi_{i2}(\Phi_{i2}^2 - \Phi_{i1}^2)\mathbf{L}_{i3}\omega_0\sin(\beta_{i1} - \beta_{i2})) = 0\end{aligned} \tag{44}$$

For $i = 1, 2$, formulae (43) and (45) give good approximation of the numerical values, e.g., for the parameter values in Fig. 3(c,d), the analytically calculated amplitudes of the upper and lower pendula are $\Phi_{11} = \Phi_{21} = 0.2581$ and $\Phi_{12} = \Phi_{22} = 0.4244$, respectively, whereas the numerical values are $\Phi_{11} = \Phi_{21} = 0.2522$ and $\Phi_{12} = \Phi_{22} = 0.3536$ for Fig. 3(c) and $\Phi_{12} = \Phi_{22} = 0.2579$ and $\Phi_{12} = \Phi_{22} = 0.3732$ for Fig. 3(d). In Fig. 3(a,d), one can see that the pendula do not pass through zero (the hanging down position) at the same moment of time, whereas in Fig. 3(b,c) the pendula cross this position simultaneously. The phase shift is observed only when the lower and upper pendula in each double pendulum are oscillating in-phase with non-zero damping between them.

We do not observe the configurations shown in Fig. 2(b,d) because each of the double pendulum has to reach different normal modes of oscillations for the same frequency for both of them. This is proven to be impossible in the low oscillation approximation [1] (the angular positions have to be much higher than the one considered in this paper).

The periodic solutions presented in Fig. 3(a,b,d) are stable, whereas the one from Fig. 3(c) is unstable. To show how a change in the natural frequency of the beam affects the stability of the periodic solutions obtained, we calculate one-parameter bifurcation diagrams. We choose the beam mass M as the bifurcation parameter and vary it in the range from 0.01 [kg] to 20.0 [kg]. In the case of two solutions: one in-phase (Fig. 3(b)) and one anti-phase (Fig. 3(d)), we do not observe any destabilization of periodic solutions. For the two others, we present bifurcation diagrams showing the maximum amplitudes of the beam oscillation $\max y_b$ on the vertical axes. The black and gray colors of branches correspond to stable and unstable periodic solutions. For the branch presented in Fig. 4(a), we start a continuation from the in-phase periodic solution shown in Fig. 3(a). Originally, the stable periodic orbit becomes unstable with a decreasing beam mass M in the Neimark-Sacker bifurcation for $M = 3.88$ [kg]. The Neimark-Sacker bifurcation point corresponds also to the maximum amplitude of the beam. In Fig. 4(b), we show a continuation of the

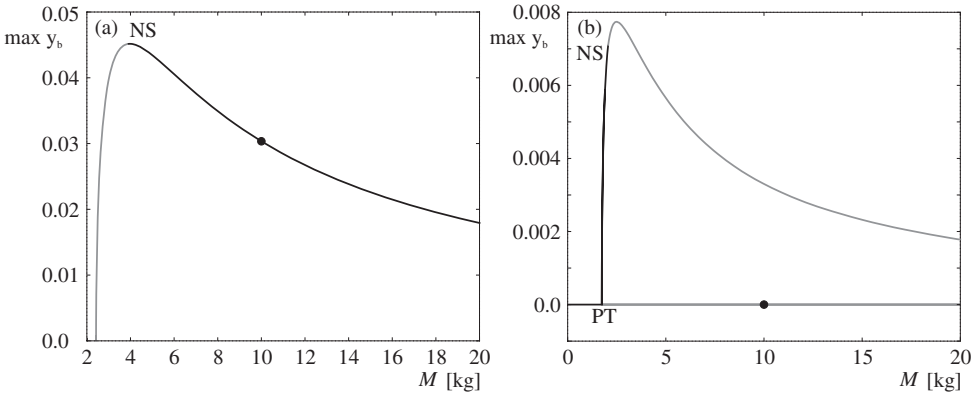

Fig. 4. One-parameter path-following of periodic solutions for the varying mass M of the beam: (a) in-phase motion from Fig. 3(a) and (b) anti-phase motion from Fig. 3(c). The black and gray lines correspond to stable and unstable periodic solutions, respectively. The abbreviation NS stands for the Neimark-Sacker bifurcation and PT denotes the pitchfork bifurcation. Bifurcations along unstable branches are neglected. The starting points of continuation are marked by black dots.

anti-phase oscillations of the pendula (Fig. 3(c)). The stabilization of this type of the periodic solution occurs in the supercritical pitchfork bifurcation (two new branches emerge) for $M = 1.737\,[\mathrm{kg}]$. In the symmetric anti-phase motion, the beam is at rest and the maximum amplitudes of the pendula remain the same. For the asymmetric periodic solutions along two overlapping branches, the beam is oscillating with a low amplitude and we observe a difference between amplitudes of the pendula. The asymmetric motion destabilizes with an increase in the beam mass M in Neimark-Sacker bifurcations for $M = 2.06\,[\mathrm{kg}]$.

4.2 Periodic solutions of the pendula with different masses – exploring symmetry

In this subsection, we investigate the stability of symmetric motion of the pendula from Fig. 3(c,d), which corresponds to anti-phase synchronization states. We decrease the masses m_{12} and m_{22} of the lower pendula in the range (0.0, 1.0] [kg]. We choose masses of the lower pendula as the bifurcation parameter because we want to avoid a situation where the lightweight upper pendula excite the much heavier lower pendula.

In Fig. 5(a,b) we present bifurcation diagrams, i.e., the maximum amplitudes of the beam (a) and the second upper pendulum (b) for decreasing masses of the lower pendula. As an initial state, we take the anti-phase periodic solution for which all pendula have identical masses (see Fig. 3(d)). For $m_{12} = m_{22} = 0.108\,[\mathrm{kg}]$, the symmetry is broken in the subcritical pitchfork bifurcation. We observe an appearance of two unstable branches which stabilize in saddle-node bifurcations for $m_{12} = m_{22} = 0.107\,[\mathrm{kg}]$, a further loss of stability occurs in the supercritical Neimark-Sacker bifurcations for $m_{12} = m_{22} = 0.105\,[\mathrm{kg}]$, hence two stable quasi-periodic solutions appear. This scenario is observed only when the system has symmetry. The bifurcation diagram for a system without symmetry ($m_{11} = 1.0\,[\mathrm{kg}]$ and $m_{12} = 0.99\,[\mathrm{kg}]$) is shown in Fig. 5(c,d). We present the maximum amplitudes of the upper pendula in the range $m_{i2} \in (0.0, 0.15]$ [kg] (for $m_{i2} \in (0.15, 1.0]$ [kg], solutions are stable). As can be easily predicted, the pitchfork bifurcation is no more present and we observe two disconnected branches of periodic solutions (the imperfect pitchfork bifurcation). As

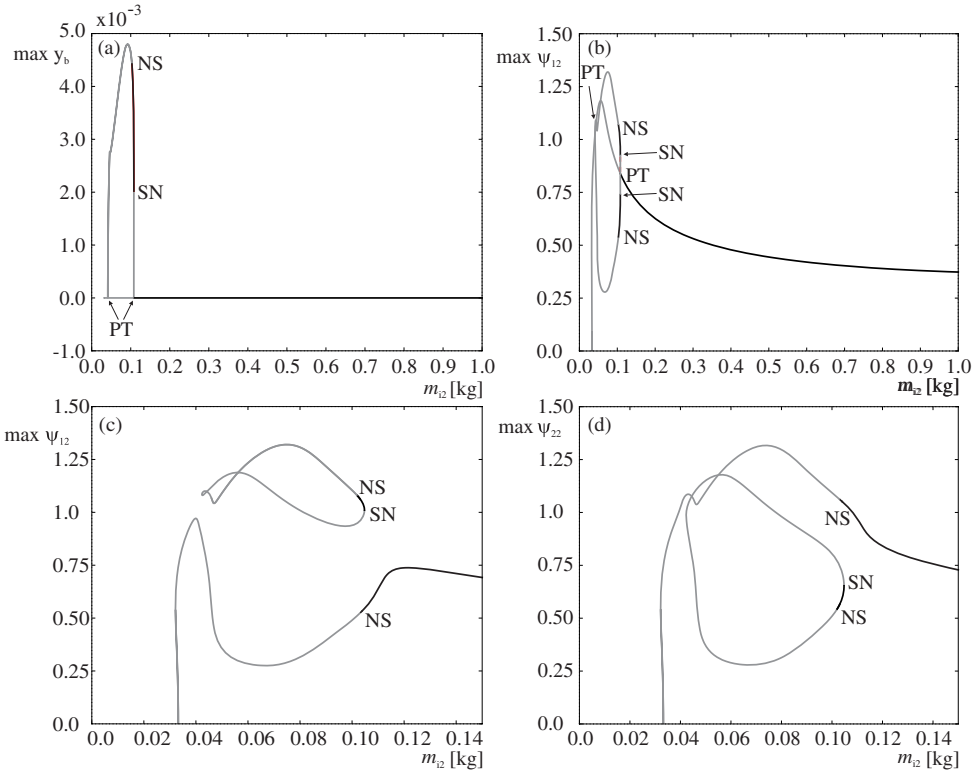

Fig. 5. In (a,b) we show one-parameter path-following of the anti-phase synchronous motion starting from the periodic solution shown in Fig. 3(d). The changes in the maximum amplitude of the beam max y_b (a) and the second upper pendulum max ψ_{12} (b) are shown for decreasing masses of the lower pendula $m_{i2} = (0.0,\ 1.0]$ [kg] $(i = 1, 2)$, whereas the upper pendula have masses equal to 1.0 [kg]. In (c,d) the same calculations are performed for asymmetrical masses of the upper pendula ($m_{11} = 1.0$ [kg] , $m_{21} = 0.99$ [kg]) in the range $m_{i2} \in (0.0,\ 0.15)$ [kg] $(i = 1, 2)$, for $m_{i2} \in (0.15,\ 1.0)$ [kg] $(i = 1, 2)$, solutions are stable. The black and gray lines correspond to stable and unstable periodic solutions, respectively. The abbreviations correspond to: PT – pitchfork bifurcation, NS – Neimark-Saker bifurcation, and SN – saddle-node bifurcation. Bifurcations along unstable branches are neglected.

one can see, the maximum amplitudes of the lower pendula start to diverge close to the destabilization and the second lower pendulum has nearly twice a higher amplitude than the first one in the Neimark-Saker bifurcation point ($m_{12} = m_{22} = 0.103$ [kg]). Close to the Neimark-Saker bifurcation located on the main branch, one can observe an appearance of the second branch which starts and disappears in saddle-node bifurcations. The stable part of this branch is bounded by the saddle-node ($m_{12} = m_{22} = 0.1019$ [kg]) and the Neimark-Sacker ($m_{12} = m_{22} = 0.1047$ [kg]) bifurcations and there is a similar difference in amplitudes between the lower and upper pendula as for the main branch. The stability range of this separated branch in the two-parameter space is studied in the next subsection.

The same analysis is performed for the periodic solution shown in Fig. 3(c), which is originally unstable. In Fig. 6(a) one can see that the maximum amplitude of the beam max y_b with decreasing masses of the lower pendula m_{12} and m_{22} remains zero (symmetry is maintained) in the whole range under consideration. For $m_{12} = m_{22} = 0.05$ [kg], we observe the subcritical pitchfork bifurcation, where symmetric solutions stabilize and stay stable nearly to $m_{12} = m_{22} \approx 0.0$ [kg]. The second

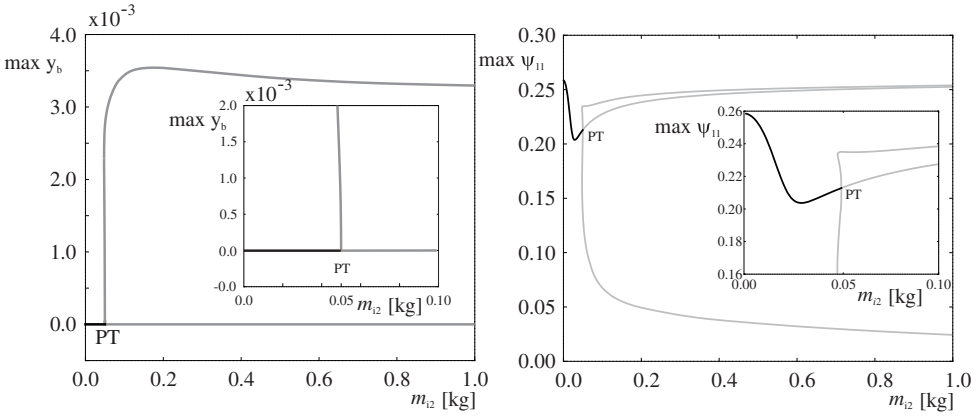

Fig. 6. One-parameter path-following of the anti-phase synchronous periodic solutions from Fig. 3(c). A change in the maximum amplitude of the beam max y_b (a) and the second upper pendulum max ψ_{12} (b) is shown for decreasing masses of the lower pendula $m_{i2} =\in (0.0,\ 1.0]$ [kg] $(i = 1, 2)$, whereas the upper pendula have masses equal to 1.0 [kg]. The black and gray lines correspond to stable and unstable periodic solutions, respectively. The abbreviation PT corresponds to the pitchfork bifurcation. Bifurcations along unstable branches are neglected.

branch corresponds to the asymmetric unstable periodic motion with low oscillations of the beam. All branches coming from the pitchfork bifurcation can be seen in Fig. 6(b), where we show the maximum amplitude of the second upper pendulum max ψ_{12}. To have a general overview, we increase the masses m_{12} and m_{22} but the stability properties do not change, hence the periodic solutions along all branches stay unstable.

4.3 Ranges of stability of synchronous solutions in the two-parameter space

In this subsection, we show how asymmetric changes of pendulum masses influence the stability of the previously present periodic solutions. In all cases we start with the pendulum configuration obtained for the identical double pendula (configurations from Fig. 3(a–d)). We change the mass of the second upper pendulum m_{21} (in different intervals for each periodic solutions) and the masses of the lower pendula $m_{12} = m_{22}$ in the interval (0.0, 1] [kg]. Our calculations are presented on the two-dimensional bifurcation diagrams (masses of the lower pendula $m_{12} = m_{22}$ versus the mass of the second upper pendulum m_{21}).

In Fig. 7(a) we show stability ranges of the configuration presented in Fig. 3(d). The solution is bounded by the Neimark-Sacker bifurcation, hence we observe an appearance of the quasi-periodic motion outside this range. The bifurcation scenario which occurs for $m_{21} = 1.0$ [kg] is different from the other ones because of the presence of symmetry. The stability at the bottom is lost not via the Neimark-Sacker but through the pitchfork bifurcation. When the symmetry is broken ($m_{21} \neq 1.0$ [kg]), the pitchfork bifurcation in no more present but there exists a disconnected stable range of periodic solutions (coming from the 'second' branch – see Fig. 5(c,d)). The area of existence of these asymmetric period solutions is presented in Fig. 7(b). As shown in Fig. 5(c,d), the stable range is bounded by the Neimark-Sacker bifurcation (from the bottom) and the saddle-node bifurcation line from the top. This area is small and when the difference of masses of the upper pendula (m_{11} and m_{21}) becomes larger than a few percent, it disappears.

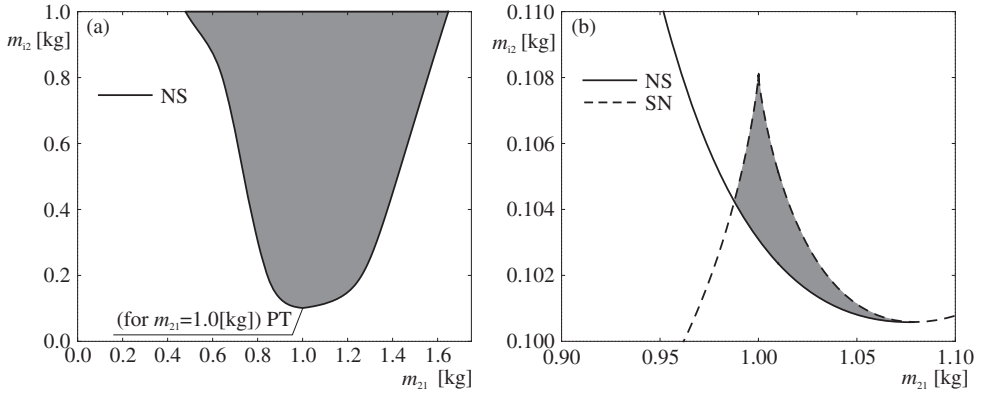

Fig. 7. In (a) two-parameter continuation of the anti-phase synchronization periodic solution (the beam is at rest - see Fig. 3(d)) for the masses m_{21} and $m_{i2} \in (0.0, 1.0]$ [kg]. The observed stable periodic solutions destabilize thought the Neimark-Sacker bifurcations. When the system is symmetric ($m_{21} = 1.0$ [kg]), the Neimark-Sacker bifurcation is interchanged by the pitchfork bifurcation. In (b) two-parameter plot for the masses m_{21} and $m_{i2} \in (0.0, 1.0]$ [kg] of the disconnected branch (see Fig. 5(c,d)). Stable periodic solutions destabilize through the Neimark-Sacker (continuous line) and saddle-node (dashed line) bifurcations. The gray shaded area corresponds to the existence of stable periodic solutions, whereas the white one to the unstable solution.

One can distinguish two types of the in-phase motion: the first one where all pendula are in-phase (Fig. 3(a)) and the second one where the upper and lower pendula are in-phase but in anti-phase to each other (Fig. 3(b)). To investigate the first type of motion, we follow the periodic solution in the two-parameter space (similarly as for the anti-phase motion). The results of calculations are presented in Fig. 8(a,b). As can be easily seen, the stable area is much larger than in the previous case. Solutions destabilize similarly in the Neimark-Sacker bifurcations, which results in an appearance of the quasi-periodic motion. For a decreasing mass m_{21}, we observe a rapid jump around $m_{21} = 0.5$ [kg] from $m_{i2} \approx 0.08$ [kg] to $m_{i2} \approx 0.7$ [kg], for an increase in m_{21}, the bound of bifurcation grows nearly linearly reaching $m_{i2} = 1.0$ [kg] for $m_{21} = 4.6$ [kg]. The zoom of the majority of the left part is presented in 8(b), where one can see that the Neimark-Sacker bifurcation line has a complex structure. The gap for m_{i2} corresponds to an appearance of the quasi-periodic motion in the Neimark-Sacker bifurcation and its disappearance in the inverse Neimark-Sacker bifurcation.

In Fig. 8(c) we present a one-parameter plot which shows a connection between the unstable anti-phase solution (Fig. 3(c)) and the stable in-phase solution (Fig. 3(b)). The starting solution is the unstable one ($m_{21} = 1.0$ [kg] and $\max y_b = 0.0$) with an increasing mass, we do not observe changes in stability – the unstable branch turns around and reaches $m_{12} \approx 0.0$ [kg]. Following the second direction results in a change of stability in the saddle-node bifurcation ($m_{21} = 0.837$ [kg]) and then destabilization in the Neimark-Sacker bifurcation ($m_{21} = 1.38$ [kg]). For $m_{21} = 1.0$ [kg], the stable solution corresponds to the solution presented in Fig. 3(b). Next, we follow the bifurcation which bounds the stable branch in the two-parameter space (m_{21} and m_{i2}), which is shown in Fig. 8(d). The stable range stays narrow up to $m_{i2} \approx 0.3$ [kg] where the Neimark-Sacker bifurcation line changes the direction and starts to go up. When the mass of the upper pendulum is large enough ($m_{21} > 11.0$ [kg]), we once again can observe a stable solution for $m_{i2} = 1.0$ [kg]. From the left-hand side, as has been mentioned before, the stable area is bounded by the saddle-node bifurcation line and is nearly a constant line around $m_{21} = 0.84$ [kg].

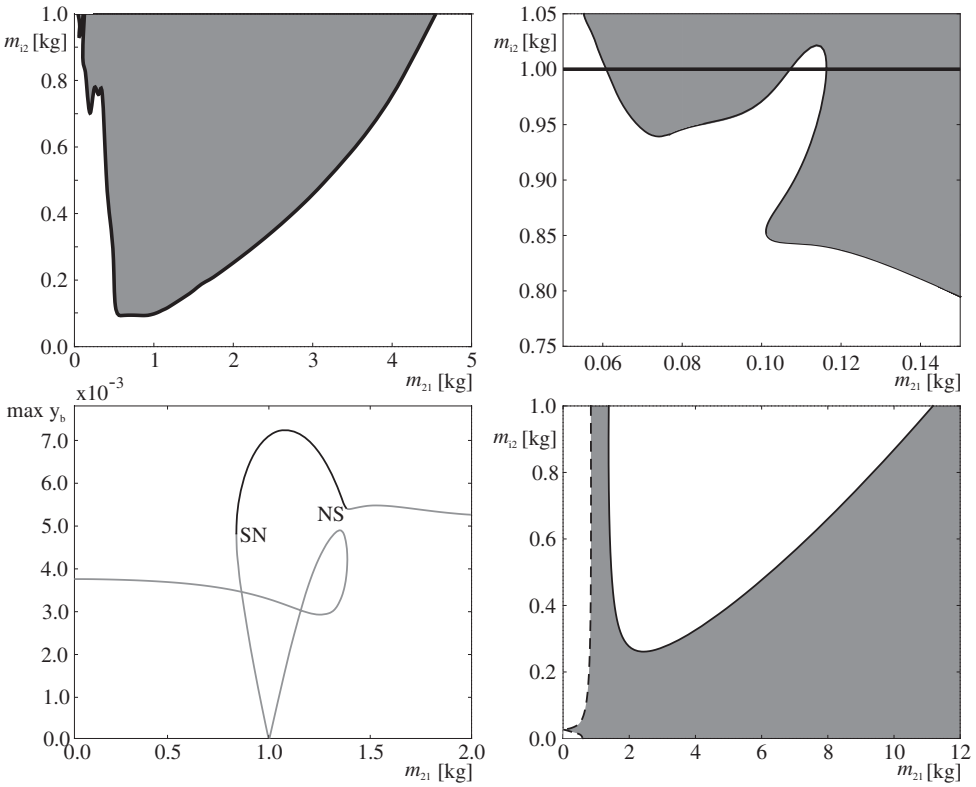

Fig. 8. In (a,b) two-parameter continuation of the in-phase synchronization periodic solution (the beam is in the anti-phase state to all pendula) for the masses m_{21} and $m_{i2} \in (0.0, 1.0]$ [kg]. The observed stable periodic solutions destabilize through the Neimark-Sacker bifurcation. In (c) one-parameter (m_{21}) plot which shows the connection between the unstable anti-phase solution (Fig. 3(c)) and the stable in-phase solution (Fig. 3(b)), where the gray and black lines correspond to stable and unstable periodic solutions. Then, in (d) two-parameter plot for the masses m_{21} and $m_{i2} \in (0.0, 1.0]$ [kg]. Stable periodic solutions destabilize through the Neimark-Sacker (continuous line) and saddle-node (dashed line) bifurcations. The gray shaded area corresponds to the existence of stable periodic solutions, whereas the white one to the unstable solution.

5 Conclusions

Our studies show that two self-excited double pendula with the van der Pol type of damping, hanging from the horizontally movable beam, can synchronize. For identical pendula, four different synchronous configurations are possible (in-phase or anti-phase), but not all of them are stable for the given parameters of the beam. When the pendula are nonidentical, i.e., have different masses, we observe synchronous states for which the phase difference between the pendula is close to 0 or π for a small parameter mismatch. With an increase in this difference, we observe a stable solution with phase shifts between 0 and π. They finally destabilize in the Neimark-Sacker saddle-node bifurcations, which results in an appearance of unsynchronized quasi-periodic oscillations or a jump to another attractor. Similar synchronous states have been observed experimentally in [28] but a special controlling procedure has been applied to stabilize them.

The observed behavior of system (1) can be explained by the energy expressions derived in Section 3, which also show why other synchronous states are not possible. We prove that the observed behavior of the system is robust as it occurs in a wide range of system parameters.

This work has been supported by the Foundation for Polish Science, Team Programme under the project TEAM/2010/5/5.

References

1. A. Andronov, A. Witt, S. Khaikin, *Theory of Oscillations* (Pergamon, Oxford 1966)
2. I.I. Blekhman, *Synchronization in Science and Technology* (ASME, New York 1988)
3. A. Pikovsky, M. Roesenblum, J. Kurths, *Synchronization: An Universal Concept in Nonlinear Sciences* (Cambridge University Press, Cambridge 2001)
4. M.P. Aghababa, H.P. Aghababa, Nonlinear Dynamics **67**, 2689 (2012)
5. M. Kapitaniak, P. Brzeski, K. Czolczynski, P. Perlikowski, A. Stefanski, T. Kapitaniak, Progress of Theoretical Physics **128**, 1141 (2012)
6. C. Huygens, 1893, Letter to de Sluse, In: Oeuveres Completes de Christian Huygens, (letters; no. 1333 of 24 February 1665, no. 1335 of 26 February 1665, no. 1345 of 6 March 1665), (Societe Hollandaise Des Sciences, Martinus Nijhoff, La Haye).
7. M. Kapitaniak, K. Czolczynski, P. Perlikowski, A. Stefanski, T. Kapitaniak, Physics Report **517**, 1 (2012)
8. M. Bennet, M.F. Schatz, H., Rockwood, K. Wiesenfeld, Proc. Roy. Soc. London A **458**, 563 (2002)
9. K. Czolczynski, P. Perlikowski, A. Stefanski, T. Kapitaniak, Prog. Theor. Phys. **122**, 1027 (2009)
10. K. Czolczynski, P. Perlikowski, A. Stefanski, T. Kapitaniak, Physica A **388**, 5013 (2009)
11. K. Czolczynski, P. Perlikowski, A. Stefanski, T. Kapitaniak, Chaos **21**, 023129 (2011)
12. R. Dilao, Chaos **19**, 023118 (2009)
13. A.L. Fradkov, B. Andrievsky, Int. J. Non-linear Mech. **42**, 895 (2007)
14. A. Yu. Kanunnikov, R.E. Lamper, J. Appl. Mech & Theor. Phys. **44**, 748 (2003)
15. J. Pantaleone, Am. J. Phys. **70**, 992 (2002)
16. P. Perlikowski, M. Kapitaniak, K. Czolczynski, A. Stefanski, T. Kapitaniak, Int. J. Bif. Chaos **22**, 1250288 (2012)
17. M. Senator, Journal Sound and Vibration, **291**, 566 (2006)
18. H. Ulrichs, A. Mann, U. Parlitz, Chaos **19**, 043120 (2009)
19. N. Rott, Z. angew. Math. Phys. **2l**, 570 (1970)
20. J. Miles, J. Appl. Math. Phys. (ZAMP) **36**, (1985)
21. A.C. Skeldon, Phys. Lett. A **166**, 224 (1992)
22. A.C. Skeldon, Physica D **75**, 541 (1994)
23. S. Samaranayake, A.K. Bajaj, Nonlinear Dynamics **4**, 605 (1993)
24. T. Morbiato, R. Vitaliani, A. Saetta, Computers & Structures **89**, 1649 (2011)
25. A.P. Willmott, J. Dapena, J. Sports Sciences **30**, 369 (2012)
26. Y. Suzukia, T. Nomuraa, M. Casadiob, P. Morassoc, J. Theor. Biol. **310**, 55 (2012)
27. K.P. Granataa, S.E. Wilsonb, Clinical Biomechanics, **16**, 650 (2001)
28. A. Fradkov, B. Andrievsky, K. Boykov, Mechatronics **15**, 1289 (2005)
29. E.J. Doedel, A.R. Champneys, T.F. Fairgrieve, Y.A. Kuznetsov, B. Sandstede, X. Wang *Auto 97: continuation and bifurcation software for ordinary differential equations* (1998)

6.2 Article 2

International Journal of Structural Stability and Dynamics
Vol. 14, No. 8 (2014) 1440028 (24 pages)

DOI: 10.1142/S0219455414400288

Dynamics of n Coupled Double Pendula Suspended to the Moving Beam

Piotr Koluda, Piotr Brzeski and Przemyslaw Perlikowski*

Lodz University of Technology, Division of Dynamics
Stefanowskiego, 1/15, Lodz, Poland
**przemyslaw.perlikowski@p.lodz.pl*

Received 7 February 2013
Accepted 2 May 2014
Published 25 July 2014

We consider the synchronization of n self-excited double pendula. For such pendula hanging on the same beam, different synchronous configurations can be obtained (in-phase and anti-phase states). An approximate analytical analysis allows to derive the synchronization condition and explain the observed types of synchronization for any number of coupled double pendula. The energy balance method is used to show how the energy between the pendula is transferred via the oscillating beam allowing their synchronization. We compute periodic solutions for $n = 2, 3, 4, 5$ coupled double pendula, based on analytical predictions. For all obtained periodic solutions, we investigate how the stability properties change with the varying natural frequency of the beam.

Keywords: Double pendula; phase synchronization; synchronization in clusters.

1. Introduction

Synchronization is common state in systems of coupled oscillators.[1–7] The interactions between connected systems often lead to oscillations where systems perform identical dynamics or oscillate with constant phase shift. The history of synchronization goes back to the 17th century. In 1673, the Dutch scientist Ch. Huygens observed the anti-phase synchronization of two pendulum clocks[8] hung on the same wall. Recently, the dynamics of coupled pendula have been the subject of investigations conducted by numerous authors.[8–17] These studies explain the phenomenon of synchronization, show its properties and give detailed explanation of interactions between single coupled pendula.

In our work, we consider an interaction between two double pendula. One of the first investigations on dynamics of the double pendulum can be found in the paper by Rott,[18] where an analytical investigation of the Hamiltonian system is presented for

*Corresponding author.

different ratios between natural frequencies of the pendula. The next results obtained by Miles[19] describe dynamics of double pendulum under parametric excitation around the 2:1 resonance. A mode interaction in the double pendulum, including a detailed bifurcation analysis near two multiple bifurcation points and a transition to quasi-periodic motion and chaos around the 2:1 parametric resonance, are presented in Refs. 20–22. Similarly, as for 2:1, the 1:1 resonance leads to dynamics that includes multiple bifurcation points, symmetry breaking points and cascades of period doubling bifurcations.[22] Double pendula can also be considered as an example of many physical systems commonly met in engineering, e.g. a model of bridge-pedestrian interactions,[23] golf or hockey swing interactions with arms,[24] human body[25] or trunk[26] models. The investigation performed for two double pendula hung on moving beam[27,28] show that in such a system we observe four types of different synchronous solutions for identical pendula. Generally speaking, such systems are globally coupled multi-dimensional networks, so one can expect a coexistence of multiple attractors of different types (periodic, quasiperiodic and chaotic), see Refs. 10, 29–31.

In this paper, we consider the synchronization of n self-excited double pendula. The oscillations of each double pendulum are self-excited by the van der Pol type of damping associated with the upper parts (upper pendula) of each double pendulum. The analytical condition which let us find the synchronous states is derived by the energy balance method. For $n = 2, 3, 4, 5$ pendula, we show possible synchronous configurations and shape of periodic solutions. Finally, the results are generalized for n coupled double pendula.

This paper is organized as follows: Section 2 describes the considered model of n coupled double pendula. In Sec. 3, we show the analytical condition which let us find synchronous states, whereas Sec. 4 presents the shape of periodic solutions, their stability changes with the change of the beam's natural frequency and generalization of obtained results for an arbitrary number of coupled double pendula. Finally, we summarize our results in Sec. 5.

2. Model of the System

The analyzed system is shown in Fig. 1. It consists of a rigid beam and n double pendula suspended on it. The beam of the mass M can move along the horizontal direction and its position is described by the coordinate x_b. The beam is connected to a linear spring with stiffness k_x and a linear damper described by the viscous damping coefficient c_x.

Each double pendulum consists of two light beams and masses mounted at their ends. The length of ith upper pendulum and ith lower pendulum is given by l_{i1} and l_{i2} $(i = 1, \ldots, n)$, respectively. Masses are concentrated at the end of ith upper and ith lower pendulum and described by m_{i1} and m_{i2}, respectively. We consider double pendula with the same lengths $l_{i1} = l_{i2} = l$ but different masses m_{i1} and m_{i2} (to maintain generality in the derivation of equations, we preserve indexes for pendula's lengths). The motion of each double pendulum is described by the angles φ_{i1}

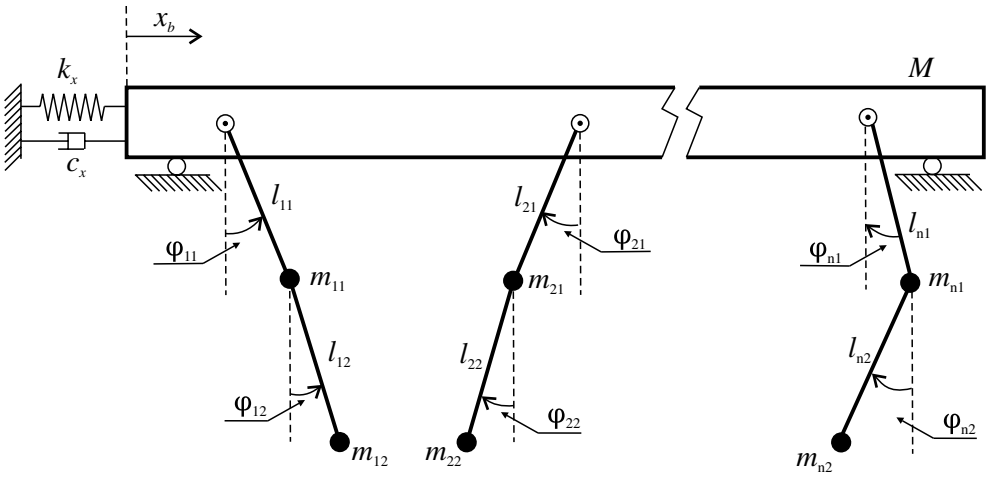

Fig. 1. Model of the system — n double pendula are mounted to the beam which can move horizontally. Each double pendulum consists of an upper pendulum of the length l_{i1} and the mass m_{i1} and a lower pendulum of the length l_{i2} and the mass m_{i2} $(i = 1, \ldots, n)$. The upper pendula are self-excited and lower pendula have damper in their pivots.

(upper pendulum) and φ_{i2} (lower pendulum). The upper pendula are self-excited by the van der Pol type of damping (not shown in Fig. 1) given by the momentum (torque) $c_{vdp}\dot{\varphi}_{1i}(1-\mu\varphi_{1i}^2)$, where c_{vdp} and μ are constant. Stable limit cycles are generated as a result of van der Pol damping.[1] The lower pendula are damped with a viscous damper with the coefficient c_{i2}. The equations of motion of the considered system are as follows:

$$\begin{aligned}
&\left(M+\sum_{i=1}^{2}\sum_{j=1}^{2}m_{ij}\right)\ddot{x}_b+\sum_{i=1}^{2}(m_{i1}+m_{i2})l_{i1}(\ddot{\varphi}_{i1}\cos\varphi_{i1}-\dot{\varphi}_{i1}^2\sin\varphi_{i1})\\
&\qquad+\sum_{i=1}^{2}m_{i2}l_{i2}(\ddot{\varphi}_{i2}\cos\varphi_{i2}-\dot{\varphi}_{i2}^2\sin\varphi_{i2})+k_x x_b+c_x\dot{x}_b=0,\\
&(m_{i1}+m_{i2})l_{i1}\ddot{x}_b\cos\varphi_{i1}+(m_{i1}+m_{i2})l_{i1}^2\ddot{\varphi}_{i1}\\
&\qquad+m_{i2}l_{i1}l_{i2}\ddot{\varphi}_{i2}\cos(\varphi_{i1}-\varphi_{i2})+m_{i2}l_{i1}l_{i2}\dot{\varphi}_{i2}^2\sin(\varphi_{i1}-\varphi_{i2})\\
&\qquad+(m_{i1}+m_{i2})l_{i1}g\sin(\varphi_{i1})+c_{vdp}(1-\mu\varphi_{i1}^2)\dot{\varphi}_{i1}+c_{i2}(\dot{\varphi}_{i2}-\dot{\varphi}_{i1})=0,\\
&m_{i2}l_{i2}\ddot{x}_b\cos\varphi_{i2}+m_{i2}l_{i1}l_{i2}\ddot{\varphi}_{i1}\cos(\varphi_{i1}-\varphi_{i2})+m_{i2}l_{i2}^2\ddot{\varphi}_{i2}\\
&\qquad-m_{i2}l_{i1}l_{i2}\dot{\varphi}_{i1}^2\sin(\varphi_{i1}-\varphi_{i2})+m_{i2}l_{i2}g\sin(\varphi_{i2})-c_{i2}(\dot{\varphi}_{i2}-\dot{\varphi}_{i1})=0,
\end{aligned}\tag{2.1}$$

where $i = 1, \ldots, n$. Introducing the dimensionless time $\tau = \omega t$, where $\omega^2 = \frac{g}{l_{11}}$ is the natural frequency of the upper pendula, we can rewrite Eq. (2.1) in the dimensionless form as:

$$\begin{aligned}
&\ddot{y}_b+\sum_{i=1}^{2}\mathbf{A}_{i1}(\ddot{\psi}_{i1}\cos\psi_{i1}-\dot{\psi}_{i1}^2\sin\psi_{i1})\\
&\qquad+\sum_{i=1}^{2}\mathbf{A}_{i2}(\ddot{\psi}_{i2}\cos\psi_{i2}-\dot{\psi}_{i2}^2\sin\psi_{i2})+\mathbf{K}y_b+\mathbf{C}\dot{y}_b=0,
\end{aligned}\tag{2.2}$$

$$\delta_{i1}\ddot{y}_b\cos\psi_{i1}+\mathbf{L}_{i1}\ddot{\psi}_{i1}+\mathbf{L}_{i3}\ddot{\psi}_{i2}\cos(\psi_{i1}-\psi_{i2})$$
$$=-\mathbf{L}_{i3}\dot{\psi}_{i2}^2\sin(\psi_{i1}-\psi_{i2})-\mathbf{G}_{i1}\sin(\psi_{i1})-\mathbf{C}_{vdp}(1-\mu\psi_{i1}^2)\dot{\psi}_{i1}$$
$$-\ \mathbf{C}_{i2}(\dot{\psi}_{i2}-\dot{\psi}_{i1}), \tag{2.3}$$

$$\delta_{i2}\ddot{y}_b\cos\psi_{i2}+\mathbf{L}_{i3}\ddot{\psi}_{i1}\cos(\psi_{i1}-\psi_{i2})+\mathbf{L}_{i2}\ddot{\psi}_{i2}$$
$$=\mathbf{L}_{i3}\dot{\psi}_{i1}^2\sin(\psi_{i1}-\psi_{i2})-\mathbf{G}_{i2}\sin(\psi_{i2})+\mathbf{C}_{i2}(\dot{\psi}_{i2}-\dot{\psi}_{i1}), \tag{2.4}$$

where

$$\mathbf{A}_{i1}=\frac{(m_{i1}+m_{i2})l_{i1}}{Ml_b},\quad \mathbf{A}_{i2}=\frac{m_{i2}l_{i2}}{Ml_b},\quad \mathbf{K}=\frac{k_x}{M\omega^2},\quad \mathbf{C}=\frac{c_x}{M\omega},$$

$$\delta_{i1}=\frac{(m_{i1}+m_{i2})l_{i1}}{Ml_{12}},\quad \delta_{i2}=\frac{m_{i2}l_{i2}}{Ml_{12}},\quad \mathbf{L}_{i1}=\frac{(m_{i1}+m_{i2})l_{i1}^2}{l_{12}l_bM},$$

$$\mathbf{L}_{i2}=\frac{m_{i2}l_{i2}^2}{l_{12}l_bM},\quad \mathbf{L}_{i3}=\frac{m_{i2}l_{i2}l_{i1}}{l_bMl_{12}},\quad \mathbf{G}_{i1}=\frac{(m_{i1}+m_{i2})l_{i1}g}{l_{12}\omega^2l_bM},$$

$$\mathbf{G}_{i2}=\frac{m_{i2}l_{i2}g}{l_{12}\omega^2l_bM},\quad \mathbf{C}_{vdp}=\frac{c_{vdp}}{\omega l_bMl_{12}}\quad\text{and}\quad \mathbf{C}_{i2}=\frac{c_{i2}}{l_{12}\omega l_bM}.$$

3. Synchronization Condition

3.1. *Synchronization condition for coupled double pendula*

In this section, we show an analytical condition for synchronous solutions of coupled double pendula (detailed analysis of two coupled double pendula is presented in Ref. 28). The derivation of synchronization condition is shown in Appendix A. In our analytical calculations, we assume that pendula have identical masses and lengths, i.e. $m_{i1}=m_{i2}=1.0\,\mathrm{kg}$ and $l_{i1}=l_{i2}=0.2485\,\mathrm{m}$ (for $i=1,\ldots,n$). The analytical condition is derived assuming that in synchronous state beam is at rest. The only exception is the case where upper and lower pendula are synchronized in phase (the upper and lower pendulum can be either in phase or in anti-phase to each other). For n coupled double pendula, the synchronization condition has the following form (see Eq. (A.39) in Appendix A):

$$\begin{aligned}
&\sin(\beta_{21}-\beta_{11})+\sin(\beta_{31}-\beta_{11})+\cdots+\sin(\beta_{i1}-\beta_{11})=0\\
&\sin(\beta_{11}-\beta_{21})+\sin(\beta_{31}-\beta_{21})+\cdots+\sin(\beta_{i1}-\beta_{21})=0\\
&\qquad\qquad\vdots\qquad\qquad\qquad\qquad\vdots\\
&\sin(\beta_{11}-\beta_{i1})+\sin(\beta_{21}-\beta_{i1})+\cdots+\sin(\beta_{i-1\,1}-\beta_{i1})=0
\end{aligned} \tag{3.1}$$

for $i = 1, \ldots, n$. This condition can be simplified using trigonometric identity: $\sin(\alpha_1 - \alpha_2) = \sin\alpha_1 \cos\alpha_2 - \cos\alpha_1 \sin\alpha_2$:

$$\begin{aligned}
&\cos\beta_{11}\left(\sum_{k=1}^{k=n}\sin\beta_{k1} - \sin\beta_{11}\right) - \sin\beta_{11}\left(\sum_{k=1}^{k=n}\cos\beta_{k1} - \cos\beta_{11}\right) = 0\\
&\cos\beta_{21}\left(\sum_{k=1}^{k=n}\sin\beta_{k1} - \sin\beta_{21}\right) - \sin\beta_{21}\left(\sum_{k=1}^{k=n}\cos\beta_{k1} - \cos\beta_{21}\right) = 0\\
&\qquad\qquad\vdots \qquad\qquad\qquad\qquad\qquad\qquad\vdots\\
&\cos\beta_{n1}\left(\sum_{k=1}^{k=n}\sin\beta_{k1} - \sin\beta_{n1}\right) - \sin\beta_{n1}\left(\sum_{k=1}^{k=n}\cos\beta_{k1} - \cos\beta_{n1}\right) = 0.
\end{aligned} \tag{3.2}$$

For $n = 2$, condition (3.2) has only two solutions: $\beta_{11} = \beta_{21} = 0 \vee \beta_{11} = 0 \wedge \beta_{21} = \pi$, i.e. upper pendula are in phase or anti-phase synchronization, the lower pendula can be in both cases in-phase or in anti-phase to upper pendula (see Figs. 2(a) and 2(b)).

For $n = 3$, Eq. (3.2) take the form:

$$\begin{aligned}
&\cos\beta_{11}(\sin\beta_{21} + \sin\beta_{31}) - \sin\beta_{11}(\cos\beta_{21} + \cos\beta_{31}) = 0,\\
&\cos\beta_{21}(\sin\beta_{11} + \sin\beta_{31}) - \sin\beta_{21}(\cos\beta_{11} + \cos\beta_{31}) = 0,\\
&\cos\beta_{31}(\sin\beta_{11} + \sin\beta_{21}) - \sin\beta_{31}(\cos\beta_{11} + \cos\beta_{21}) = 0.
\end{aligned}$$

Therefore, the possible solutions are as follows: $\beta_{11} = 0 \wedge \beta_{21} = \frac{2\pi}{3} \wedge \beta_{31} = \frac{4\pi}{3}$ or $\beta_{11} = \beta_{21} = \beta_{31}$. Hence, four different configurations, that are presented in Figs. 2(c)–2(f), can appear.

For $n = 4$, system (3.2) takes the form:

$$\begin{aligned}
&\cos\beta_{11}(\sin\beta_{21} + \sin\beta_{31} + \sin\beta_{41}) - \sin\beta_{11}(\cos\beta_{21} + \cos\beta_{31} + \cos\beta_{41}) = 0,\\
&\cos\beta_{21}(\sin\beta_{11} + \sin\beta_{31} + \sin\beta_{41}) - \sin\beta_{21}(\cos\beta_{11} + \cos\beta_{31} + \cos\beta_{41}) = 0,\\
&\cos\beta_{31}(\sin\beta_{11} + \sin\beta_{21} + \sin\beta_{41}) - \sin\beta_{31}(\cos\beta_{11} + \cos\beta_{21} + \cos\beta_{41}) = 0,\\
&\cos\beta_{41}(\sin\beta_{11} + \sin\beta_{21} + \sin\beta_{31}) - \sin\beta_{41}(\cos\beta_{11} + \cos\beta_{21} + \cos\beta_{31}) = 0.
\end{aligned}$$

Its solutions give us the following phase shifts: $\beta_{11} = \beta_{21} = 0 \wedge \beta_{31} = \beta_{41} = \pi$ or $\beta_{11} = \beta_{21} = \beta_{31} = \beta_{41}$. The lower pendula can be in phase or in anti-phase to the upper pendula. The possible configurations are shown in Figs. 2(g)–2(j). In case when the number of pendula is greater than four, even one can even observe the anti-phase synchronization in pairs. In each pair, because of the anti-phase motion, forces acting on the beam cancel themselves, hence the beam stays at rest. There is no assumption on the phase shift between pairs of double pendula, hence it can be any number from 0 to 2π.

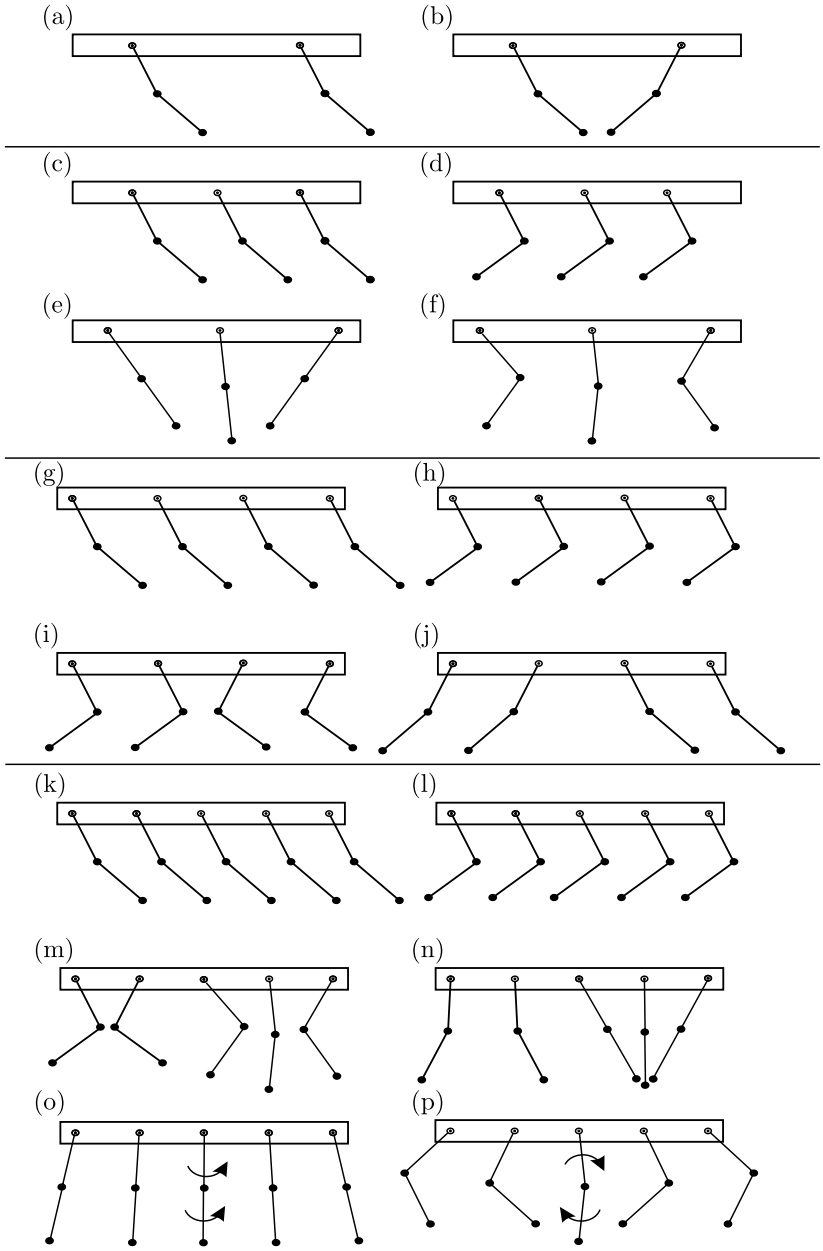

Fig. 2. Synchronous states of the system (2.2)–(2.4): (a), (b) for $n = 2$ coupled double pendula: (a) upper and lower pendula in phase: $\beta_{11} = \beta_{21}$ and $\beta_{12} = \beta_{22}$, (b) upper and lower pendula in anti-phase: $\beta_{11} = -\beta_{21}$ and $\beta_{12} = -\beta_{22}$; (c)–(f) for $n = 3$ coupled double pendula: (c), (d) upper and lower pendula in phase: $\beta_{11} = \beta_{21} = \beta_{31}$ and $\beta_{12} = \beta_{22} = \beta_{32}$, (e), (f) upper and lower pendula shifted by $\frac{2\pi}{3}$: $\beta_{11} = 0 \wedge \beta_{21} = \frac{2\pi}{3} \wedge \beta_{31} = \frac{4\pi}{3}$ and $\beta_{12} = 0 \wedge \beta_{22} = \frac{2\pi}{3} \wedge \beta_{32} = \frac{4\pi}{3}$; (g)–(j) for $n = 4$ coupled double pendula: (g), (h) upper and lower pendula in phase: $\beta_{11} = \beta_{21} = \beta_{31} = \beta_{41}$ and $\beta_{12} = \beta_{22} = \beta_{32} = \beta_{42}$, (i), (j) upper and lower pendula in anti-phase in pairs: $\beta_{11} = -\beta_{31}$, $\beta_{21} = -\beta_{41}$ and $\beta_{12} = -\beta_{32}$, $\beta_{22} = -\beta_{42}$; (k)–(p) for $n = 5$ coupled double pendula: (k), (l) upper and lower pendula in phase: $\beta_{11} = \beta_{21} = \beta_{31} = \beta_{41} = \beta_{51}$ and $\beta_{12} = \beta_{22} = \beta_{32} = \beta_{42} = \beta_{52}$, (m), (n) upper and lower pendula synchronized in phase in two anti-phase clusters, (o), (p) upper and lower pendula shifted by $\frac{2\pi}{5}$: $\beta_{11} = 0 \wedge \beta_{21} = \frac{2\pi}{5} \wedge \beta_{31} = \frac{4\pi}{5} \wedge \beta_{41} = \frac{6\pi}{5} \wedge \beta_{51} = \frac{8\pi}{5}$ and $\beta_{12} = 0 \wedge \beta_{22} = \frac{2\pi}{5} \wedge \beta_{32} = \frac{4\pi}{5} \wedge \beta_{42} = \frac{6\pi}{5} \wedge \beta_{52} = \frac{8\pi}{5}$.

For $n = 5$, system (3.2) has the following solution:

$$\begin{aligned}
&\cos\beta_{11}(\sin\beta_{21} + \sin\beta_{31} + \sin\beta_{41} + \sin\beta_{51}) \\
&\quad - \sin\beta_{11}(\cos\beta_{21} + \cos\beta_{31} + \cos\beta_{41} + \cos\beta_{51}) = 0, \\
&\cos\beta_{21}(\sin\beta_{11} + \sin\beta_{31} + \sin\beta_{41} + \sin\beta_{51}) \\
&\quad + \sin\beta_{21}(\cos\beta_{11} + \cos\beta_{31} + \cos\beta_{41} + \cos\beta_{51}) = 0, \\
&\cos\beta_{31}(\sin\beta_{11} + \sin\beta_{21} + \sin\beta_{41} + \sin\beta_{51}) \\
&\quad - \sin\beta_{31}(\cos\beta_{11} + \cos\beta_{21} + \cos\beta_{41} + \cos\beta_{51}) = 0, \\
&\cos\beta_{41}(\sin\beta_{11} + \sin\beta_{21} + \sin\beta_{31} + \sin\beta_{51}) \\
&\quad - \sin\beta_{41}(\cos\beta_{11} + \cos\beta_{21} + \cos\beta_{31} + \cos\beta_{51}) = 0, \\
&\cos\beta_{51}(\sin\beta_{11} + \sin\beta_{21} + \sin\beta_{31} + \sin\beta_{41}) \\
&\quad - \sin\beta_{51}(\cos\beta_{11} + \cos\beta_{21} + \cos\beta_{31} + \cos\beta_{41}) = 0.
\end{aligned}$$

Hence, the synchronization condition takes the form: $\beta_{11} = 0 \wedge \sin\beta_{21} + \sin\beta_{31} + \sin\beta_{41} + \sin\beta_{51} = 0$. That implies the flowing solutions: $\beta_{21} = 0 \wedge \beta_{31} = 0 \wedge \beta_{41} = 0 \wedge \beta_{51} = 0$ or $\beta_{11} = 0 \wedge \beta_{21} = \frac{2}{5}\pi \wedge \beta_{31} = \frac{4}{5}\pi \wedge \beta_{41} = \frac{6}{5}\pi \wedge \beta_{51} = \frac{8}{5}\pi$ or combinations when two double pendula are in anti-phase synchronization and three are shifted by $2\pi/3$ (see phase shifted state of three coupled double pendula). All described configuration are presented in Figs. 2(k)–2(p).

3.2. *Synchronization condition for n number of coupled pendula*

According to detailed analysis of synchronization in system of $n = 2, 3, 4, 5$ coupled double pendula we can generalize obtained results for an arbitrary number n of systems. Despite the value of n we can observe the state where all double pendula are synchronized in phase which means that all upper and similarly all lower pendula are completely synchronized. They act on the beam causing its oscillations. Considering other possible configurations we have to recall our assumptions which are used to derive the analytical condition of synchronization: the beam is at rest and double pendula perform harmonic motion. As it is shown in Figs. 2(m) and 2(n) double pendula can group in clusters. The minimum number of double pendula in cluster is two because for two and more double pendula in cluster, forces acting on beam vanish. As clusters are not acting on one another via the beam, the phase shift between clusters can be an arbitrary number from 0 to 2π. The number of double pendula in each cluster is a prime number because any other number can be expressed as a sum of prime numbers.[34] The phase shift between double pendula in cluster is $2\pi/n_1$, where n_1 is a number of double pendula in the cluster (n_1 is a prime number). For example, for $n = 11$, we can observe the following numbers of double pendula in clusters: $(3, 2, 2, 2, 2)$ or $(3, 3, 3, 2)$ or $(5, 3, 3)$ or $(5, 2, 2, 2)$ or $(7, 2, 2)$ or (11). Note that $(9, 2)$ is not a possible solution — the cluster of nine double pendula

can be created from three clusters with three pendula shifted by $2\pi/3$. The formula which let us calculate the number of possible configurations is complex,[34] hence it is better to base on an algorithm (see Appendix B) which gives us explicit results (number of clusters and number of double pendula in each cluster). As soon as we do not consider a large n, the time of calculation is short. The number of possible clusters grows much faster than the number n of double pendula (the tendency is close to exponential), e.g. for $n = 10$ (5 clusters), $n = 30$ (98 clusters), $n = 60$ (2198 clusters), $n = 90$ (38,257 clusters), $n = 120$ (145,627 clusters). Additionally, when number of double pendula is a prime number we have a case where double pendula are equally distributed with phase shift $2\pi/n$, so for our example with $n = 11$ double pendula we observe a seventh possible configuration. When number of double pendula is not a prime number such configuration can only be created from other clusters with properly chosen phase shifts between clusters, e.g. for eight double pendula, configuration consists of four clusters each with two pendula $(2, 2, 2, 2)$ with exactly $\pi/4$ phase shift between clusters give equally distributed eight double pendula. Moreover, for all mentioned above types of synchronization in each double pendulum the upper and lower pendulum can be synchronized in phase or anti-phase, hence the number of possible synchronous states is two times bigger than the number of possible clusters.

4. Numerical Results

In this section, we show the shapes of possible periodic solutions and analyze their stability. Numerical calculations are performed using the Auto 07p[32] continuation toolbox. Auto07p lets us obtain periodic solutions of the system independently on their stability. To start continuation we need to have periodic solutions, hence each periodic solution is firstly calculated by numerical integration using the fourth-order Runge–Kutta method and then corrected by applying Newton–Raphson scheme in Auto07p. In our numerical studies, we use the following parameters of Eqs. (2.2)–(2.4): $m_{i1} = m_{i2} = 1.0\,\mathrm{kg}$, $M = 10.0\,\mathrm{kg}$, $l_{i1} = l_{i2} = 0.2485\,\mathrm{m}$, $k_x = 4.0\,\mathrm{N/m}$, $c_x = 1.53\,\mathrm{Ns/m}$, $c_{vdp} = -0.1\,\mathrm{Ns/m}$, $\mu = 60.0\,\mathrm{m}^{-2}$, $c_{i2} = 0.0016\,\mathrm{Ns/m}$, which yield the following dimensionless coefficients: for $n = 3$: $\mathbf{A}_{i1} = 0.031063$, $\mathbf{A}_{i2} = 0.015531$, $\delta_{i1} = 0.125000$, $\delta_{i2} = 0.062500$, $\mathbf{L}_{i1} = 0.031063$, $\mathbf{L}_{i2} = 0.015531$, $\mathbf{L}_{i3} = 0.015531$, $\mathbf{G}_{i1} = 0.031063$, $\mathbf{G}_{i2} = 0.015531$, $\mathbf{C}_{vdp} = -0.004003$, $\mathbf{C}_{i2} = 0.000063$, $\mathbf{C} = 0.015219$, $\mathbf{K} = 0.00633$; for $n = 4$: $\mathbf{A}_{i1} = 0.027311$, $\mathbf{A}_{i2} = 0.013806$, $\delta_{i1} = 0.111111$, $\delta_{i2} = 0.055556$, $\mathbf{L}_{i1} = 0.027611$, $\mathbf{L}_{i2} = 0.013806$, $\mathbf{L}_{i3} = 0.013806$, $\mathbf{G}_{i1} = 0.027611$, $\mathbf{G}_{i2} = 0.013806$, $\mathbf{C}_{vdp} = -0.003558$, $\mathbf{C}_{i2} = 0.000056$, $\mathbf{C} = 0.013528$, $\mathbf{K} = 0.005629$; and for $n = 5$: $\mathbf{A}_{i1} = 0.024850$, $\mathbf{A}_{i2} = 0.012425$, $\delta_{i1} = 0.100000$, $\delta_{i2} = 0.05000$, $\mathbf{L}_{i1} = 0.024850$, $\mathbf{L}_{i2} = 0.012425$, $\mathbf{L}_{i3} = 0.012425$, $\mathbf{G}_{i1} = 0.024850$, $\mathbf{G}_{i2} = 0.012425$, $\mathbf{C}_{vdp} = -0.003202$, $\mathbf{C}_{i2} = 0.000050$, $\mathbf{C} = 0.012176$, $\mathbf{K} = 0.005066$ $(i = 1, \ldots, n)$. Our bifurcation parameter is the mass M of the beam. To hold an intuitive physical interpretation, we change dimensional mass, but all the calculations are performed for dimensionless equations.

4.1. *Shape of periodic solutions*

The shapes of periodic solutions of two self-excited double-pendula and detailed analysis of their stability are presented in our previous paper,[28] hence we do not present the results here. Shapes of periodic solutions for four coupled double pendula are nearly the same as for two coupled double pendula (periods are slightly different because of different ratio between mass of the beam and masses of the pendula).

In Fig. 3, we show shapes of four different periodic solutions for three coupled double pendula. In Fig. 3(a), one can observe a case where all pendula are synchronized in-phase, while beam is moving in anti-phase to them. Hence, the time traces of two lower and two upper pendula overlap. In Fig. 3(b), the upper and lower

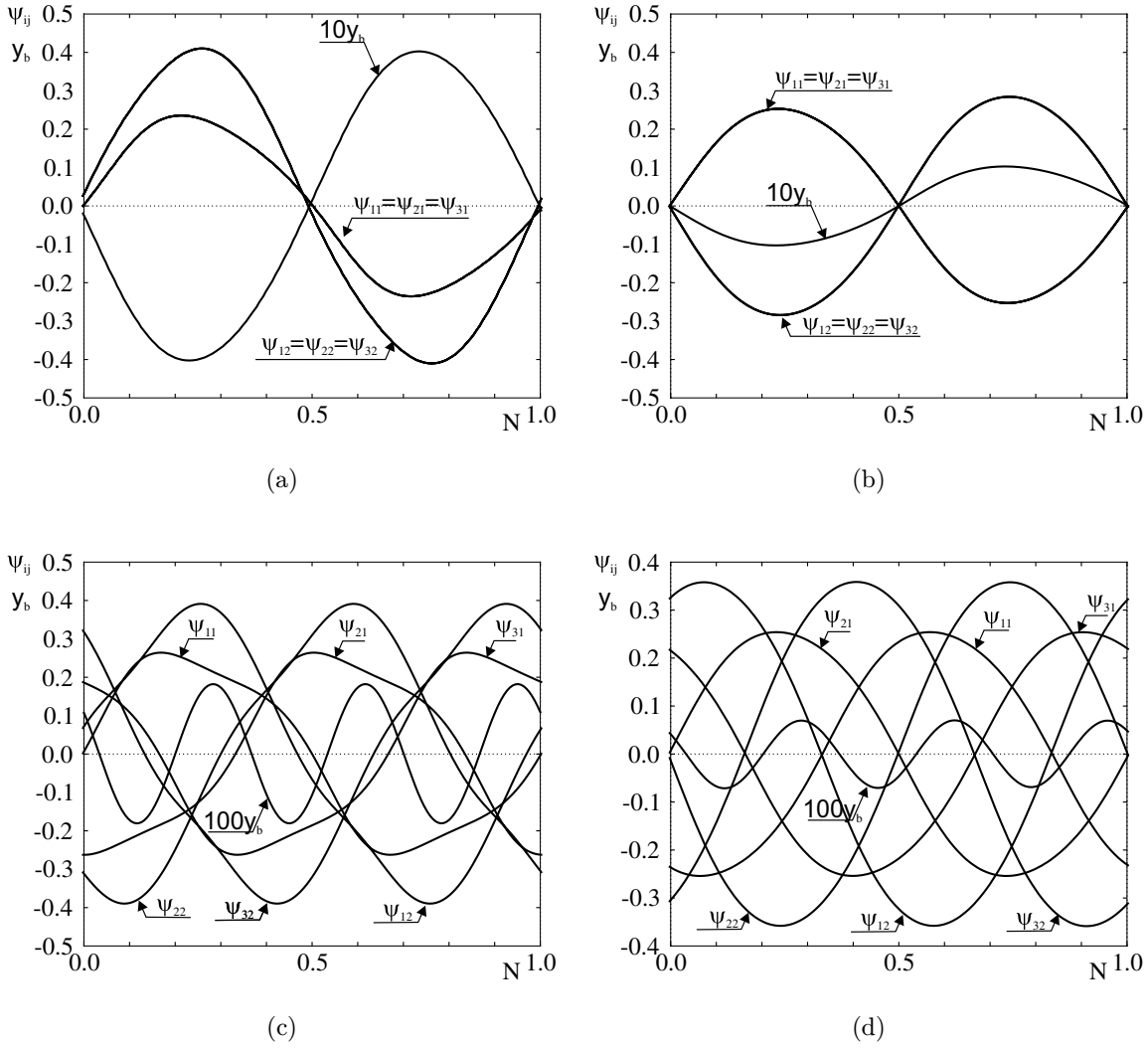

Fig. 3. Pendula and beam displacements for one period of motion ($N = 1$) for four different periodic solutions assuming identical masses of the $n = 3$ coupled double pendula: $m_{i1} = m_{i2} = 1.0\,\mathrm{kg}$ ($i = 1, \ldots, n$). The displacement y_b of the beam is shown 10 or 100 times magnified. (a) pendula configuration from Fig. 2(c) with the period $T = 6.89$, (b) pendula configuration from Fig. 2(d) with the period $T = 3.53$, (c) pendula configuration from Fig. 2(e) with the period $T = 8.28$, and (d) pendula configuration from Fig. 2(f) with the period $T = 3.77$.

pendula are in anti-phase and the beam is moving is in phase with lower pendula. The next synchronous state is observed when pendula are shifted by $2\pi/3$, where we also observe two cases presented in Fig. 3(c) (upper and lower pendula are in-phase) and in Fig. 3(d) (upper and lower pendula are in anti-phase). One can see that the period of the beam is three times shorter than the period of the pendula, hence the beam performs three full periods of motion every one period of the whole system. It is worth to notice, that contrary to even number of double pendula case, for odd number of double pendula the beam is always oscillating. For equally phase shifted double pendula (by $2\pi/3$), the amplitude of the beam is approximately 10 times smaller than for in phase synchronization. The oscillation of the beam for phase shifted cases is observed because periodic solutions of each pendulum is not

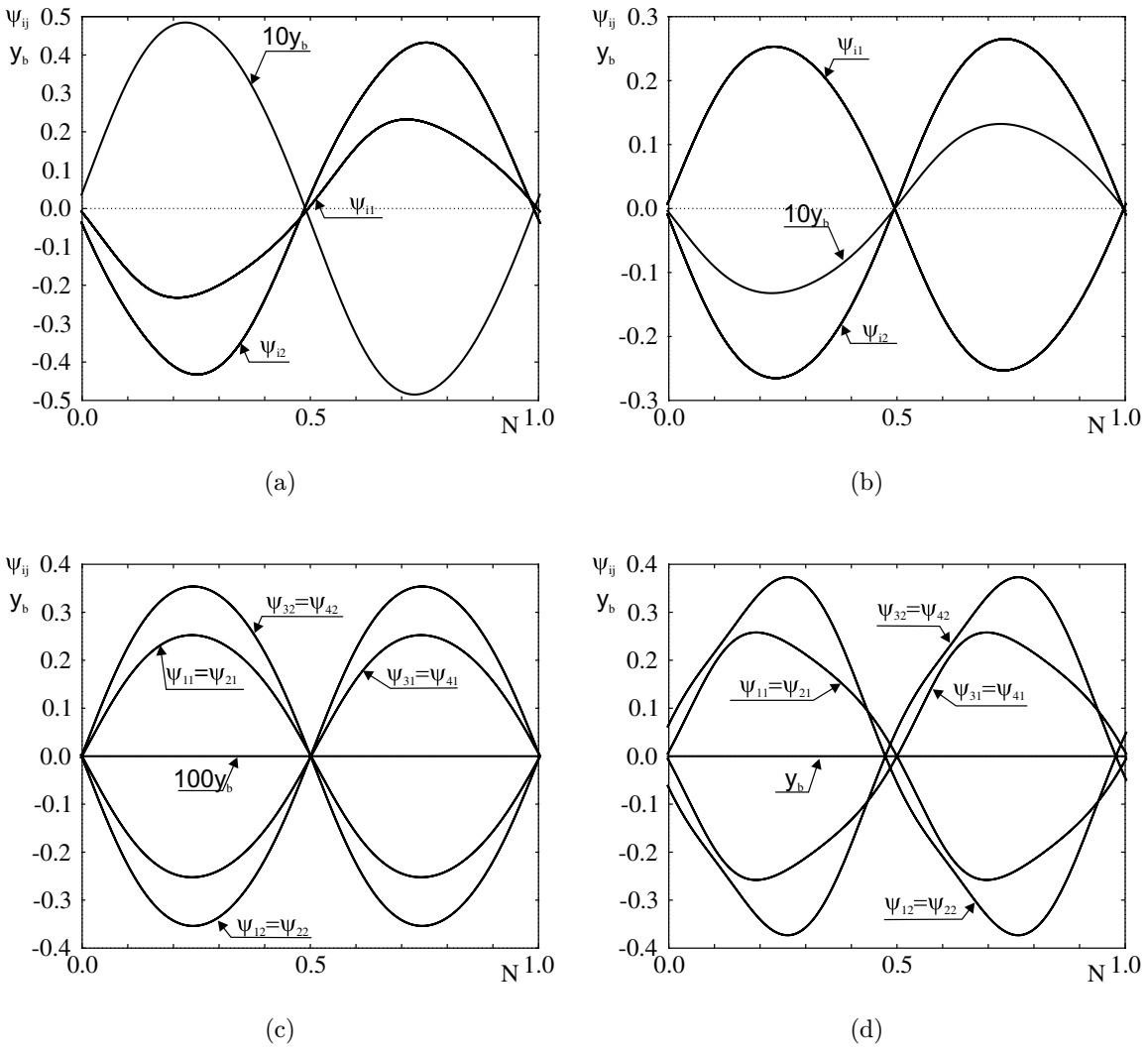

Fig. 4. Pendula and beam displacements for one period of motion ($N = 1$) for four different periodic solutions assuming identical masses of the $n = 4$ coupled double pendula: $m_{i1} = m_{i2} = 1.0\,\mathrm{kg}$ ($i = 1, \ldots, n$). The displacement y_b of the beam M is shown 10 or 100 times magnified. (a) pendula configuration from Fig. 2(g) with the period $T = 6.65$, (b) pendula configuration from Fig. 2(h) with the period $T = 3.48$, (c) pendula configuration from Fig. 2(i) with the period $T = 3.75$, and (d) pendula configuration from Fig. 2(j) with the period $T = 8.22$.

harmonic, hence the reacting forces acting on the beam do not vanish. This property is visible in Fig. 3(d) where solutions are closer to harmonic ones than in Fig. 3(c), resulting in twice smaller amplitude of the beam.

The shapes of synchronous periodic solutions for $n = 4$ coupled double pendula are presented in Fig. 4. As we mention before they are nearly the same as for two coupled double pendula (see Ref. 28). In Figs. 4(a) and 4(b) we show in-phase motion of double pendula — in Fig. 4(a) the pendula in each double pendulum are in-phase while in Fig. 4(b) they are in anti-phase. As always, for this type of synchronous motion the beam is oscillating. In Figs. 4(c) and 4(d) double pendula are grouped in two pairs (in each pair there are two anti-phase synchronized double

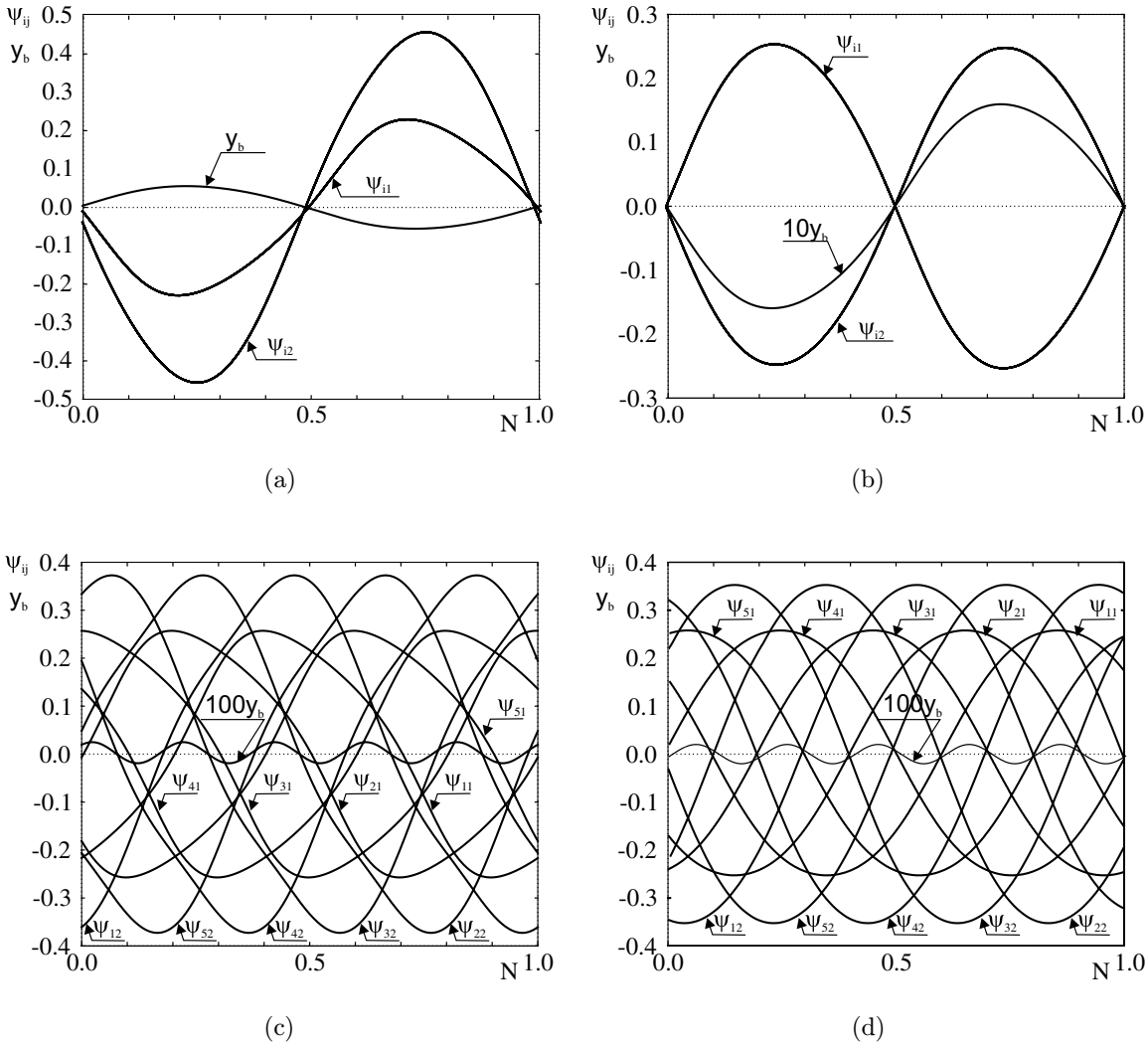

Fig. 5. Pendula and beam displacements for one period of motion ($N = 1$) for four different periodic solutions assuming identical masses of the $n = 5$ coupled double pendula: $m_{i1} = m_{i2} = 1.0\,\mathrm{kg}$ ($i = 1, \ldots, n$). The displacement y_b of the beam M is in (b)–(d) magnified. (a) pendula configuration from Fig. 2(k) with the period $T = 6.44$, (b) pendula configuration from Fig. 2(l) with the period $T = 3.42$, (c) pendula configuration from Fig. 2(m) with the period $T = 3.77$, (d) pendula configuration from Fig. 2(n) with the period $T = 8.25$, (e) pendula configuration from Fig. 2(o) with the period $T = 8.25$ and (f) pendula configuration from Fig. 2(p) with the period $T = 3.83$.

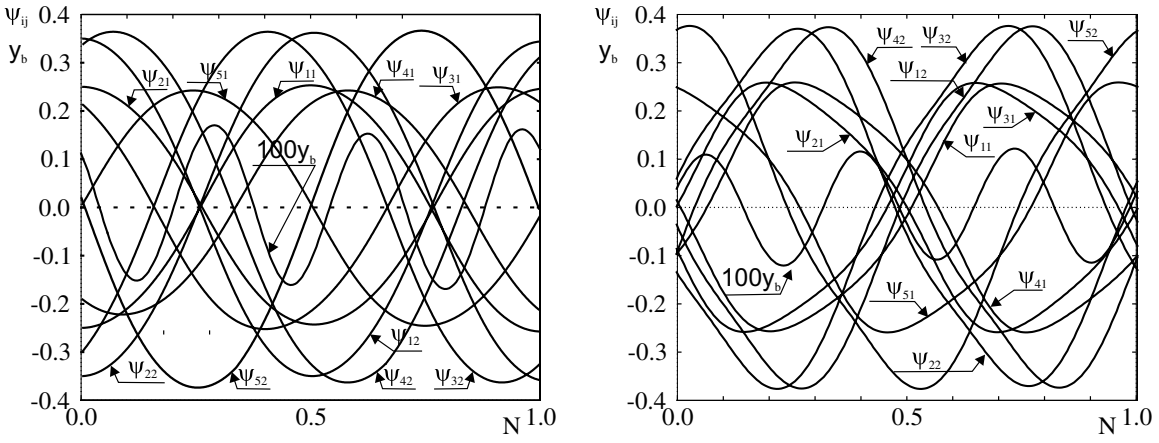

Fig. 5. (*Continued*)

pendula). Generally, there is no assumption on phase shift between pairs — it can be an arbitrary phase angle form 0 to 2π, because the reacting forces that act on the beam annul themselves in each pair. This implies that for even number of double pendula ($n \geq 4$) we observe infinite number of possible synchronous configurations.

For $n = 5$, we obtain six possible synchronous states which are shown in Fig. 5. In Figs. 5(a) and 5(b) we show the in-phase synchronization of double pendula — in Fig. 5(a) the pendula in each double pendulum are in phase while in Fig. 5(b) they are in anti-phase. One can see that when the mass M of the beam is constant the increase of the number of double pendula results in the growth of the beam and pendula amplitudes. By changing the mass M of the beam, one can obtain the same amplitude of system's motion for any number of coupled pendula.

In Fig. 5(c), we show the solution where pendula are equally distributed in phase space (shifted by $2\pi/5$) and in each double pendulum we observe in-phase synchronization between upper and lower pendula. The second configuration of equally phase distributed pendula is presented in Fig. 5(d) where in each double pendulum we observe anti-phase synchronization between upper and lower pendulum. Comparing both figures with Figs. 3(c) and 3(d) we notice that amplitudes of beam are much smaller. Hence, the increase in the number of coupled double pendula reduce the beam amplitude. Therefore, we assume that when n is odd number and $n \to \infty$ the amplitude of beam tends to zero ($\max y_b \to 0$). In Fig. 5(e), we show synchronization in two clusters, i.e. two double pendula are in anti-phase synchronization and three are equally distributed in phase space (phase shift $2\pi/3$). The same type of solution is presented in Fig. 5(f) but in each double pendulum pendula are in anti-phase configuration. The anti-phase pair (cluster consists of two pendula) do not act on the motion of the beam (no resultant force). The motion of the beam is governed by the dynamics of three double pendula cluster, hence the beam is performing three periods of motion for one period of system (similarly as for three coupled systems).

4.2. *Stability of periodic solutions*

In this section, we show how the change in the natural frequency of the beam affects the stability of obtained periodic solutions. We present one-parameter bifurcation diagrams calculated using AUTO-07p. We choose the beam mass M as the bifurcation parameter and vary it in the range from 0.01 kg to 80.0 kg (in some plots we reduce the range to 20.0 kg or 50.0 kg because for larger masses of the beam the stability does not change). In all plots on the vertical axis we show the maximum amplitude of the beam $\max y_b$. The black dots in figures mark the starting point of calculation — from this point we follow the solution in both directions — increasing and decreasing the mass M of the beam (we start form periodic solutions presented in previous subsection). The changes in line types of branches of periodic solutions correspond to changes of stability, i.e. the black solid line of branches mean that periodic solutions are stable and black dashed that the solution is unstable.

In Fig. 6, we show bifurcation diagrams for three coupled double pendula. We observe changes in stability properties of all considered periodic solutions. Figure 6(a) shows periodic solutions where all pendula are in-phase (see Fig. 3(a)). One can see that with the decrease of beam's mass, solutions along the branch are stable up to Neimark-Sacker bifurcation (for $M = 4.3$ kg) when they become unstable. With increasing mass M, we do not notice any change in stability. The similar scenario occurs for periodic solution presented in Fig. 3(b) — the destabilization takes place for $M = 2.71$ kg. Subsequent subplots — Figs. 6(c) and 6(d) present continuation of the solutions from Figs. 3(c) and 3(d) where double pendula are shifted by $2\pi/3$. For periodic solution shown in 6(c) the starting orbit is unstable, we observe the stabilization in Neimark–Sacker bifurcation for $M = 1.54$ kg. For the second branch (Fig. 6(d)) we start from the stable solution and it remains stable up to $M = 61.48$ kg. In both branches the increase of beam's mass M causes the decrease of its amplitude ($\max y_b$). As one can notice the varying natural frequency of the beam changes the stability of solutions and there is no value of M for which all of them are stable. The maximum number of stable coexisting solutions is three and minimum is one, hence parameter M is crucial to obtain given periodic solution.

Figure 7 is devoted to stability analysis of periodic solutions obtained for four coupled double pendula. We present only branches of periodic solutions for which we observe changes in stability. We do not show continuation of orbits presented in Figs. 4(b) and 4(d) because they are stable in the whole considered range of the mass M of the beam. In Fig. 7(a), we start from solution presented in Fig. 4(a). Similarly to previous in phase solutions this branch is stable when mass M of the beam increases, but with decreasing mass M it becomes unstable in the Neimark–Sacker bifurcation for $M = 4.77$ kg. The starting point of the branch presented in Fig. 4(b) corresponds to periodic solution shown in Fig. 4(c).

At the beginning, the branch is unstable (around black dot), then for $M = 3.8$ kg in the symmetry breaking pitchfork bifurcation we observe an appearance of three

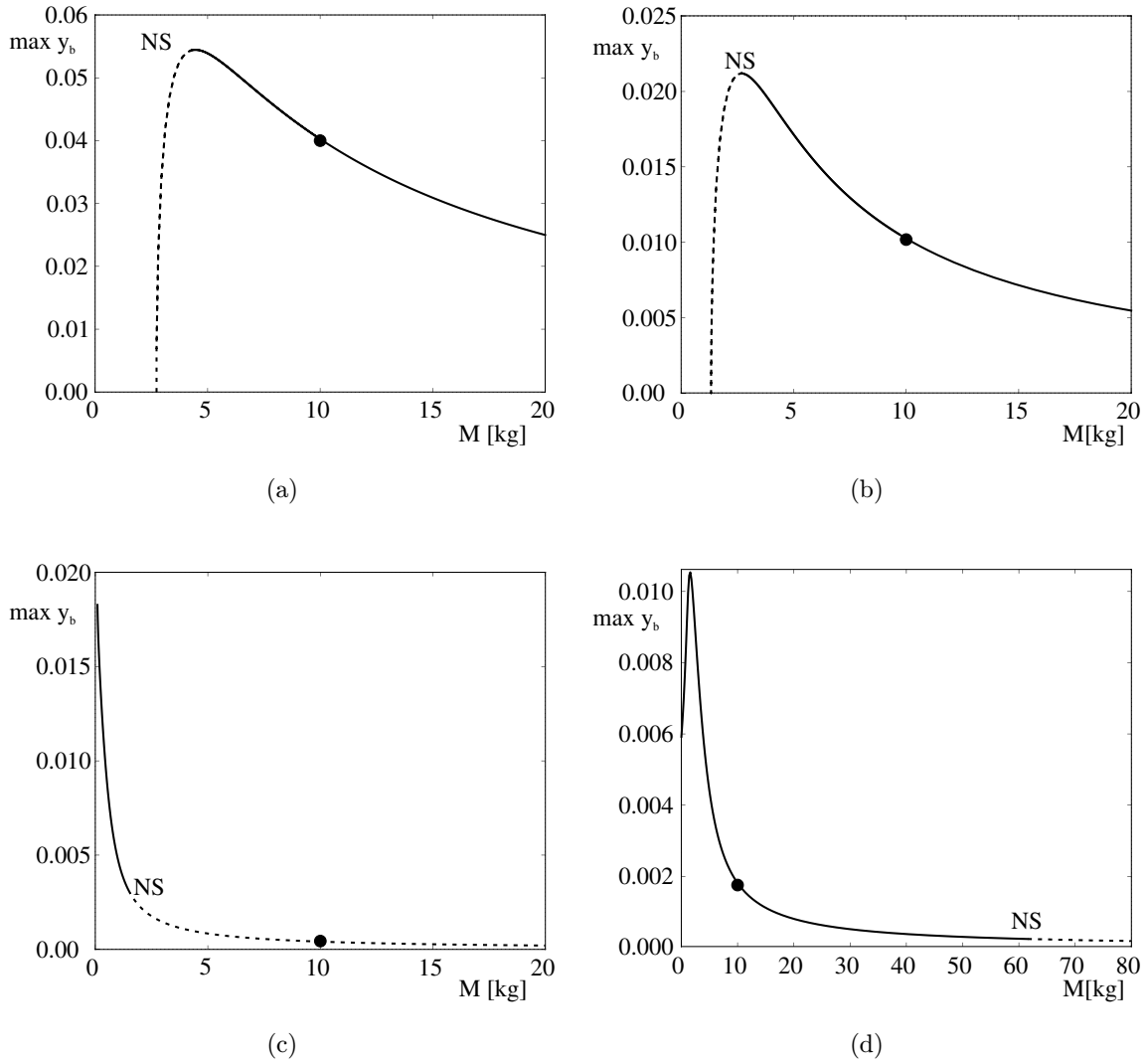

Fig. 6. One-parameter path-following of periodic solutions for the varying mass M of the beam for $n = 3$ coupled double pendula: (a) in-phase motion from Fig. 3(a), (b) anti-phase motion from Fig. 3(b), (c) the equally spaced motion with phase shift $2\pi/3$ between double pendula with in phase motion from Figs. 3(c) and 3(d) the equally spaced motion with phase shift $2\pi/3$ between double pendula with anti-phase motion in each double pendulum from Fig. 3(d). The black solid and black dashed lines correspond to stable and unstable periodic solutions, respectively. The abbreviation NS stands for the Neimark–Sacker bifurcation and PT denotes the pitchfork bifurcation. Bifurcations along unstable branches are neglected. The starting points of continuation are marked by black dots.

stable branches — one symmetric (the beam stays unmovable) and two asymmetric periodic solutions (the lines presenting amplitudes of beam overlap for them, so we just see one curve). The asymmetric branches lose stability simultaneously in Neimark–Sacker bifurcations for $M = 4.1\,\mathrm{kg}$. The further increase of mass M along branches corresponding to asymmetric solutions cause decrease of beam's amplitude. Shapes of asymmetric orbits are similar to those for single pendula — both solutions are shifted — one in clockwise and the other in counter clockwise direction from hanging down position of pendulum.

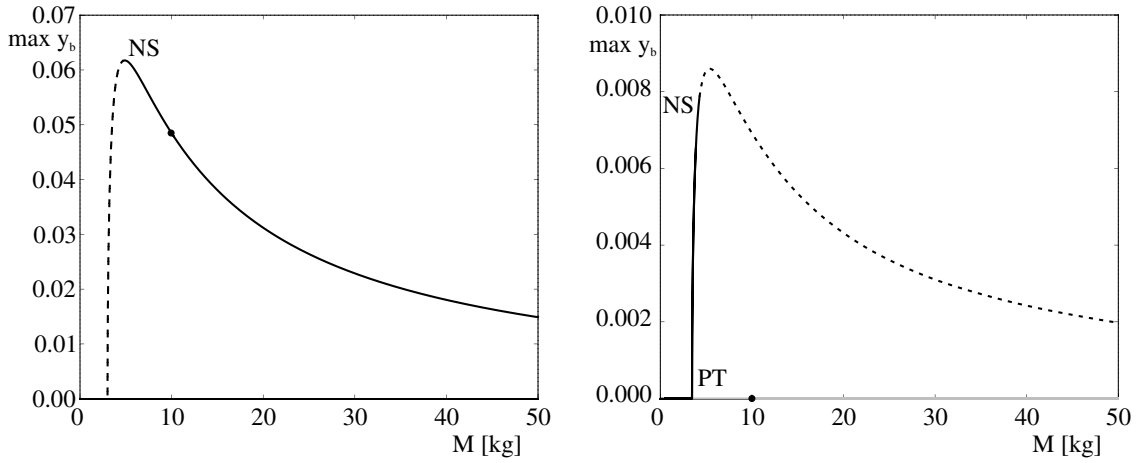

Fig. 7. One-parameter path-following of periodic solutions for the varying mass M of the beam for $n = 4$ coupled double pendula: (a) in-phase motion from Fig. 4(a), (b) motion of double pendulum from Fig. 4(c). The black solid and black dashed lines correspond to stable and unstable periodic solutions, respectively. The abbreviation NS stands for the Neimark–Sacker bifurcation and PT denotes the pitchfork bifurcation. Bifurcations along unstable branches are neglected. The starting points of continuation are marked by black dots.

The solutions obtained for five coupled double pendula are mostly unstable. Branches which starts from orbits presented in Figs. 5(c)–5(e) are unstable in the whole considered range of parameter M. Contrary, the solution shown in Fig. 5(b) remains stable. Because of that we do not present their bifurcation diagrams. First form remaining solutions is a periodic orbit shown in Fig. 5(a)), its bifurcation

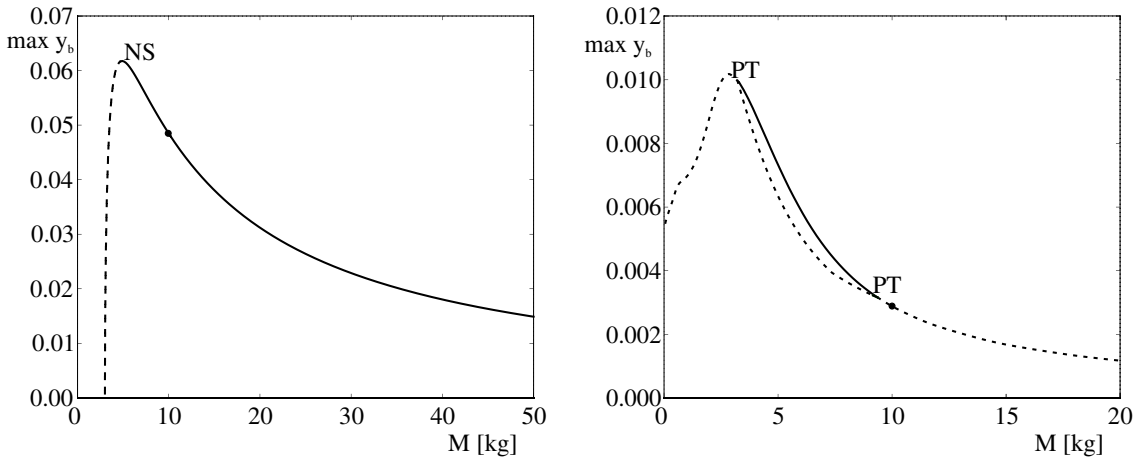

Fig. 8. One-parameter path-following of periodic solutions for the varying mass M of the beam for $n = 5$ coupled double pendula: (a) in-phase motion from Fig. 5(a), (b) the equally spaced motion with phase shift $2\pi/5$ between double pendula with in phase motion from Fig. 5(f). The black solid and black dashed lines correspond to stable and unstable periodic solutions, respectively. The abbreviation NS stands for the Neimark–Sacker bifurcation and PT denotes the pitchfork bifurcation. Bifurcations along unstable branches are neglected. The starting points of continuation are marked by black dots.

digram is presented in Fig. 8(a). Starting from stable solution (black dot) it becomes unstable with decreasing mass of the beam in Neimark–Sacker bifurcation for $M = 4.97\,\mathrm{kg}$. Increase of beam's mass causes only slow decrease of its amplitude. Interesting behavior can be observed for synchronization in two clusters with anti-phase synchronization in each double pendulum (see Fig. 5(f)). We start continuation from unstable solution, which in symmetry breaking pitchfork bifurcation for $M = 9.37\,\mathrm{kg}$ divides into three branches — the symmetric branch stays unstable and two asymmetric branches become stable (curves overlap as for four double pendula). Both asymmetric branches merge with symmetric one for $M = 3.21\,\mathrm{kg}$ in the inverse pitchfork bifurcation.

5. Conclusion

In this paper, we show different synchronous solutions which exist in the system of n coupled double pendula suspended on the beam. We derive the analytical condition which enable calculation of the possible periodic solutions for any number of double pendula. For each periodic solution obtained from derived condition, we observe two states of synchronization between pendula in each double pendulum (upper and lower pendula are in phase or anti-phase). The number of possible configurations grows with the number of coupled pendula. We show shapes of periodic solutions for $n = 3, 4, 5$ coupled double pendula, which can be stable or unstable depending on system's parameters. We examine how stability of each considered periodic solution changes with varying natural frequency of the beam. Using path-following toolbox Auto07p we detect all types of bifurcations along the branches of analyzed periodic solutions. In the considered system, the typical bifurcation that stabilizes/destabilizes periodic solutions is a Neimark–Sacker bifurcation. Hence, we observe appearance or disappearance of quasiperiodic oscillations. Moreover, by the proper choice of beam's mass parameter one can ensure that only selected solutions are stable. We claim that obtained results give a good overview of the dynamics of systems with coupled double pendula, and show that stability of such systems is strongly dependent on natural frequency of the beam. Therefore, to obtain desired synchronous state one has to adjust beam's natural frequency.

Acknowledgments

This work has been supported by the Foundation for Polish Science, Team Programme under project TEAM/2010/5/5. We also acknowledge valuable discussions with Patrycja Kuzma and Blazej Witkowski.

Appendix A

In this appendix, we derive an analytical condition for the double pendula synchronization in the considered system. We base on energy balance method and assumption of small oscillation of the pendula.

A.1. *Equation of the beam motion*

Assuming that the double pendula are identical and perform periodic oscillations with the frequency ω_0 and low amplitudes, one can describe displacements, velocities and accelerations of the upper and lower pendula in the following way:

$$\psi_{ij} = \Phi_{ij} \sin(\omega\tau + \beta_{ij}), \tag{A.1}$$

$$\dot{\psi}_{ij} = \omega\Phi_{ij} \cos(\omega\tau + \beta_{ij}), \tag{A.2}$$

$$\ddot{\psi}_{ij} = -\omega^2\Phi_{ij} \sin(\omega\tau + \beta_{ij}) \tag{A.3}$$

for $i = 1, \ldots, n$ and $j = 1, 2$, where Φ_{ij} are amplitudes and β_{ij} are phase difference between pendula.

Equation (2.2) allows to estimate the force generated by the pendula that acts on the beam:

$$F = -\sum_{i=1}^{n} \mathbf{A}_{i1}(\ddot{\psi}_{i1} \cos\psi_{i1} - \dot{\psi}_{i1}^2 \sin\psi_{i1}) - \sum_{i=1}^{n} \mathbf{A}_{i2}(\ddot{\psi}_{i2} \cos\psi_{i2} - \dot{\psi}_{i2}^2 \sin\psi_{i2}). \tag{A.4}$$

Substituting Eqs. (A.1)–(A.3) into Eq. (A.4) and considering the relation $\cos^2\alpha \sin\alpha = 0.25 \sin\alpha + 0.25 \sin 3\alpha$, one gets:

$$\begin{aligned} F = \sum_{i=1}^{n} \sum_{j=1}^{2} \mathbf{A}_{ij} [&\omega^2\Phi_{ij}(1 + 0.25\Phi_{ij}^2) \sin(\omega\tau + \beta_{ij}) \\ &+ \omega^2\Phi_{ij}^3 0.25 \sin(3\omega\tau + 3\beta_{ij})]. \end{aligned} \tag{A.5}$$

Substituting Eq. (A.5) in the equation of the beam's motion (2.2) we have:

$$\begin{aligned} \ddot{y}_b + \mathbf{K}y_b + \mathbf{C}\dot{y}_b = \sum_{i=1}^{n} \sum_{j=1}^{2} \mathbf{A}_{ij} [&\omega^2\Phi_{ij}(1 + 0.25\Phi_{ij}^2) \sin(\omega\tau + \beta_{ij}) \\ &+ \omega^2\Phi_{ij}^3 0.25 \sin(3\omega\tau + 3\beta_{ij})]. \end{aligned} \tag{A.6}$$

Assuming that damping coefficient $\mathbf{C}$ is small, one gets:

$$\begin{aligned} y_b &= \sum_{i=1}^{n} \sum_{j=1}^{2} \mathbf{X}_{1ij}\mathbf{A}_{ij} \sin(\omega\tau + \beta_{ij}) + \sum_{i=1}^{2} \sum_{j=1}^{2} \mathbf{X}_{3ij}\mathbf{A}_{ij} \sin(3\omega\tau + 3\beta_{ij}), \\ \ddot{y}_b &= \sum_{i=1}^{n} \sum_{j=1}^{2} \mathbf{A}_{1ij}\mathbf{A}_{ij} \sin(\omega\tau + \beta_{ij}) + \sum_{i=1}^{2} \sum_{j=1}^{2} 9\mathbf{A}_{3ij}\mathbf{A}_{ij} \sin(3\omega\tau + 3\beta_{ij}), \end{aligned} \tag{A.7}$$

where

$$\begin{aligned} X_{1ij} &= \frac{\omega^2\Phi_{ij}(1 + 0.25\Phi_{ij}^2)}{\mathbf{K} - \omega^2} \quad X_{3ij} = \frac{0.25\omega^2\Phi_{ij}^3}{\mathbf{K} - 9\omega^2}, \\ \mathbf{A}_{1ij} &= \frac{-\omega^4\Phi_{ij}(1 + 0.25\Phi_{ij}^2)}{\mathbf{K} - \omega^2} \quad \mathbf{A}_{3ij} = \frac{-0.25\omega^4\Phi_{ij}^3}{\mathbf{K} - 9\omega^2}. \end{aligned} \tag{A.8}$$

Equation (A.7) represent the displacement and the acceleration of the beam with mass M respectively.

A.2. *Energy balance of the system*

Multiplying Eq. (2.2) by the velocity of the beam $\dot{y}_b$, we obtain:

$$\ddot{y}_b\dot{y}_b + \mathbf{K}y_b\dot{y}_b = -\mathbf{C}\dot{y}_b^2 - \sum_{i=1}^{n}\mathbf{A}_{i1}(\ddot{\psi}_{i1}\dot{y}_b\cos\psi_{i1} - \dot{\psi}_{i1}^2\dot{y}_b\sin\psi_{i1}) - \sum_{i=1}^{n}\mathbf{A}_{i2}(\ddot{\psi}_{i2}\dot{y}_b\cos\psi_{i2} - \dot{\psi}_{i2}^2\dot{y}_b\sin\psi_{i2}). \tag{A.9}$$

Assuming that the motion of the pendulum is periodic with period T ($T = 2\pi/\omega$) and integrating Eq. (A.9), we obtain the following energy balance:

$$\int_0^T \ddot{y}_b\dot{y}_b d\tau + \int_0^T \mathbf{K}y_b\dot{y}_b d\tau = -\int_0^T \mathbf{C}\dot{y}_b^2 d\tau - \int_0^T \sum_{j=1}^{2}\left(\sum_{i=1}^{2}\mathbf{A}_{ij}(\ddot{\psi}_{ij}\cos\psi_{ij} - \dot{\psi}_{ij}^2\sin\psi_{ij})\right)\dot{y}_b d\tau. \tag{A.10}$$

The left-hand side of Eq. (A.10) represents the increase in the total energy of the beam which for the periodic oscillations is equal to zero:

$$\int_0^T \ddot{y}_b\dot{y}_b d\tau + \int_0^T \mathbf{K}y_b\dot{y}_b d\tau = 0. \tag{A.11}$$

The first component of the right-hand side of the Eq. (A.10) represents the energy dissipated by linear damper $\mathbf{C}$

$$W_{\text{beam}}^{\text{DAMP}} = \int_0^T \mathbf{C}\dot{y}_b^2 d\tau \tag{A.12}$$

while the second component represents the work performed by horizontal components of the force generated by the double pendula that acts on the beam and causing its motion:

$$W_{\text{beam}}^{\text{DRIVE}} = -\int_0^T \sum_{j=1}^{2}\left(\sum_{i=1}^{n}\mathbf{A}_{ij}(\ddot{\psi}_{ij}\cos\psi_{ij} - \dot{\psi}_{ij}^2\sin\psi_{ij})\right)\dot{y}_b d\tau. \tag{A.13}$$

Substituting Eqs. (A.12) and (A.13) to Eq. (A.10) we get:

$$W_{\text{beam}}^{\text{DRIVE}} - W_{\text{beam}}^{\text{DAMP}} = 0. \tag{A.14}$$

Multiplying the equation of the upper pendulum Eq. (A.2) by velocity $\dot{\psi}_{i1}$, we obtain:

$$\begin{aligned}\delta_{i1}\ddot{y}_b\dot{\psi}_{i1}\cos\psi_{i1} + \mathbf{L}_{i1}\ddot{\psi}_{i1}\dot{\psi}_{i1} + \mathbf{L}_{i3}\ddot{\psi}_{i2}\dot{\psi}_{i1}\cos(\psi_{i1}-\psi_{i2})\\ = -\mathbf{L}_{i3}\dot{\psi}_{i1}\dot{\psi}_{i2}^2\sin(\psi_{i1}-\psi_{i2}) - \mathbf{G}_{i1}\dot{\psi}_{i1}\sin(\psi_{i1})\\ - \mathbf{C}_{vdp}(1-\mu\psi_{i1}^2)\dot{\psi}_{i1}^2 + \mathbf{C}_{i2}(\dot{\psi}_{i2}-\dot{\psi}_{i1})\dot{\psi}_{i1}.\end{aligned} \tag{A.15}$$

Assuming that the oscillations of the pendula are periodic with period T and integrating Eq. (A.15), one obtains the following energy balance:

$$\begin{aligned}&\int_0^T \mathbf{L}_{i1}\ddot{\psi}_{i1}\dot{\psi}_{i1}d\tau + \int_0^T \mathbf{G}_{i1}\dot{\psi}_{i1}\sin\psi_{i1}d\tau\\ &\quad = -\int_0^T \delta_{i1}\ddot{y}_b\dot{\psi}_{i1}\cos\psi_{i1}d\tau - \int_0^T \mathbf{L}_{i3}(\dot{\psi}_{i1}\dot{\psi}_{i2}^2\sin(\psi_{i1}-\psi_{i2})\\ &\quad + \ddot{\psi}_{i2}\dot{\psi}_{i1}\cos(\psi_{i1}-\psi_{i2}))d\tau - \int_0^T \mathbf{C}_{vdp}\dot{\psi}_{i1}^2 d\tau + \int_0^T \mathbf{C}_{vdp}\mu\psi_{i1}^2\dot{\psi}_{i1}^2 d\tau\\ &\quad + \int_0^T \mathbf{C}_{i2}\dot{\psi}_{i2}\dot{\psi}_{i1}d\tau - \int_0^T \mathbf{C}_{i2}\dot{\psi}_{i1}^2 d\tau.\end{aligned} \tag{A.16}$$

The left-hand side of Eq. (A.16) represents the total energy of the upper pendula which in the case of periodic oscillations is equal to zero:

$$\int_0^T \mathbf{L}_{i1}\ddot{\psi}_{i1}\dot{\psi}_{i1}d\tau + \int_0^T \mathbf{G}_{i1}\dot{\psi}_{i1}\sin\psi_{i1}d\tau = 0 \quad i = 1,2. \tag{A.17}$$

The first component of the right-hand side of Eq. (A.16) represents the energy which is transferred to the beam:

$$W_{i1}^{\mathrm{SYN}} = \int_0^T \delta_{i1}\ddot{y}_b\dot{\psi}_{i1}\cos\psi_{i1}d\tau. \tag{A.18}$$

The second component describes the energy which is transferred to lower pendulum:

$$W_{i1}^{\mathrm{SYNP}} = -\int_0^T \mathbf{L}_{i3}(\dot{\psi}_{i1}\dot{\psi}_{i2}^2\sin(\psi_{i1}-\psi_{i2}) + \ddot{\psi}_{i2}\dot{\psi}_{i1}\cos(\psi_{i1}-\psi_{i2}))d\tau \tag{A.19}$$

and the third component describes the energy, which is supplied to the system by van der Pol damper in one period of oscillations:

$$W_{i1}^{\mathrm{DAMP}} = -\int_0^T (\mathbf{C}_{vdp}+\mathbf{C}_{i2})\dot{\psi}_{i1}^2 - \mathbf{C}_{i2}\dot{\psi}_{i2}\dot{\psi}_{i1}d\tau. \tag{A.20}$$

Finally, the last component represents the energy dissipated by van der Pol damper:

$$W_{i1}^{\mathrm{SELF}} = -\int_0^T \mu\mathbf{C}_{vdp}\psi_{i1}^2\dot{\psi}_{i1}^2 d\tau \tag{A.21}$$

substituting Eqs. (A.18)–(A.21) to Eq. (A.16), we obtain the following relation:

$$W_{i1}^{\mathrm{SYNP}} - W_{i1}^{\mathrm{SYN}} + W_{i1}^{\mathrm{SELF}} + W_{i1}^{\mathrm{DAMP}} = 0 \quad \text{for } i = 1, \ldots, n.$$

Multiplying the equation of the lower pendulum Eq. (2.4) by velocity $\dot{\psi}_{i2}$, one gets:

$$\begin{aligned}\delta_{i2}\ddot{y}_b\dot{\psi}_{i2}\cos\psi_{i2} + \mathbf{L}_{i3}\ddot{\psi}_{i1}\dot{\psi}_{i2}\cos(\psi_{i1}-\psi_{i2}) + \mathbf{L}_{i2}\dot{\psi}_{i2}\ddot{\psi}_{i2}\\ = \mathbf{L}_{i3}\dot{\psi}_{i1}^2\dot{\psi}_{i2}\sin(\psi_{i1}-\psi_{i2}) - \mathbf{G}_{i2}\dot{\psi}_{i2}\sin(\psi_{i2}) - \mathbf{C}_{i2}(\dot{\psi}_{i2}-\dot{\psi}_{i1})\dot{\psi}_{i2}. \qquad \text{(A.22)}\end{aligned}$$

Assuming that the oscillations of the pendulum are periodic with period T, the integration of Eq. (A.22) gives the following energy balance:

$$\begin{aligned}\int_0^T \mathbf{L}_{i2}\dot{\psi}_{i2}\ddot{\psi}_{i2}d\tau + \int_0^T \mathbf{G}_{i2}\dot{\psi}_{i2}\sin(\psi_{i2})d\tau\\ = -\int_0^T \beta_{i2}\ddot{y}_b\dot{\psi}_{i2}\cos\psi_{i2}d\tau + \int_0^T \mathbf{L}_{i3}(\dot{\psi}_{i1}^2\dot{\psi}_{i2}\sin(\psi_{i1}-\psi_{i2})\\ - \ddot{\psi}_{i1}\dot{\psi}_{i2}\cos(\psi_{i1}-\psi_{i2}))d\tau + \int_0^T \mathbf{C}_{i2}\dot{\psi}_{i2}^2 d\tau + \int_0^T \mathbf{C}_{i2}\dot{\psi}_{i1}\dot{\psi}_{i2}d\tau. \qquad \text{(A.23)}\end{aligned}$$

The left-hand side of Eq. (A.23) represents the total energy of the lower pendulum which in case of periodic oscillations is equal to zero

$$\int_0^T \mathbf{L}_{i2}\dot{\psi}_{i2}\ddot{\psi}_{i2}d\tau + \int_0^T \mathbf{G}_{i2}\dot{\psi}_{i2}\sin(\psi_{i2})d\tau = 0 \quad i = 1, 2. \qquad \text{(A.24)}$$

The first component of the right-hand side of Eq. (A.23) represents the energy which is transferred to the beam via the upper pendulum or to the next pendulum via the upper pendulum and the beam:

$$W_{i2}^{\mathrm{SYN}} = \int_0^T \delta_{i2}\ddot{y}_b\dot{\psi}_{i2}\cos\psi_{i2}d\tau \qquad \text{(A.25)}$$

The second component describes the energy which is transferred to the upper pendulum:

$$W_{i2}^{\mathrm{SYNP}} = -\int_0^T \mathbf{L}_{i3}(\dot{\psi}_{i1}^2\dot{\psi}_{i2}\sin(\psi_{i1}-\psi_{i2}) - \ddot{\psi}_{i1}\dot{\psi}_{i2}\cos(\psi_{i1}-\psi_{i2}))d\tau \qquad \text{(A.26)}$$

and the last component represents the energy dissipated by the damper:

$$W_{i2}^{\mathrm{DAMP}} = -\int_0^T \mathbf{C}_{i2}(\dot{\psi}_{i2}-\dot{\psi}_{i1})\dot{\psi}_{i2}d\tau. \qquad \text{(A.27)}$$

Substituting Eqs. (A.25)–(A.27) to Eq. (A.23), one obtains the following relation:

$$W_{i2}^{\mathrm{SYNP}} - W_{i2}^{\mathrm{SYN}} + W_{i2}^{\mathrm{DAMP}} = 0,$$

where $i = 1, \ldots, n$.

A.3. *Synchronization between the upper and lower pendula*

The energy transferred from the upper to the lower pendulum is given by:

$$W_{i1}^{\mathrm{SYNP}} = -\int_0^T \mathbf{L}_{i3}(\ddot{\psi}_{i2}\cos(\psi_{i1}-\psi_{i2}) + \dot{\psi}_{i2}^2\sin(\psi_{i1}-\psi_{i2}))\dot{\psi}_{i1}d\tau \tag{A.28}$$

and the energy transferred from the lower to the upper pendulum as:

$$W_{i2}^{\mathrm{SYNP}} = -\int_0^T \mathbf{L}_{i3}(\ddot{\psi}_{i1}\cos(\psi_{i1}-\psi_{i2}) - \dot{\psi}_{i1}^2\sin(\psi_{i1}-\psi_{i2}))\dot{\psi}_{i2}d\tau \tag{A.29}$$

Taking into account Eqs. (A.1)–(A.3) and Eq. (A.29) takes the form:

$$\begin{aligned} W_{i1}^{\mathrm{SYNP}} = & -\mathbf{L}_{i3}\int_0^T (-\omega^2\Phi_{i2}\sin(\omega\tau+\beta_{i2})\cos(\Phi_{i1}\sin(\omega\tau+\beta_{i1}) \\ & - \Phi_{i2}\sin(\omega\tau+\beta_{i2})) + \omega^2\Phi_{i2}^2\cos^2(\omega\tau+\beta_{i2})\sin(\Phi_{i1}\sin(\omega\tau+\beta_{i1}) \\ & - \Phi_{i2}\sin(\omega\tau+\beta_{i2})))\omega\Phi_{i1}\cos(\omega\tau+\beta_{i1})d\tau \\ = & \mathbf{L}_{i3}\pi\omega^2\Phi_{i1}\Phi_{i2}\sin(\beta_{i2}-\beta_{i1}) \end{aligned} \tag{A.30}$$

and

$$W_{i2}^{\mathrm{SYNP}} = \mathbf{L}_{i3}\pi\omega^2\Phi_{i1}\Phi_{i2}\sin(\beta_{i1}-\beta_{i2}) = -W_{i1}^{\mathrm{SYNP}}. \tag{A.31}$$

The synchronization between the lower and upper pendula occurs when:

$$W_{i1}^{\mathrm{SYNP}} = 0 \Rightarrow \sin(\beta_{i1}-\beta_{i2}) = 0. \tag{A.32}$$

The condition (A.32) is fulfilled when:

$$\beta_{i1} = \beta_{i2} \vee (\beta_{i1} = 0 \wedge \beta_{i2} = \pi). \tag{A.33}$$

In the first case, the oscillations of the upper and lower pendula are in-phase, i.e. the pendula move in the same directions, whereas in the second case they are in anti-phase, i.e. the pendula move in the opposite directions. For low oscillations, limit conditions (A.33) define two normal modes of oscillations.[1]

A.4. *Synchronization between the upper pendula*

In each equation of the pendulum's motion, there is a component influencing the beam's motion

$$M_{ij}^{\mathrm{SYN}} = \delta_{ij}\ddot{y}_b\cos\psi_{ij}, \tag{A.34}$$

which is called the synchronization momentum (torque). The work done by this momentum during one period is equal to zero.

$$W_{ij}^{\mathrm{SYN}} = \int_0^T \delta_{ij}\ddot{y}_b\cos\psi_{ij}\dot{\psi}_{ij}dt = 0 \tag{A.35}$$

substituting Eqs. (A.7), (A.1) and (A.2) into (A.35) and performing the linearization, we arrive at:

$$W_{kl}^{\mathrm{SYN}} = \xi\delta_{kl}\Phi_{kl}\left[\sum_{i=1}^{n}\sum_{j=1}^{2}\Theta_{ij}M_{ij}\sin(\beta_{ij}-\beta_{kl})\right] = 0 \quad k = 1,\ldots,n \; l = 1,2, \tag{A.36}$$

where

$$\begin{aligned} \xi &= \frac{-\omega_0^5\pi}{Ml_b(\mathbf{K}-\omega_0^2)}, \quad M_{i1} = (m_{i1}+m_{i2})l_{i1}, \\ M_{i2} &= m_{i2}l_{i2}, \quad \Theta_{ij} = \Phi_{ij}(1+0.25\Phi_{ij}^2) \end{aligned} \tag{A.37}$$

and n is number of double pendula.

Equation (A.36) allow the calculation of phase angle β_{ij} for which the synchronization of the periodic pendula oscillations occurs. We assume that pendula are identical, hence we can introduce the following substitution:

$$A = \Theta_{i1}M_{i1}; \quad B = \Theta_{i2}M_{i2} \quad \text{for } i = 1,\ldots,n. \tag{A.38}$$

The synchronization between lower and upper pendula can either be in phase ($\beta_{i1} = \beta_{i2}$) or in anti-phase ($\beta_{i1} - \beta_{i2} = \pi$). In both cases the condition $\sin(\beta_{i1} - \beta_{i2}) = 0$ is fulfilled. That allows to rewrite Eq. (A.36) in simpler form:

$$\begin{aligned} &(A+B)[\sin(\beta_{21}-\beta_{11}) + \sin(\beta_{31}-\beta_{11}) + \cdots + \sin(\beta_{i1}-\beta_{11})] = 0 \\ &(A+B)[\sin(\beta_{11}-\beta_{21}) + \sin(\beta_{31}-\beta_{21}) + \cdots + \sin(\beta_{i1}-\beta_{21}) = 0 \\ &\qquad\qquad\vdots \qquad\qquad\qquad\qquad\qquad\vdots \\ &(A+B)[\sin(\beta_{11}-\beta_{i1}) + \sin(\beta_{21}-\beta_{i1}) + \cdots + \sin(\beta_{i-11}-\beta_{i1})] = 0 \end{aligned} \tag{A.39}$$

for $i = 1,\ldots,n$.

Equation (A.39) can be divided by $(A+B)$ which gives us the condition for synchronization between the upper pendula.

Appendix B

Code[33] in Mathematica which let us calculate number of possible clusters and number of pendula in each cluster:

```
f[n_] := Length@IntegerPartitions[n, All, Prime@Range@PrimePi@n];
w[n_] := Select[IntegerPartitions[n], And @@ PrimeQ/@ # &];
number = 21;
f[number]
w[number]
```

References

1. A. Andronov, A. Witt and S. Khaikin, *Theory of Oscillations* (Pergamon, Oxford, 1966).
2. I. I. Blekhman, *Synchronization in Science and Technology* (ASME, New York, 1988).
3. A. Pikovsky, M. Roesenblum and J. Kurths, *Synchronization: An Universal Concept in Nonlinear Sciences* (Cambridge University Press, Cambridge, 2001).
4. M. P. Aghababa and H. P. Aghababa, Synchronization of nonlinear chaotic electromechanical gyrostat systems with uncertainties, *Nonlin. Dynam.* **67** (2012) 2689–2701.
5. P. Perlikowski, A. Stefanski and T. Kapitaniak, 1:1 Mode locking and generalized synchronization in mechanical oscillators, *J. Sound Vibr.* **318**(1–2) (2008) 329–340.
6. A. Silchenko, T. Kapitaniak and V. Anishchenko, Noise-enhanced phase locking in a stochastic bistable system driven by a chaotic signal, *Phys. Rev. E* **59**(2) (1999) 1593–1599.
7. P. Brzeski, P. Perlikowski, S. Yanchuk and T. Kapitaniak, The dynamics of the pendulum suspended on the forced Duffing oscillator, *J. Sound Vibr.* **331**(24) (2012) 5347–5357.
8. C. Huygens, 1893, Letter to de Sluse, In: Oeuveres Completes de Christian Huygens, (letters; No. 1333 of 24 February 1665, no. 1335 of 26 February 1665, No. 1345 of 6 March 1665) (Societe Hollandaise Des Sciences, Martinus Nijhoff, La Haye).
9. M. Bennet, M. F. Schatz, H. Rockwood and K. Wiesenfeld, Huygens's clocks, *Proc. Roy. Soc. Lond. A* **458** (2002) 563–579.
10. K. Czolczynski, P. Perlikowski, A. Stefanski and T. Kapitaniak, Clustering of Huygens' Clocks, *Prog. Theor. Phys.* **122** (2009) 1027–1033.
11. R. Dilao, Antiphase and in-phase synchronization of nonlinear oscillators: The Huygens's clocks system, *Chaos* **19** (2009) 023118.
12. A. L. Fradkov and B. Andrievsky, Synchronization and phase relations in the motion of twopendulum system, *Int. J. Nonlin. Mech.* **42** (2007) 895.
13. A. Yu. Kanunnikov and R. E. Lamper, Synchronization of pendulum clocks suspended on an elastic beam. *J. Appl. Mech. Theor. Phys.* **44** (2003) 748–752.
14. J. Pantaleone, Synchronization of metronomes, *Am. J. Phys.* **70** (2002) 992.
15. P. Perlikowski, M. Kapitaniak, K. Czolczynski, A. Stefanski and T. Kapitaniak, Chaos in coupled clocks, *Int. J. Bif. Chaos* **22** (2012) 1250288.
16. M. Senator, Synchronization of two coupled escapement-driven pendulum clocks, *J. Sound Vibr.* **291** (2006) 566–603.
17. H. Ulrichs, A. Mann and U. Parlitz, Synchronization and chaotic dynamics of coupled mechanical metronomes, *Chaos* **19** (2009) 043120.
18. N. Rott, A multiple pendulum for the demonstration of non-linear coupling, *Z. Angew. Math. Phys.* **2l**(570) (1970) 570–582.
19. J. Miles, Parametric excitation of an internally resonant double pendulum, *J. Appl. Math. Phys. (ZAMP)* **36** (1985) 337–345.
20. A. C. Skeldon, Mode interaction in a double pendulum, *Phys. Lett. A* **166** (1992) 224–229.
21. A. C. Skeldon, Dynamics of a parametrically excited double, *Physica D* **75** (1994) 541–558.
22. S. Samaranayake and A. K. Bajaj, Bifurcations in the dynamics of an orthogonal double pendulum, *Nonlin. Dynam.* **4** (1993) 605–633.
23. T. Morbiato, R. Vitaliani and A. Saetta, Numerical analysis of a synchronization phenomenon: Perdestrian stucture interaction, *Comput. Struct.* **89** (2011) 1649–1663.
24. A. P. Willmott and J. Dapena, The planarity of the stickface motion in the field hockey hit, *J. Sports Sci.* **30** (2012) 369–377.

25. Y. Suzukia, T. Nomuraa, M. Casadiob and P. Morassoc, Intermittent control with ankle, hip, and mixed strategies during quiet standing: A theoretical proposal based on a double inverted pendulum model, *J. Theoret. Biol.* **310** (2012) 55–79.
26. K. P. Granataa and S. E. Wilsonb, Trunk posture and spinal stability, *Clin. Biomech.* **16**(8) (2001) 650–659.
27. P. Koluda, P. Perlikowski, K. Czolczynski and T. Kapitaniak, Synchronization configurations of two coupled double pendula, *Commun. Nonlin. Sci. Numer. Simul.* **19** (2014) 977–990.
28. P. Koluda, P. Perlikowski, K. Czolczynski and T. Kapitaniak, Synchronization of two self-excited double-pendula, *The Eur. Phys. J. Special Topics* (2014) (http://arxiv.org/abs/1402.1375).
29. B. Blazejczyk-Okolewska and T. Kapitaniak, Co-existing attractors of impact oscillator, *Chaos Solitons Fractals* **9**(8) (1998) 1439–1443.
30. T. Kapitaniak, Stochastic response with bifurcations to nonlinear duffing oscillator, *J. Sound Vibr.* **102**(3) (1995) 440–441.
31. T. Kapitaniak, Generating strange nonchaotic trajectories, *Phys. Rev. E* **47**(2) (1993) 1408–1410.
32. E. J. Doedel, A. R. Champneys, T. F. Fairgrieve, Y. A. Kuznetsov, B. Sandstede and X. Wang, in *Auto 97: Continuation and Bifurcation Software for Ordinary Differential Equations* (1998).
33. http://oeis.org/A000607.
34. R. C. Vaughan, On the number of partitions into primes, *Ramanujan J.* **15**(1) (2008) 109–121.

6.3 Article 3

Commun Nonlinear Sci Numer Simulat 19 (2014) 977–990

Contents lists available at ScienceDirect

Commun Nonlinear Sci Numer Simulat

journal homepage: www.elsevier.com/locate/cnsns

Synchronization configurations of two coupled double pendula

Piotr Koluda, Przemyslaw Perlikowski, Krzysztof Czolczynski, Tomasz Kapitaniak *

Division of Dynamics, Technical University of Lodz, Stefanowskiego 1/15, Lodz, Poland

ARTICLE INFO

Article history:
Received 1 August 2013
Accepted 9 August 2013
Available online 22 August 2013

Keywords:
Double pendulum
Synchronization
Energy balance

ABSTRACT

We consider the synchronization of two self-excited double pendula hanging from a horizontal beam which can roll on the parallel surface. We show that such pendula can obtain four different robust synchronous configurations. Our approximate analytical analysis allows to derive the synchronization conditions and explains the observed types of synchronizations. We consider the energy balance in the system and show how the energy is transferred between the pendula via the oscillating beam allowing the pendula' synchronization.

1. Introduction

Groups of oscillators are observed to synchronize in a diverse variety of systems [1,3,15,18,24–26], despite the inevitable differences between the oscillators. Synchronization is commonly the process where two or more systems interact with each other and come to oscillate together. The history of synchronization goes back to the 17th century when Ch. Huygens observed weak synchronization of two pendulum clocks [9]. Recently the phenomenon of the synchronization of the clocks hanging on a common movable beam has been the subject of research by a number of authors [2,4–8,10–14,16,17,19–21]. These studies have explained the phenomenon of synchronization of a number of single pendula. The problem of the synchronization of double pendula is less investigated. Fradkov et al. [22] developed the control system which allows the experimental synchronization of two double pendula. The occurrence of the synchronous rotation of a set of four uncoupled nonidentical double pendula arranged into a cross structure mounted on a vertically excited platform has been studied in [23]. It has been shown that after a transient, many different types of synchronous configurations with the constant phase difference between the pendula can be observed.

In this paper we consider the synchronization of two self-excited double-pendula. The oscillations of each pendulum are self-excited by the escapement mechanism associated with the lower parts (lower pendula) of each double-pendulum. We show that two such double-pendula hanging on the same beam can synchronize both in phase and in antiphase. We give evidence that the observed synchronous states are robust as they exit in the wide range of system parameters and are preserved for the parameters' mismatch (the pendula with different lengths are considered). The performed approximate analytical analysis allows to derive the synchronization conditions and explains the observed types of synchronizations. The energy balance in the system allows to show how the energy is transferred between the pendula via the oscillating beam.

This paper is organized as follows. Section 2 describes the considered model of the coupled double pendula. In Section 3 we derive the energy balance of the synchronized identical pendula. Stable synchronous configurations of double pendula have been identified in Section 4. Section 5 presents the results of our numerical simulations and describes the observed synchronization states. Finally, we summarize our results in Section 6.

* Corresponding author. Tel.: +48 426312231.
E-mail addresses: tomasz.kapitaniak@p.lodz.pl, tomaszka@p.lodz.pl (T. Kapitaniak).

1007-5704/$ - see front matter © 2013 Elsevier B.V. All rights reserved.
http://dx.doi.org/10.1016/j.cnsns.2013.08.008

2. The model

The analyzed system is shown in Fig. 1. It consists of the rigid beam and two double pendula suspended on it. The beam of mass M can move in horizontal direction, its movement is described by coordinate X. The beam is connected to the refuge by a linear spring with stiffness coefficient K_X and linear damper with damping coefficient C_X. Each double pendulum consists of two light beams of lengths L_{ci}, L_{si} and two masses M_{ci} and M_{si}, where $i = 1,2$, mounted at beam's ends. Subscripts s and c describe respectively upper and lower parts (pendula) of each double pendulum (see Fig. 1). The lower parts (pendula) are mounted to the upper parts (pendula) at the distances L_{ai} from the points in which double pendula are mounted to the beam M. The motion of each double-pendulum is described by angles φ_{ci} (lower pendulum) and φ_{si} (upper pendulum). The oscillations of the double pendula are damped by the viscous dampers C_{si} and C_{ci} (not shown in Fig. 1). The lower pendula of each double pendulum are excited by the clock escapement mechanism (described in details in [10]) represented by momentum M_{Di} which provide the energy needed to compensate the energy dissipation due to the viscous friction C_{si}, C_{ci} and to keep the pendula oscillating [1]. This mechanism acts in two successive steps (the first step is followed by the second one and the second one by the first one). In the first step if $0 < (\varphi_{ci} - \varphi_{si}) < \gamma_N$ then $M_{Di} = M_{Ni}$ and when $(\varphi_{ci} - \varphi_{si}) < 0$ or $\gamma_N < (\varphi_{ci} - \varphi_{si})$ then $M_{Di} = 0$, where γ_N and M_{Ni} are constant values which characterize the mechanism. For the second stage one has for $-\gamma_N < (\varphi_{ci} - \varphi_{si}) < 0$ $M_{Di} = -M_{Ni}$ and $M_{Di} = 0$ for $0 < (\varphi_{ci} - \varphi_{si})$ or $-\gamma_N > (\varphi_{ci} - \varphi_{si})$.

Note that the system shown in Fig. 1 can be considered as the two-dimensional model of Huygens' experiment (upper pendula represent clocks' cases and lower pendula clocks' pendula) [10].

The equations of motion of the considered system are as follows:

$$M_{ci}L_{ci}^2\frac{d^2\varphi_{ci}}{dt^2} + M_{ci}L_{ai}L_{ci}\frac{d^2\varphi_{si}}{dt^2}\cos(\varphi_{ci}-\varphi_{si}) + M_{ci}L_{ai}L_{ci}\left(\frac{d\varphi_{si}}{dt}\right)^2\sin(\varphi_{ci}-\varphi_{si}) + M_{ci}L_{ci}\frac{d^2X}{dt^2}\cos\varphi_{ci} + C_{\varphi ci}\left(\frac{d\varphi_{ci}}{dt}-\frac{d\varphi_{si}}{dt}\right) + M_{ci}L_{ci}g\sin\varphi_{ci} = M_{Di}, \quad i = 1,2 \tag{1}$$

$$M_{si}L_{si}^2\frac{d^2\varphi_{si}}{dt^2} + M_{ci}L_{ai}^2\frac{d^2\varphi_{si}}{dt^2} + M_{ci}L_{ai}L_{ci}\frac{d^2\varphi_{ci}}{dt^2}\cos(\varphi_{ci}-\varphi_{si}) - M_{ci}L_{ai}L_{ci}\left(\frac{d\varphi_{ci}}{dt}\right)^2\sin(\varphi_{ci}-\varphi_{si}) + M_{si}L_{si}\frac{d^2X}{dt^2}\cos\varphi_{si} + M_{ci}L_{ai}\frac{d^2X}{dt^2}\cos\varphi_{si} + C_{\varphi si}\frac{d\varphi_{si}}{dt} - C_{\varphi ci}\left(\frac{d\varphi_{ci}}{dt}-\frac{d\varphi_{si}}{dt}\right) + M_{si}L_{si}g\sin\varphi_{si} + M_{ci}L_{ai}g\sin\varphi_{si} = -M_{Di}, \tag{2}$$

$$\left(M_B + \sum_{i=1}^{2}(M_{ci}+M_{si})\right)\frac{d^2X}{dt^2} + C_X\frac{dX}{dt} + K_XX = \sum_{i=1}^{2}(M_{si}L_{si}+M_{ci}L_{ai})\left(-\frac{d^2\varphi_{si}}{dt^2}\cos\varphi_{si} + \left(\frac{d\varphi_{si}}{dt}\right)^2\sin\varphi_{si}\right) + \sum_{i=1}^{2}M_{ci}L_{ci}\left(-\frac{d^2\varphi_{ci}}{dt^2}\cos\varphi_{ci} + \left(\frac{d\varphi_{ci}}{dt}\right)^2\sin\varphi_{ci}\right), \tag{3}$$

where $i = 1,2$.

Considering mass M_{c1}, length L_{c1} of the first lower pendulum and gravitational acceleration g as reference parameters one can rewrite Eqs. (1)–(3) in the dimensionless form:

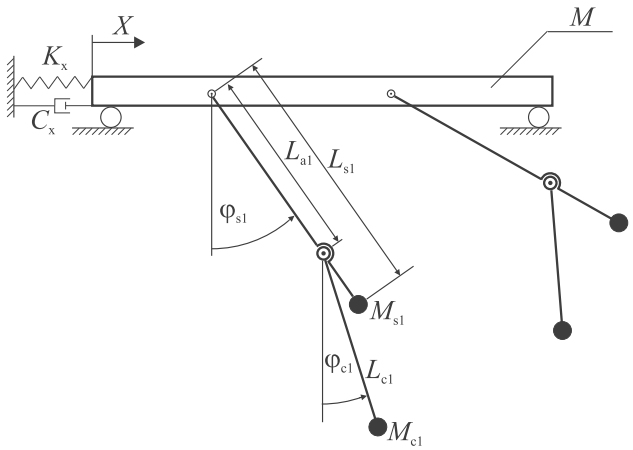

Fig. 1. The model of two double pendula hanging from a horizontal beam.

$$m_{ci}l_{ci}^2\ddot{\varphi}_{ci}+m_{ci}l_{ai}l_{ci}\ddot{\varphi}_{si}\cos(\varphi_{ci}-\varphi_{si})+m_{ci}l_{ai}l_{ci}\dot{\varphi}_{si}^2\sin(\varphi_{ci}-\varphi_{si})+m_{ci}l_{ci}\ddot{x}\cos\varphi_{ci}+c_{\varphi ci}(\dot{\varphi}_{ci}-\dot{\varphi}_{si})+m_{ci}l_{ci}\sin\varphi_{ci}=N_{Di},\quad i=1,2, \tag{4}$$

$$m_{si}l_{si}^2\ddot{\varphi}_{si}+m_{ci}l_{ai}^2\ddot{\varphi}_{si}+m_{ci}l_{ai}l_{ci}\ddot{\varphi}_{ci}\cos(\varphi_{ci}-\varphi_{si})-m_{ci}l_{ai}l_{ci}\dot{\varphi}_{ci}^2\sin(\varphi_{ci}-\varphi_{si})+m_{si}l_{si}\ddot{x}\cos\varphi_{si}+m_{ci}l_{ai}\ddot{x}\cos\varphi_{si}+c_{\varphi si}\dot{\varphi}_{si}-c_{\varphi ci}(\dot{\varphi}_{ci}-\dot{\varphi}_{si})+m_{si}l_{si}\sin\varphi_{si}+m_{ci}l_{ai}\sin\varphi_{si}=-N_{Di},\quad i=1,2, \tag{5}$$

$$\left(m_B+\sum_{i=1}^{2}(m_{ci}+m_{si})\right)\ddot{x}+c_x\dot{x}+k_xx=\sum_{i=1}^{2}(m_{si}l_{si}+m_{ci}l_{ai})(-\ddot{\varphi}_{si}\cos\varphi_{si}+\dot{\varphi}_{si}^2\sin\varphi_{si})+\sum_{i=1}^{2}m_{ci}l_{ci}(-\ddot{\varphi}_{ci}\cos\varphi_{ci}+\dot{\varphi}_{ci}^2\sin\varphi_{ci}), \tag{6}$$

where:

$$m_{ci}=\frac{M_{ci}}{M_{c1}},\quad m_{si}=\frac{M_{si}}{M_{c1}},\quad m_B=\frac{M_B}{M_{c1}},\quad l_{ci}=\frac{L_{ci}}{L_1},\quad l_{si}=\frac{L_{si}}{L_1},\quad x=\frac{X}{L_{c1}},$$

$$c_{\varphi ci}=\frac{C_{\varphi ci}\sqrt{L_{c1}}}{M_{c1}L_{c1}^2\sqrt{g}},\quad c_{\varphi si}=\frac{C_{\varphi si}\sqrt{L_{c1}}}{M_{c1}L_{c1}^2\sqrt{g}},\quad c_x=\frac{C_X\sqrt{L_{c1}}}{M_{c1}\sqrt{g}},\quad k_x=\frac{K_XL_{c1}}{M_{c1}g},\quad N_{Di}=\frac{M_{Di}}{M_{c1}L_{c1}g},$$

$\tau=\alpha t$ (dimensionless time), $\alpha=\sqrt{\frac{g}{L_{c1}}}$, symbols $\ddot{}$ and $\dot{}$ denote respectively $\frac{d^2}{d\tau^2}$ and $\frac{d}{d\tau}$.

3. Energy balance

Assume that the motion of both pendula is periodic with period T. Multiplying Eq. (4) by the angular velocity of the lower pendula and integrating it over the period T we obtain the equation of the energy balance:

$$\int_0^T m_{ci}l_{ci}^2\ddot{\varphi}_{ci}\dot{\varphi}_{ci}d\tau+\int_0^T m_{ci}l_{ai}l_{ci}\ddot{\varphi}_{si}\dot{\varphi}_{ci}\cos(\varphi_{ci}-\varphi_{si})d\tau+\int_0^T m_{ci}l_{ai}l_{ci}\dot{\varphi}_{si}^2\dot{\varphi}_{ci}\sin(\varphi_{ci}-\varphi_{si})d\tau+\int_0^T m_{ci}l_{ci}\ddot{x}\dot{\varphi}_{ci}\cos\varphi_{ci}d\tau+\int_0^T c_{\varphi ci}(\dot{\varphi}_{ci}-\dot{\varphi}_{si})\dot{\varphi}_{ci}d\tau+\int_0^T m_{ci}l_{ci}\dot{\varphi}_{ci}\sin\varphi_{ci}d\tau=\int_0^T N_{Di}\dot{\varphi}_{ci}d\tau, \tag{7}$$

where $i=1,2$. The first three components of Eq. (7) represent the work performed by the forces with which the lower pendula act on the upper pendula:

$$W_{ci}^{INERT}=\int_0^T m_{ci}l_{ci}^2\ddot{\varphi}_{ci}\dot{\varphi}_{ci}d\tau+\int_0^T m_{ci}l_{ai}l_{ci}\ddot{\varphi}_{si}\dot{\varphi}_{ci}\cos(\varphi_{ci}-\varphi_{si})d\tau+\int_0^T m_{ci}l_{ai}l_{ci}\dot{\varphi}_{si}^2\dot{\varphi}_{ci}\sin(\varphi_{ci}-\varphi_{si})d\tau. \tag{8}$$

The fourth component describes the energy transferred by the lower pendula (via the upper pendula) to the oscillating beam:

$$W_{ci}^{SYN}=\int_0^T m_{ci}l_{ci}\ddot{x}\dot{\varphi}_{ci}\cos\varphi_{ci}d\tau. \tag{9}$$

The part of energy dissipated by lower pendula in the joints which connect lower and upper pendula is given by the following component:

$$W_{csi}^{DAMP}=\int_0^T c_{\varphi ci}(\dot{\varphi}_{ci}-\dot{\varphi}_{si})\dot{\varphi}_{ci}d\tau. \tag{10}$$

The last component on the left hand side of Eq. (7) represents the work performed by the gravitational force during one period of oscillations which due to the potential character of this force is equal to zero:

$$W_{ci}^{POT}=\int_0^T m_{ci}l_{ci}\dot{\varphi}_{ci}\sin\varphi_{ci}d\tau=0. \tag{11}$$

Integral on the right hand side of Eq. (7) describes the part of the work performed by the escapement mechanism, i.e., the part of this work which is connected with the motion of the lower pendula:

$$W_{ci}^{DRIVE}=\int_0^T N_{Di}\dot{\varphi}_{ci}d\tau. \tag{12}$$

Substituting Eqs. (8)–(12) into Eq. (7) one gets the energy balance of the lower pendula:

$$W_{ci}^{INERT}+W_{ci}^{SYN}+W_{csi}^{DAMP}=W_{ci}^{DRIVE}. \tag{13}$$

Next multiplying Eq. (5) by the angular velocity of the upper pendula and integrating it over the period T we obtain the equation of the energy balance:

$$\int_0^T m_{si}l_{si}^2\ddot{\varphi}_{si}\dot{\varphi}_{si}d\tau+\int_0^T m_{ci}l_{ai}^2\ddot{\varphi}_{si}\dot{\varphi}_{si}d\tau+\int_0^T m_{ci}l_{ai}l_{ci}\ddot{\varphi}_{ci}\dot{\varphi}_{si}\cos(\varphi_{ci}-\varphi_{si})d\tau-\int_0^T m_{ci}l_{ai}l_{ci}\dot{\varphi}_{ci}^2\dot{\varphi}_{si}\sin(\varphi_{ci}-\varphi_{si})d\tau$$
$$+\int_0^T m_{si}l_{si}\ddot{x}\dot{\varphi}_{si}\cos\varphi_{si}d\tau+\int_0^T m_{ci}l_{ai}\ddot{x}\dot{\varphi}_{si}\cos\varphi_{si}d\tau+\int_0^T c_{\varphi si}\dot{\varphi}_{si}\dot{\varphi}_{si}d\tau-\int_0^T c_{\varphi ci}(\dot{\varphi}_{ci}-\dot{\varphi}_{si})\dot{\varphi}_{si}d\tau$$
$$+\int_0^T m_{si}l_{si}\dot{\varphi}_{si}\sin\varphi_{si}d\tau+\int_0^T m_{ci}l_{ai}\dot{\varphi}_{si}\sin\varphi_{si}d\tau=\int_0^T -N_{Di}\dot{\varphi}_{si}d\tau. \tag{14}$$

The first four components on the left hand side of Eq. (14) represent the work performed by the forces with which the upper pendula act on the lower pendula:

$$W_{si}^{INERT}=\int_0^T m_{si}l_{si}^2\ddot{\varphi}_{si}\dot{\varphi}_{si}d\tau+\int_0^T m_{ci}l_{ai}^2\ddot{\varphi}_{si}\dot{\varphi}_{si}d\tau+\int_0^T m_{ci}l_{ai}l_{ci}\ddot{\varphi}_{ci}\dot{\varphi}_{si}\cos(\varphi_{ci}-\varphi_{si})d\tau-\int_0^T m_{ci}l_{ai}l_{ci}\dot{\varphi}_{ci}^2\dot{\varphi}_{si}\sin(\varphi_{ci}-\varphi_{si})d\tau. \tag{15}$$

The next two components represent the energy transferred to the oscillating beam by upper pendula:

$$W_{si}^{SYN}=\int_0^T m_{si}l_{si}\ddot{x}\dot{\varphi}_{si}\cos\varphi_{si}d\tau+\int_0^T m_{ci}l_{ai}\ddot{x}\dot{\varphi}_{si}\cos\varphi_{si}d\tau. \tag{16}$$

The energy dissipated in the joints which connect upper pendula to the beam M is given by the following component:

$$W_{si}^{DAMP}=\int_0^T c_{\varphi si}\dot{\varphi}_{si}\dot{\varphi}_{si}d\tau. \tag{17}$$

The next component represents the part of the energy dissipated in the joints which connect lower and upper pendula (the part connected with the motion of the upper pendula):

$$W_{sci}^{DAMP}=-\int_0^T c_{\varphi ci}(\dot{\varphi}_{ci}-\dot{\varphi}_{si})\dot{\varphi}_{si}d\tau. \tag{18}$$

The last two components on the left hand side of Eq. (14) represent the work performed by the gravitational force during one period of oscillations which due to the potential character of this force is equal to zero:

$$W_{si}^{POT}=\int_0^T m_{si}l_{si}\dot{\varphi}_{si}\sin\varphi_{si}d\tau+\int_0^T m_{ci}l_{ai}\dot{\varphi}_{si}\sin\varphi_{si}d\tau=0. \tag{19}$$

The integral on the right hand side of Eq. (14) describes the part of the work performed by the escapement mechanism, i.e., the part of this work which is connected with the motion of the upper pendula:

$$W_{si}^{DRIVE}=\int_0^T -N_{Di}\dot{\varphi}_{si}d\tau. \tag{20}$$

Substituting Eqs. (15)–(20) into Eq. (14) one gets the energy balance of the upper pendula:

$$W_{si}^{INERT}+W_{si}^{SYN}+W_{si}^{DAMP}+W_{sci}^{DAMP}=W_{si}^{DRIVE}. \tag{21}$$

Adding Eq. (13) to Eq. (21) we get the equation describing the energy balance of the double pendula:

$$W_{ci}^{INERT}+W_{ci}^{SYN}+W_{csi}^{DAMP}+W_{si}^{INERT}+W_{si}^{SYN}+W_{si}^{DAMP}+W_{sci}^{DAMP}=W_{ci}^{DRIVE}+W_{si}^{DRIVE}. \tag{22}$$

Taking into consideration that $W_{ci}^{INERT}+W_{si}^{INERT}=0$ one can rewrite Eq. (22) in the following form:

$$W_{i}^{SYN}+W_{ci}^{DAMP}+W_{si}^{DAMP}=W_{i}^{DRIVE}, \tag{23}$$

where the synchronization energy, i.e., the energy transferred by each double pendulum to the beam is given by:

$$W_{i}^{SYN}=\int_0^T m_{ci}l_{ci}\ddot{x}\dot{\varphi}_{ci}\cos\varphi_{ci}d\tau+\int_0^T (m_{ci}l_{ai}+m_{si}l_{si})\ddot{x}\dot{\varphi}_{si}\cos\varphi_{si}d\tau, \tag{24}$$

the energy dissipated in the joint connecting upper and lower pendula by:

$$W_{csi}^{DAMP}=\int_0^T c_{\varphi ci}(\dot{\varphi}_{ci}-\dot{\varphi}_{si})^2d\tau, \tag{25}$$

the energy dissipated in the joint connecting double pendula to the beam by:

$$W_{si}^{DAMP} = \int_0^T c_{\varphi si}\dot{\varphi}_{si}^2 d\tau \tag{26}$$

and the energy given by the escapement mechanizm by:

$$W_i^{DRIVE} = \int_0^T N_{Di}(\dot{\varphi}_{ci} - \dot{\varphi}_{si})d\tau. \tag{27}$$

Multiplying Eq. (6) by the velocity of the beam and integrating it over the period T we obtain the equation of the energy balance of the beam:

$$\begin{aligned}&\int_0^T \left(m_B + \sum_{i=1}^{2}(m_{ci}+m_{si})\right)\ddot{x}\dot{x}d\tau + \int_0^T c_x\dot{x}\dot{x}d\tau + \int_0^T k_x x\dot{x}d\tau \\ &= \int_0^T \left(\sum_{i=1}^{2}(m_{si}l_{si}+m_{ci}l_{ai})(-\ddot{\varphi}_{si}\cos\varphi_{si} + \dot{\varphi}_{si}^2\sin\varphi_{si})\right)\dot{x}d\tau + \int_0^T \left(\sum_{i=1}^{2} m_{ci}l_{ci}(-\ddot{\varphi}_{ci}\cos\varphi_{ci} + \dot{\varphi}_{ci}^2\sin\varphi_{ci})\right)\dot{x}d\tau.\end{aligned} \tag{28}$$

The first component on the left hand side of Eq. (28) represents the increase of the kinematic energy of the beam M and both double pendula during period T which should be equal to zero (as the oscillations are periodic):

$$W_b^{INERT} = \int_0^T \left(m_B + \sum_{i=1}^{2}(m_{ci}+m_{si})\right)\ddot{x}\dot{x}d\tau = 0. \tag{29}$$

The next component represents the energy dissipated in the damper c_x:

$$W_b^{DAMP} = \int_0^T c_x\dot{x}\dot{x}d\tau. \tag{30}$$

The last component on the left hand side described the work performed by the force in the spring k_x which due to the potential character of this force is equal to zero:

$$W_b^{POT} = \int_0^T k_x x\dot{x}d\tau = 0. \tag{31}$$

The right hand side of Eq. (28) gives the resultant force with which both double pendula act on the beam so:

$$W_b^{SYN} = \int_0^T \left(\sum_{i=1}^{2}(m_{si}l_{si}+m_{ci}l_{ai})(-\ddot{\varphi}_{si}\cos\varphi_{si} + \dot{\varphi}_{si}^2\sin\varphi_{si})\right)\dot{x}d\tau + \int_0^T \left(\sum_{i=1}^{2} m_{ci}l_{ci}(-\ddot{\varphi}_{ci}\cos\varphi_{ci} + \dot{\varphi}_{ci}^2\sin\varphi_{ci})\right)\dot{x}d\tau. \tag{32}$$

Substituting Eqs. (29)–(32) into Eq. (28) one gets the energy balance of the beam in the form:

$$W_b^{DAMP} = W_b^{SYN}. \tag{33}$$

Adding together Eqs. (23) and (33) we get the energy balance of the whole system in the following form:

$$W_1^{SYN} + W_{c1}^{DAMP} + W_{s1}^{DAMP} + W_2^{SYN} + W_{c2}^{DAMP} + W_{s2}^{DAMP} + W_b^{DAMP} = W_1^{DRIVE} + W_2^{DRIVE} + W_b^{SYN}. \tag{34}$$

During the steady periodic oscillations the energy supplied by the escapement mechanisms is dissipated by the dampers, i.e.:

$$W_{c1}^{DAMP} + W_{s1}^{DAMP} + W_{c2}^{DAMP} + W_{s2}^{DAMP} + W_b^{DAMP} = W_1^{DRIVE} + W_2^{DRIVE} \tag{35}$$

and

$$W_1^{SYN} + W_2^{SYN} = W_b^{SYN}, \tag{36}$$

i.e., energy transferred to the beam by double pendula is equal to the work performed by the reaction forces in the joints connecting the pendula to the beam.

4. Synchronous configurations in the system with identical pendula

Let us consider the system with identical double pendula ($l_{c1} = l_{c2},\ l_{s1} = l_{s2},\ l_{a1} = l_{a2},\ m_{c1} = m_{c2},\ m_{s1} = m_{s2}$). Neglecting the damping and the energy supplied by the escapement mechanism (see Eq. 25) one can rewrite Eq. (23) in the following form:

$$W_i^{SYN} = 0, \quad i = 1,2 \tag{37}$$

and considering Eq. (33):

$$W_b^{SYN} = W_b^{DAMP} = 0 \tag{38}$$

In the small amplitudes' limit the oscillations of the double pendula can be approximated by harmonic functions:

$$\begin{aligned} \varphi_{ci} &= \Phi_{ci} \sin(\tau + \beta_{ci}) \\ \varphi_{si} &= \Phi_{si} \sin(\tau + \beta_{si}) \end{aligned} \tag{39}$$

so their velocities and accelerations are as follow:

$$\begin{aligned} \dot{\varphi}_{ci} &= \Phi_{ci} \cos(\tau + \beta_{ci}) \\ \dot{\varphi}_{si} &= \Phi_{si} \cos(\tau + \beta_{si}) \\ \ddot{\varphi}_{ci} &= -\Phi_{ci} \sin(\tau + \beta_{ci}) \\ \ddot{\varphi}_{si} &= -\Phi_{si} \sin(\tau + \beta_{si}) \end{aligned} \tag{40}$$

Substituting Eqs. (39) and (40) into Eq. (6) (and neglecting damping) one gets:

$$\begin{aligned} \left(m_B + \sum_{i=1}^{2}(m_{ci} + m_{si})\right)\ddot{x} + k_x x = &\sum_{i=1}^{2}(m_{si}l_{si} + m_{ci}l_{ai})\left(\Phi_{si}\sin(\tau + \beta_{si}) + \Phi_{si}^3 \cos^2(\tau + \beta_{si})\sin(\tau + \beta_{si})\right) \\ &+ \sum_{i=1}^{2} m_{ci}l_{ci}\left(\Phi_{ci}\sin(\tau + \beta_{ci}) + \Phi_{ci}^3 \cos^2(\tau + \beta_{ci})\sin(\tau + \beta_{ci})\right). \end{aligned} \tag{41}$$

Taking into account the relation:

$$\cos^2\gamma \sin\gamma = 0.25\sin\gamma + 0.25\sin 3\gamma$$

and indicating

$$U = m_b + \sum_{i=1}^{2}(m_{ci} + m_{si})$$

Eq. (41) can be rewriten in the following form:

$$U\ddot{x} + k_x x = \sum_{i=1}^{2}(F_{si}\sin(\tau + \beta_{si}) + G_{si}\sin(3\tau + 3\beta_{si})) + \sum_{i=1}^{2}(F_{ci}\sin(\tau + \beta_{ci}) + G_{ci}\sin(3\tau + 3\beta_{ci})), \tag{42}$$

where

$$\begin{aligned} F_{si} &= (m_{si}l_{si} + m_{ci}l_{ai})\left(\Phi_{si} + \frac{1}{4}\Phi_{si}^3\right), \quad G_{si} = \frac{1}{4}(m_{si}l_{si} + m_{ci}l_{ai})\Phi_{si}^3, \\ F_{ci} &= (m_{ci}l_{ci})\left(\Phi_{ci} + \frac{1}{4}\Phi_{ci}^3\right), G_{ci} = \frac{1}{4}(m_{ci}l_{ci})\Phi_{ci}^3. \end{aligned}$$

The particular solution of Eq. (42) is given by:

$$x = \sum_{i=1}^{2}(X_{si}\sin(\tau + \beta_{si}) + Q_{si}\sin(3\tau + 3\beta_{si})) + \sum_{i=1}^{2}(X_{ci}\sin(\tau + \beta_{ci}) + Q_{ci}\sin(3\tau + 3\beta_{ci})), \tag{43}$$

where

$$X_{si} = \frac{F_{si}}{k_x - U}, \quad Q_{si} = \frac{G_{si}}{k_x - 9U}, \quad X_{ci} = \frac{F_{ci}}{k_x - U}, \quad Q_{ci} = \frac{F_{ci}}{k_x - 9U}.$$

The acceleration of the beam is given in the following form:

$$\ddot{x} = \sum_{i=1}^{2}(A_{si}\sin(\tau + \beta_{si}) + D_{si}\sin(3\tau + 3\beta_{si})) + \sum_{i=1}^{2}(A_{ci}\sin(\tau + \beta_{ci}) + D_{ci}\sin(3\tau + 3\beta_{ci})) \tag{44}$$

where $A_{si} = -X_{si},\ D_{si} = -9Q_{si},\ A_{ci} = -X_{ci},\ D_{ci} = -9Q_{ci}$.

In the state of synchronization of the periodic oscillations of identical pendula the phase angles β_{ci} and β_{si} are constant and independent of the initial conditions. There is no energy transfer from one double pendulum to the other one via the beam so the synchronization energy (24) has to be equal to zero. Substituting Eq. (24) into Eq. (37) and considering Eqs. (40) and (44) one gets:

$$W_k^{SYN} = \int_0^T m_{ck} l_{ck} \ddot{x} \dot{\varphi}_{ck} \cos\varphi_{ck} d\tau + \int_0^T (m_{ck} l_{ak} + m_{sk} l_{sk}) \ddot{x} \dot{\varphi}_{sk} \cos\varphi_{sk} d\tau$$
$$= \int_o^T m_{ck} l_{ck} \left(\sum_{i=1}^{2} (A_{si} \sin(\tau + \beta_{si}) + D_{si} \sin(3\tau + 3\beta_{si})) + \sum_{i=1}^{2} (A_{ci} \sin(\tau + \beta_{ci}) + D_{ci} \sin(3\tau + 3\beta_{ci})) \right)$$
$$\Phi_{ck} \cos(\tau + \beta_{ck}) d\tau + \int_o^T (m_{ck} l_{ak} + m_{sk} l_{sk}) \left(\sum_{i=1}^{2} (A_{si} \sin(\tau + \beta_{si}) + D_{si} \sin(3\tau + 3\beta_{si})) + \sum_{i=1}^{2} (A_{ci} \sin(\tau + \beta_{ci}) \right.$$
$$\left. + D_{ci} \sin(3\tau + 3\beta_{ci})) \right) \Phi_{sk} \cos(\tau + \beta_{sk}) d\tau = 0, \tag{45}$$

where $k = 1,2$. Further calculations lead to the following form:

$$W_k^{SYN} = m_{ck} l_{ck} \Phi_{ck} \pi \left(\sum_{i=1}^{2} (A_{si} \sin(\beta_{si} - \beta_{ck}) + A_{ci} \sin(\beta_{ci} - \beta_{ck})) \right)$$
$$+ (m_{ck} l_{ck} + m_{sk} l_{sk}) \Phi_{sk} \pi \left(\sum_{i=1}^{2} (A_{si} \sin(\beta_{si} - \beta_{sk}) + A_{ci} \sin(\beta_{ci} - \beta_{sk})) \right) = 0. \tag{46}$$

Eq. (46) is fulfilled for both double pendula (i.e., for $i = 1,2$, $k = 1,2$) when:

$$\begin{aligned} &\sin(\beta_{si} - \beta_{ck}) = 0.0, \\ &\sin(\beta_{ci} - \beta_{ck}) = 0.0, \\ &\sin(\beta_{si} - \beta_{sk}) = 0.0, \\ &\sin(\beta_{ci} - \beta_{sk}) = 0.0. \end{aligned} \tag{47}$$

Assuming that $\beta_{c1} = 0^o$ (one phase angle can be arbitrarily taken) one can show that Eq. (47) is fulfilled by all combinations of phase angles where $\beta_{c2}, \beta_{s1}, \beta_{s2} = 0$ or π, i.e., both double pendula simultaneously go through the stable equilibrium position and simultaneously reach the maximum displacements.

Eqs. (47) and (39) allow the identification of the following synchronous configurations:

(i) $\beta_{s1} = 0,\ \beta_{s2} = \pi,\ \beta_{c1} = 0,\ \beta_{c2} = \pi$, the upper pendula are in the antiphase, i.e., $\varphi_{s1} = -\varphi_{s2},\ \varphi_{c1} = -\varphi_{c2}$ and the upper and the lower pendula of both double pendula are in the phase, i.e., $\dot{\varphi}_{c1} > 0 \Rightarrow \dot{\varphi}_{s1} > 0,\ \dot{\varphi}_{c2} < 0,\ \dot{\varphi}_{s2} < 0$ (**AAP** in Fig. 2(a)).

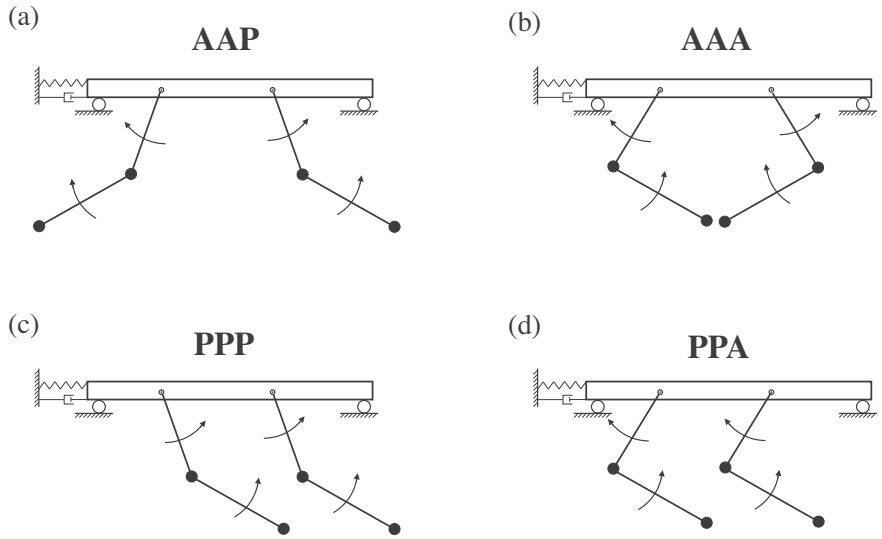

Fig. 2. Synchronous configurations of two identical double pendula: (a) $\beta_{s1} = 0,\ \beta_{s2} = \pi,\ \beta_{c1} = 0,\ \beta_{c2} = \pi$, the upper and the lower pendula of both double pendula are in the antiphase, i.e., $\varphi_{s1} = -\varphi_{s2},\ \varphi_{c1} = -\varphi_{c2}$ and the upper and the lower pendula of both double pendula are in the phase, i.e., $\dot{\varphi}_{c1} > 0 \Rightarrow \dot{\varphi}_{s1} > 0,\ \dot{\varphi}_{c2} < 0,\ \dot{\varphi}_{s2} < 0$ (**AAP**), (b) $\beta_{s1} = 0,\ \beta_{s2} = \pi,\ \beta_{c1} = \pi,\ \beta_{c2} = 0$, the upper and the lower pendula of both double pendula are in the antiphase, i.e., $\varphi_{s1} = -\varphi_{s2},\ \varphi_{c1} = -\varphi_{c2}$ and the upper and the lower pendula of both double pendula are in the antiphase, i.e., $\dot{\varphi}_{c1} > 0 \Rightarrow \dot{\varphi}_{s1} < 0,\ \dot{\varphi}_{c2} < 0,\ \dot{\varphi}_{s2} > 0$ (**AAA**), (c) $\beta_{s1} = 0,\ \beta_{s2} = 0,\ \beta_{c1} = 0,\ \beta_{c2} = 0$, both double pendula move identically, i.e., $\varphi_{s1} = \varphi_{s2},\ \varphi_{c1} = \varphi_{c2}$ and the upper and the lower pendula of both double pendula are in the phase, i.e., $\dot{\varphi}_{c1} > 0 \Rightarrow \dot{\varphi}_{s1} > 0,\ \dot{\varphi}_{c2} > 0,\ \dot{\varphi}_{s2} > 0$ (**PPP**), (d) $\beta_{s1} = 0,\ \beta_{s2} = 0,\ \beta_{c1} = \pi,\ \beta_{c2} = \pi$, both double pendula move identically, i.e., $\varphi_{s1} = \varphi_{s2},\ \varphi_{c1} = \varphi_{c2}$ and the upper and the lower pendula of both double pendula are in the antiphase, i.e., $\dot{\varphi}_{c1} > 0 \Rightarrow \dot{\varphi}_{s1} < 0,\ \dot{\varphi}_{c2} > 0,\ \dot{\varphi}_{s2} < 0$ (**PPA**).

(ii) $\beta_{s1}=0,\ \beta_{s2}=\pi,\ \beta_{c1}=\pi,\ \beta_{c2}=0$, the upper pendula of both double pendula are in the antiphase, i.e., $\varphi_{s1}=-\varphi_{s2},\ \varphi_{c1}=-\varphi_{c2}$ and the upper and the lower pendula of both double pendula are in the antiphase, i.e., $\dot{\varphi}_{c1}>0\Rightarrow\dot{\varphi}_{s1}<0,\ \dot{\varphi}_{c2}<0,\ \dot{\varphi}_{s2}>0$ (**AAA** in Fig. 2(b)).
(iii) $\beta_{s1}=0,\ \beta_{s2}=0,\ \beta_{c1}=0,\ \beta_{c2}=0$, both double pendula move identically, i.e., $\varphi_{s1}=\varphi_{s2},\ \varphi_{c1}=\varphi_{c2}$ and the upper and the lower pendula of both double pendula are in the phase, i.e., $\dot{\varphi}_{c1}>0\Rightarrow\dot{\varphi}_{s1}>0,\ \dot{\varphi}_{c2}>0,\ \dot{\varphi}_{s2}>0$ (**PPP** in Fig. 2(c)).
(iv) $\beta_{s1}=0,\ \beta_{s2}=0,\ \beta_{c1}=\pi,\ \beta_{c2}=\pi$, both double pendula move identically, i.e., $\varphi_{s1}=\varphi_{s2},\ \varphi_{c1}=\varphi_{c2}$ and the upper and the lower pendula of both double pendula are in the antiphase, i.e., $\dot{\varphi}_{c1}>0\Rightarrow\dot{\varphi}_{s1}<0,\ \dot{\varphi}_{c2}>0,\ \dot{\varphi}_{s2}<0$ (**PPA** in Fig. 2(d)). In the cases (i–ii) the beam is at rest while in the cases (iii–iv) it oscillates harmonically and its oscillations are in the antiphase to the oscillations of the upper pendula.

Note that the conditions given by Eq. (45) allow also for non-symmetrical configurations given by $(\beta_{s1}=0,\ \beta_{s2}=0,\ \beta_{c1}=0,\ \beta_{c2}=\pi)$, $(\beta_{s1}=0,\ \beta_{s2}=\pi,\ \beta_{c1}=0,\ \beta_{c2}=0)$, $(\beta_{s1}=0,\ \beta_{s2}=0,\ \beta_{c1}=\pi,\ \beta_{c2}=0)$ or $(\beta_{s1}=0,\ \beta_{s2}=\pi,\ \beta_{c1}=\pi,\ \beta_{c2}=\pi)$. In these configurations both double pendula have to reach different normal modes of oscillations for the same frequency (as required by Eqs. (39)), which is proven to be impossible in the small oscillations' approximation [1].

5. Numerical results

5.1. Two identical double pendula

We consider the examples of synchronous configurations and the bifurcation diagrams showing the dependence of the type of the synchronous state on the initial conditions and system parameters. Our results have been obtained by numerical integration (by 4th order Runge–Kutta method) of Eqs. (4)–(6). In our calculations we consider the following values of the system parameters (identical double pendula):$m_{ci}=1,\ m_{si}=1,\ m_B=10,\ l_{ci}=1,\ l_{si}=1,\ c_{\varphi ci}=0.01,\ c_{\varphi si}=0.01,\ c_x=3.4147,\ N_{Di}=0.02,\ i=1,2$. The escapement mechanisms work In the range $-\gamma_c<\varphi_{ci}<\gamma_c,\ \gamma_c=5^\circ$. The damping coefficient of the beam c_x gives the assumed logarithmic decrement of damping $\Delta=\ln(1.5)$ for the stiffness coefficient $k_x=50.0$. The stiffness coefficient k_x has been taken as a bifurcation parameter.

Fig. 3(a)–(d) presents the examples of four synchronous configurations introduced in Section 4 (Fig. 2(a)–(d)). We show time series of the double pendula's $\varphi_{ci}, \varphi_{si}$ and beam's x (for better visibility 10 times enlarged) displacements versus dimensionless time τ. The intervals of existence of these configurations and energy balances which are associated with them are presented in Figs. 4(a)–(d), 5(a)–(c) and 6(a)–(c).

Fig. 3(a) shows the configurations **AAP**: the upper pendula of both double pendula are in the antiphase, i.e., $\varphi_{s1}=-\varphi_{s2},\ \varphi_{c1}=-\varphi_{c2}$ and the upper and the lower pendula of both double pendula are in the phase, i.e., $\dot{\varphi}_{c1}>0\Rightarrow\dot{\varphi}_{s1}>0,\ \dot{\varphi}_{c2}<0,\ \dot{\varphi}_{s2}<0$. This configuration is stable for $5.0<k_x<500.0$. The energy supplied by the escapement mechanism is dissipated by the pendula's dampers and the beam is at rest:

$$W_{c1}^{DAMP}+W_{s1}^{DAMP}=W_1^{DRIVE},$$
$$W_{c2}^{DAMP}+W_{s2}^{DAMP}=W_2^{DRIVE},$$
$$W_1^{SYN}=W_2^{SYN}=W_b^{SYN}=W_b^{DAMP}=0.0.$$

The energy balance during this configuration is shown in Fig. 5(a). Synchronous configuration **AAA** is shown in Fig. 3(b): the upper pendula of both double pendula are in the antiphase, i.e., $\varphi_{s1}=-\varphi_{s2},\ \varphi_{c1}=-\varphi_{c2}$ and the upper and the lower pendula of both double pendula are in the antiphase, i.e., $\dot{\varphi}_{c1}>0\Rightarrow\dot{\varphi}_{s1}<0,\ \dot{\varphi}_{c2}<0,\ \dot{\varphi}_{s2}>0$. This configuration coexists with the configuration **AAP** for $5.0<k_x<500.0$. The energy balances of **AAP** and **AAA** configurations are the same (see Fig. 5(a)). Fig. 3(c) shows **PPP** configuration: both double pendula move identically, i.e., $\varphi_{s1}=\varphi_{s2},\ \varphi_{c1}=\varphi_{c2}$ and the upper and the lower pendula of both double pendula are in the phase, i.e., $\dot{\varphi}_{c1}>0\Rightarrow\dot{\varphi}_{s1}>0,\ \dot{\varphi}_{c2}>0,\ \dot{\varphi}_{s2}>0$. At this configuration part of the energy supplied by the escapement mechanisms is dissipated by the pendula dampers and the rest (synchronization energy) is transferred to the beam. The energy transferred by double pendula excites the beam's oscillations and is dissipated by the beam damper c_x:

$$W_{c1}^{DAMP}+W_{s1}^{DAMP}+W_1^{SYN}=W_1^{DRIVE},$$
$$W_{c2}^{DAMP}+W_{s2}^{DAMP}+W_2^{SYN}=W_2^{DRIVE}.$$
$$W_1^{SYN}+W_2^{SYN}=W_b^{SYN}=W_b^{DAMP}$$

The energy balance during this configuration is shown in Fig. 5(b). The configuration **PPA** is shown in Fig. 3(d): both double pendula move identically, i.e., $\varphi_{s1}=\varphi_{s2},\ \varphi_{c1}=\varphi_{c2}$ and the upper and the lower pendula of both double pendula are in the antiphase, i.e., $\dot{\varphi}_{c1}>0\Rightarrow\dot{\varphi}_{s1}<0,\ \dot{\varphi}_{c2}>0,\ \dot{\varphi}_{s2}<0$. The energy balance for **PPA** and **PPP** configurations are the same (see Fig. 5(b)).

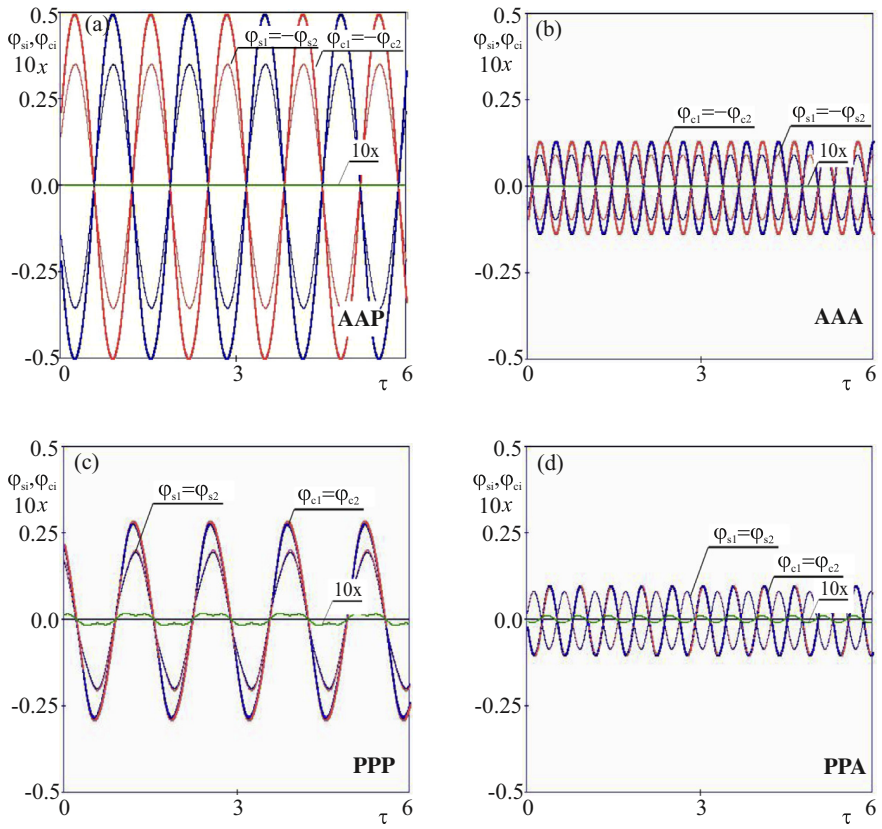

Fig. 3. Time series of double pendula' φ_{ci}, φ_{si} and beam's x (for better visibility 10 times enlarged) displacements versus dimensionless time τ illustrating different synchronous configurations of two identical double pendula: $m_{ci}=1,\ m_{si}=1,\ m_B=10,\ l_{ci}=1,\ l_{si}=1,\ c_{\varphi ci}=0.01,\ c_{\varphi si}=0.01,\ c_x=3.4147,\ N_{Di}=0.02,\ i=1,2$, ($\varphi_{c1}$ – bold line, φ_{c2} – bold blue line, φ_{s1} – red line, φ_{s1} – blue line, x – green line), (a) **AAP** synchronization, $k_x=50.0$, (b) **AAA** synchronization, $k_x=300.0$, (c) **PPP** synchronization, $k_x=50.0$ (different initial conditions than in (a)), (d) **PPA** synchronization, $k_x=5.0$. (For interpretation of the references to colour in this figure legend, the reader is referred to the web version of this article.)

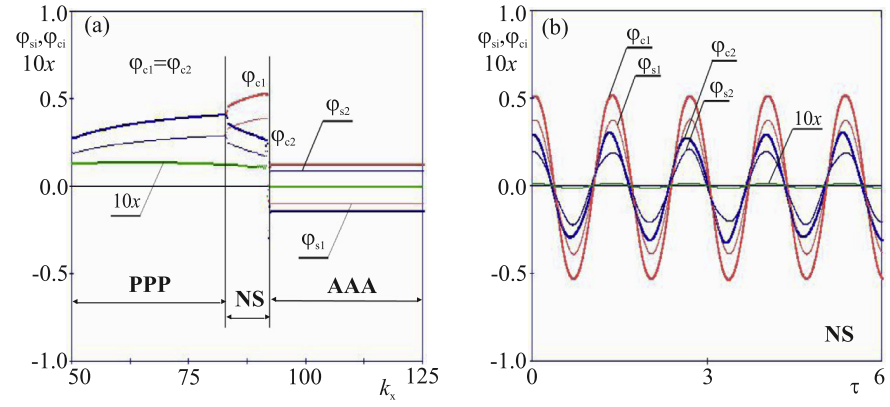

Fig. 4. Transition from **PPP** to **AAA** synchronous configurations of two identical double pendula: $m_{ci}=1,\ m_{si}=1,\ m_B=10,\ l_{ci}=1,\ l_{si}=1,\ c_{\varphi ci}=0.01,\ c_{\varphi si}=0.01,\ c_x=3.4147,\ N_{Di}=0.02,\ i=1,2$, ($\varphi_{c1}$ – bold line, φ_{c2} – bold blue line, φ_{s1} – red line, φ_{s1} – blue line, x – green line); (a) bifurcation diagram showing the transition from **AAP** to **AAA** synchronous configurations, (b) time series of the double pendula φ_{ci}, φ_{si} and the beam's x (for better visibility 10 times enlarged) displacements versus dimensionless time τ illustrating **NS** synchronous configuration, $k_x=88.0$. (For interpretation of the references to colour in this figure legend, the reader is referred to the web version of this article.)

Configurations **PPP** and **PPA** coexist with configurations **AAP** and **AAA** only in particular intervals of stiffness coefficient k_x. Fig. 4(a) presents the bifurcation diagram $\varphi_{si}, \varphi_{si}, x$ versus k_x. The calculations started for $k_x=50.0$ and the following initial conditions:

$$\varphi_{c1}=0.5,\quad \varphi_{s1}=0.5,\quad \varphi_{c2}=0.5,\quad \varphi_{s2}=0.5,\quad \dot{\varphi}_{c1}=0.0,\quad \dot{\varphi}_{s1}=0.0,\quad \dot{\varphi}_{c2}=0.0,\quad \dot{\varphi}_{s2}=0.0,$$
$$x=\dot{x}=0,$$

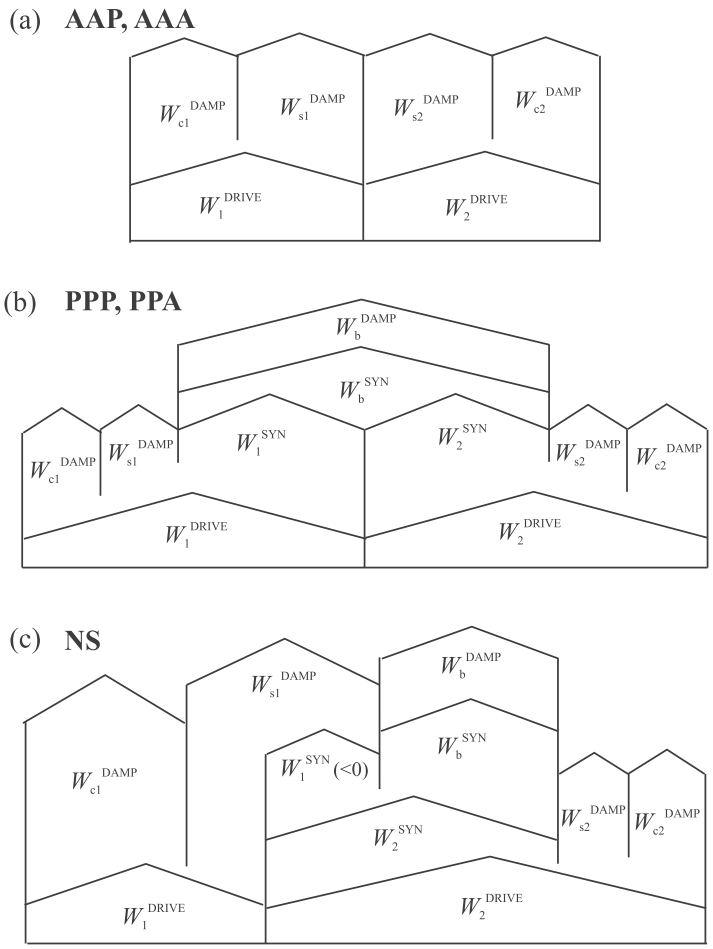

Fig. 5. Energy balances for different synchronous configurations; (a) **AAP** and **AAA** configurations, (b) **PPP** and **PPA** configurations, (c) **NS** configuration.

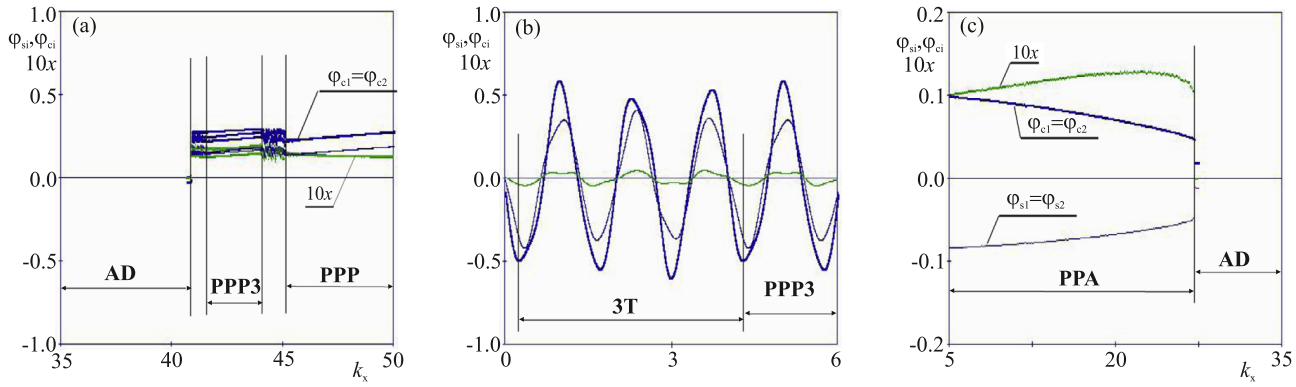

Fig. 6. Regions of existence of **PPP** and **PPA** synchronous configurations of two identical double pendula:$m_{ci}=1,\ m_{si}=1,\ m_B=10,\ l_{ci}=1,\ l_{si}=1,\ c_{\varphi ci}=0.01,\ c_{\varphi si}=0.01,\ c_x=3.4147,\ N_{Di}=0.02,\ i=1,2$, ($\varphi_{c1}$ – bold line, φ_{c2} – bold blue line, φ_{s1} – red line, φ_{s1} – blue line, x – green line); (a) bifurcation diagram showing the transition from **PPP** configuration to amplitude death **AD**, (b) time series of the double pendula' $\varphi_{ci}, \varphi_{si}$ and the beam's x (for better visibility 10 times enlarged) displacements versus dimensionless time τ illustrating **PPP3** synchronous configuration, $k_x=42.5$, (c) bifurcation diagram showing the transition from **PPA** configuration to amplitude death **AD**. (For interpretation of the references to colour in this figure legend, the reader is referred to the web version of this article.)

which lead to **PPP** configuration. The increase of the bifurcation parameter k_x leads to the loss of configuration's stability for $k_x=81.5$. In the interval $81.5<k_x<91.6$ we observe previously unpredicted nonsymetrical synchronization NS. For $k_x>91.6$ nonsymmetrical synchronization is replaced by the synchronous configuration AAA. Fig. 4(b) presents time series of the double pendula's $\varphi_{ci}, \varphi_{si}$ and beam's x (for better visibility 10 times enlarged) displacements versus dimensionless time τ during NS synchronization. The double pendula' oscillations during this type of synchronization are similar to the oscillations at **PPP** configuration, but pendula' amplitudes are not equal, i.e., $\varphi_{c1}\neq\varphi_{c2}$ and $\varphi_{s1}\neq\varphi_{s2}$. The amplitudes of

the oscillations of the lower and upper pendula of the first double pendulum are larger than the equivalent amplitudes of the second double pendulum, i.e., the first double pendulum is excited by the second one. Note that the phase shifts between the oscillations of both double pendula visible in Fig. 4(b) also indicate the energy transfer between double pendula. In this synchronous state the part of the energy supplied by the escapement mechanism of the second double pendulum is dissipated by the pendulum's dampers and the other part is transferred to the beam (synchronization energy W_2^{SYN}). Part of W_2^{SYN} excites the beam (W_b^{SYN}) and is dissipated in the beam damper c_x. The rest of synchronization energy W_2^{SYN} (denoted as W_1^{SYN})is transferred to the first double pendulum via the beam. The dampers of the first double pendulum dissipate the energy supplied by the escapement mechanism and the energy transferred from the second pendulum:

$$W_{c2}^{DAMP} + W_{s2}^{DAMP} + W_2^{SYN} = W_2^{DRIVE},$$
$$W_2^{SYN} = W_b^{SYN} + \left|W_1^{SYN}\right|; \quad W_1^{SYN} < 0,$$
$$W_b^{SYN} = W_b^{DAMP},$$
$$W_{c1}^{DAMP} + W_{s1}^{DAMP} = W_2^{DRIVE} + \left|W_1^{SYN}\right|.$$

The energy balance for nonsymmetrical configuration is shown in Fig. 5(c).

Fig. 6(a) shows the bifurcation diagram for decreasing values of k_x. We start from the configuration **PPP** (we use the same initial conditions as for the calculation of the diagram of Fig. 4(a)). The configuration **PPP** is stable down to the value $k_x = 45.2$. The deacrease of k_x causes the decrease of the amplitudes of both double pendula. At $k_x = 45.2$ the difference between amplitudes of upper and lower pendula $\varphi_{ci} - \varphi_{si}$ ($i = 1,2$) decreases below the γ_c what disturbs the regular operation of the escapement mechanisms. First, we observe chaotic oscillations of both double pendula for $45.2 > k_x > 44.0$. In the interval $44.0 > k_x > 41.4$ the escapement mechanisms become regular again but they supply smaller amounts of energy as every third impulse is missing. We observe synchronization **PPP3** which is similar to **PPP** but the pendula oscillate with three times longer periods. Time series of the pendula displacements during this synchronization are shown in Fig. 6(b).

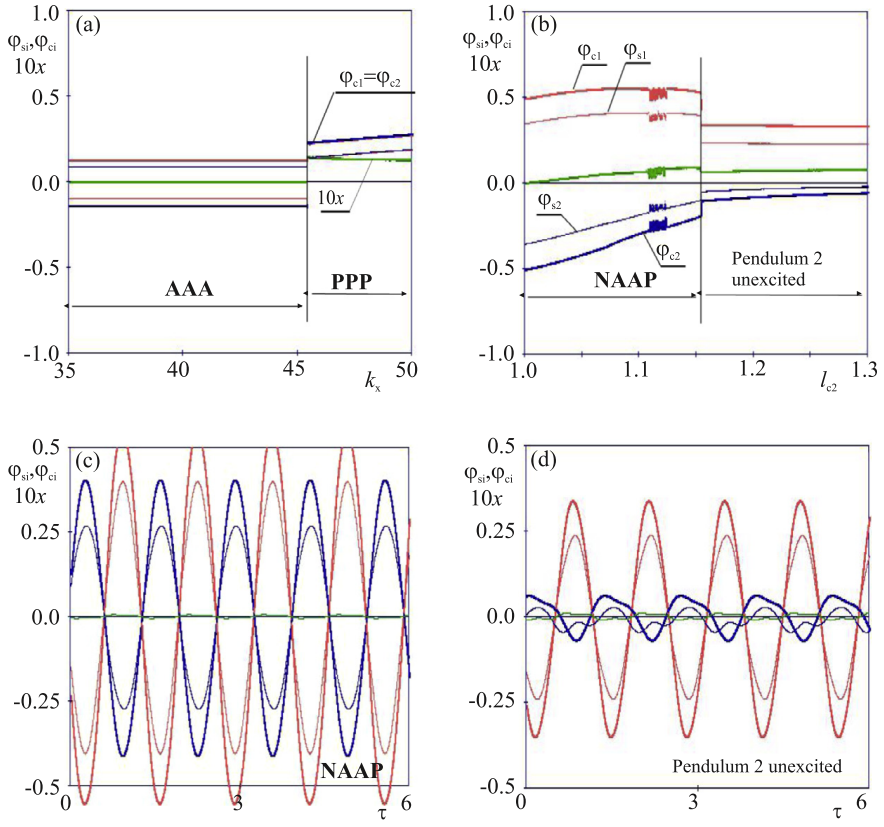

Fig. 7. Synchronization of the system with two nonidentical double pendula with different length (the length of the lower pendulum of double pendulum 2 l_{c2} has been taken as a control parameter, φ_{c1} – bold line, φ_{c2} – bold blue line, φ_{s1} – red line, φ_{s1} – blue line, x – green line); (a) bifurcation diagram showing the transition from **PPP** to AAA configuration $l_{c2} = 1.001$, (b) bifurcation diagram showing the transition from **NAAP** configuration to the turn off of the escapement mechanism of double pendulum 2, (c) time series of the double pendula $\varphi_{ci}, \varphi_{si}$ and the beam's x (for better visibility 10 times enlarged) displacements versus dimensionless time τ illustrating **NAAP** synchronous configuration, $l_{c2} = 1.051$, (d) time series of the double pendula $\varphi_{ci}, \varphi_{si}$ and the beam's x (for better visibility 10 times enlarged) displacements versus dimensionless time τ illustrating the oscillations in the case when the escapement mechanism of double pendulum 2 is turned off, $l_{c2} = 1.25$. (For interpretation of the references to colour in this figure legend, the reader is referred to the web version of this article.)

Further decrease of k_x leads to the chaotic oscillations in the interval $41.4 > k_x > 40.9$ and next to the amplitude death as the result of the turn off of the escapement mechanisms. Fig. 6(c) presents k_x interval for which the configuration **PPA** can be observed. In the numerical calculations we start from $k_x = 5.0$ and the following initial conditions:

$$\varphi_{c1} = -0.08, \quad \varphi_{s1} = 0.1, \quad \varphi_{c2} = -0.08, \quad \varphi_{s2} = 0.1, \quad \dot{\varphi}_{c1} = 0.0, \quad \dot{\varphi}_{s1} = 0.0, \quad \dot{\varphi}_{c2} = 0.0, \quad \dot{\varphi}_{s2} = 0.0,$$
$$x = 0.01, \quad \dot{x} = 0.0,$$

which lead to the stable **PPA** configuration. The increase of the stiffness coefficient k_x leads to the decrease of the amplitudes of the double pendula oscillations, the escapement mechanisms' turn off and finally to the amplitude death **AD** at $k_x = 27.0$.

5.2. Two nonidentical double pendula

To observe how the behavior of the system is sensitive to small parameter mismatch consider the bifurcation diagram shown in Fig. 7(a). Only one value of the system parameters slightly differs from that used in the calculations of bifurcation diagram of Fig. 6(a). We take $l_{c2} = 1.001$ (previously $l_{c2} = 1.000$ has been taken). The region of existence of the **PPP** configuration is the same as in Fig. 6(a) but at $k_x = 45.2$ we observe the jump to **AAA** configuration which is stable in the whole range of the considered values of k_x. In the bifurcation diagrams of Fig. 7(b) and 8(a) we fixed the value of $k_x = 50.0$ and consider the length l_{c2}as a bifurcation parameter. Calculating the bifurcation diagram of Fig. 7(b) we start from $l_{c2} = 1.0$ and the following initial conditions:

$$\varphi_{c1} = 0.5, \quad \varphi_{s1} = 0.5, \quad \varphi_{c2} = -0.5, \quad \varphi_{s2} = -0.5, \quad \dot{\varphi}_{c1} = 0.0, \quad \dot{\varphi}_{s1} = 0.0, \quad \dot{\varphi}_{c2} = 0.0, \quad \dot{\varphi}_{s2} = 0.0,$$
$$x = 0.0, \quad \dot{x} = 0.0,$$

which lead to stable **AAP** configuration shown in Fig. 3(a). The increase of length l_{c2} leads to the loss of symmetry. (For the case of unmovable beam the period of oscillations of double pendulum 2 would be larger than the period of double pendulum 1.) The oscillations of the beam cause the energy transfer from double pendulum 2 to double pendulum 1. The loss of the

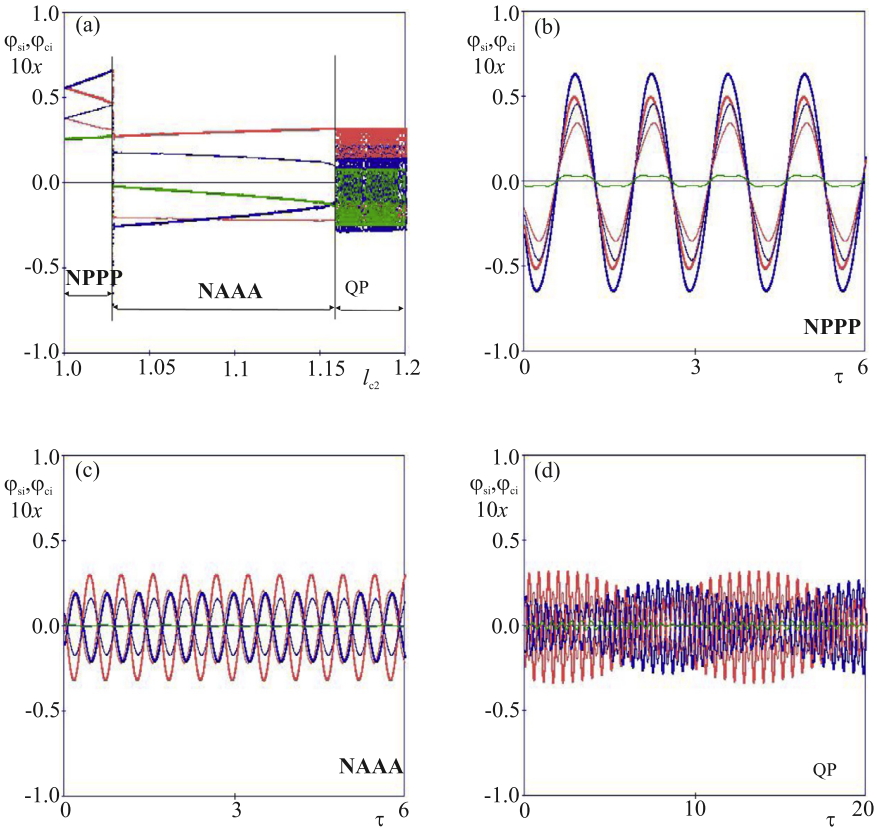

Fig. 8. Synchronization of the system with two double pendula with different length (the length of the lower pendulum of double pendulum 2 l_{c2} has been taken as a control parameter), (φ_{c1} – bold line, φ_{c2} – bold blue line, φ_{s1} – red line, φ_{s1} – blue line, x – green line); (a) bifurcation diagram showing the transition from **NPPP** configuration to quasiperiodic oscillations via **NAAA**configuration, (b) time series of the double pendula' $\varphi_{ci}, \varphi_{si}$ and the beam's x (for better visibility 10 times enlarged) displacements versus dimensionless time τ illustrating **NPPP** synchronous configuration, $l_{c2} = 1.02$, (c) time series of the double pendula' $\varphi_{ci}, \varphi_{si}$ and the beam's x (for better visibility 10 times enlarged) displacements versus dimensionless time τ illustrating **NAAA** synchronous configuration, $l_{c2} = 1.1005$, (d) time series of the double pendula's $\varphi_{ci}, \varphi_{si}$ and beam's x (for better visibility 10 times enlarged) displacements versus dimensionless time τ illustrating quasiperiodic oscillations **QP**, $l_{c2} = 1.19$. (For interpretation of the references to colour in this figure legend, the reader is referred to the web version of this article.)

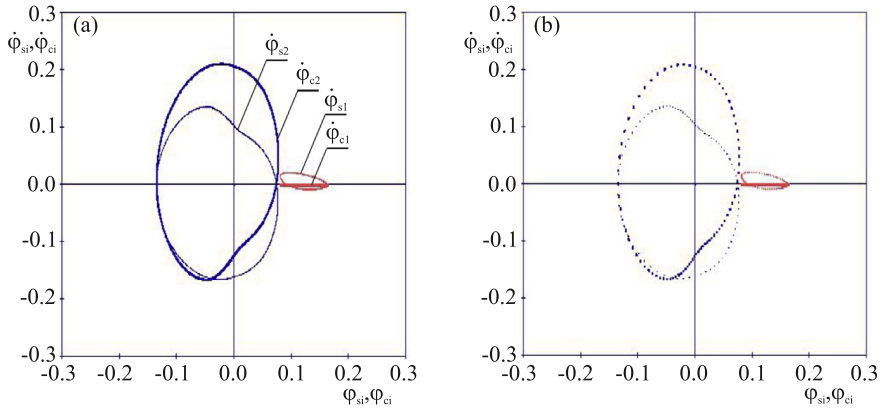

Fig. 9. Synchronization of the system with two double pendula with different length (the length of the lower pendulum of double pendulum 2 l_{c2} has been taken as a control parameter): (φ_{c1} – bold line, φ_{c2} – bold blue line, φ_{s1} – red line, φ_{s1} – blue line) (a) Poincare map showing quasiperiodic behavior, $l_{c2} = 1.19$, (b) Poincare map showing the long periodic window in quasiperiodic regime, $l_{c2} = 1.194$. (For interpretation of the references to colour in this figure legend, the reader is referred to the web version of this article.)

energy by double pendulum 2 and the increase of the energy of double pendulum 1 causes that the amplitudes of the pendulum 1 are larger than the amplitudes of pendulum 2 and the periods of oscillations of both double pendula are equal (due to the beam's oscillations). This type of nonsymmetrical synchronization is illustrated in Fig. 7(c) and indicated as **NAAP**. The energy balance during this synchronization is qualitatively similar to the balance of **NS** synchronization (see Fig. 5(c)). Synchronization configuration **NAAP** is stable up to the value $l_{c2} = 1.155$. Decreasing the amplitudes of the pendula' oscillations causes that for larger values of l_{c2} the escapement mechanism of double pendulum 2 is switched off and the whole system is excited by the escapement mechanism of double pendulum 1. Double pendulum 2 oscillates due to the energy supplied by pendulum 1 (via the beam). This behavior is illustrated in Fig. 7(d).

Fig. 8(a) shows the next bifurcation diagram where the length l_{c2} is a bifurcation parameter. It starts from $l_{c2} = 1.0$ and configuration **PPP** of Fig. 3(c) (we use the same initial conditions as in the calculations of Fig. 4(a)). The increase of l_{c2} leads to the loss of symmetry. We observe the energy transfer from double pendulum 1 to double pendulum 2 (the opposite case to the one described in Fig. 7(b)). The loss of energy by double pendulum 1 and the increase of the energy of double pendulum 2 causes that the amplitudes of pendulum 2 are larger than the amplitudes of pendulum 1 and the periods of oscillations of both double pendula are equal. **PPP** synchronous configuration is replaced by nonsymmetrical configuration **NPPP**. The time series of pendula's displacements characteristic for this configuration are shown in Fig. 8(b). The energy balance during this configuration is qualitatively the same as during **NS** configuration. Configuration **NPPP** is stable up to $l_{c2} = 1.029$ when we observe transition to next configuration **NAAA** shown in Fig. 8(c). **NAAA** configuration is stable in the interval $1.029 < l_{c2} < 1.16$. For larger values of l_{c2} double pendula' oscillations become quasiperiodic (the amount of energy transferred from double pendulum 2 to double pendulum 1 is not sufficient to keep the periods of both pendula equal). Time series characteristic for quasiperiodic oscillations are shown in Fig. 8(d).

The quasiperiodic character of the oscillations shown in Fig. 8(d) is proven on Poincare maps shown in Fig. 9(a) (for $l_{c2} = 1.19$). The map shows the angular velocities of the upper and lower pendula of both double pendula versus the displacements of these pendula. Both angular velocities and displacements are taken at the moments when the angular velocity of the lower pendulum of the first double pendulum changes the sign from positive to negative one. The maps shown in Fig. 9(a) consist of the closed curves which is characteristic for quasiperiodic behavior. Note the existence of the high-periodic windows in the quasiperiodic regime as can be seen in Fig. 9(b) (for $l_{c2} = 1.194$). The period oscillations is equal to 82T.

6. Conclusions

Our studies show that two double pendula self-exited by the escapement mechanism hanging from the horizontally movable beam can synchronize. For identical pendula four different synchronous configurations are possible: (i) the upper pendula of both double pendula are in the antiphase, (i.e., $\varphi_{s1} = -\varphi_{s2},\ \varphi_{c1} = -\varphi_{c2}$) and the upper and the lower pendula of both double pendula are in the phase, i.e., $\dot\varphi_{c1} > 0 \Rightarrow \dot\varphi_{s1} > 0,\ \dot\varphi_{c2} < 0,\ \dot\varphi_{s2} < 0$ (**AAP** in Fig. 2(a)), (ii) the upper pendula of both double pendula are in the antiphase, (i.e., $\varphi_{s1} = -\varphi_{s2}, \varphi_{c1} = -\varphi_{c2}$) and the upper and the lower pendula of both double pendula are in the antiphase, i.e., $\dot\varphi_{c1} > 0 \Rightarrow \dot\varphi_{s1} < 0,\ \dot\varphi_{c2} < 0,\ \dot\varphi_{s2} > 0$ (**AAA** in Fig. 2(b)), (iii) both double pendula move identically, i.e., $\varphi_{s1} = \varphi_{s2},\ \varphi_{c1} = \varphi_{c2}$ and the upper and the lower pendula of both double pendula are in the phase, i.e., $\dot\varphi_{c1} > 0 \Rightarrow \dot\varphi_{s1} > 0,\ \dot\varphi_{c2} > 0,\ \dot\varphi_{s2} > 0$ (**PPP** in Fig. 2(c)), (iv) both double pendula move identically, i.e., $\varphi_{s1} = \varphi_{s2},\ \varphi_{c1} = \varphi_{c2}$ and the upper and the lower pendula of both double pendula are in the antiphase, i.e., $\dot\varphi_{c1} > 0 \Rightarrow \dot\varphi_{s1} < 0,\ \dot\varphi_{c2} > 0,\ \dot\varphi_{s2} < 0$ (**PPA** in Fig. 2(d)). In the cases (i–ii) the beam is at rest while in the cases (iii–iv) it oscillates harmonically and its oscillations are in the antiphase to the oscillations of the upper pendula. When the pendula are nonidentical, i.e., have different lengths (and periods of oscillations) for small parameters' mismatch we observe the

synchronous states for which the phase difference between the pendula is close to 0 or π but for larger differences unsynchronized quasiperiodic or chaotic oscillations dominate. Similar synchronous states have been observed experimentally in [22] but to stabilize them the special controlling procedure has been applied.

The observed behavior of system (1) can be explained by the energy expressions derived in Section 3. which also show why other synchronous states are not possible. We give the evidence that the observed behavior of the system is robust as it occurs in the wide range of system parameters and can be observed experimentally.

Acknowledgment

This work was supported by the Foundation for Polish Science, Team Programme: Project No. TEAM-2010/5/5.

References

[1] Andronov A, Witt A, Khaikin S. Theory of oscillations. Oxford: Pergamon; 1966.
[2] Bennet M, Schatz MF, Rockwood H, Wiesenfeld K. Huygens's clocks. Proc R Soc Lond A 2002;458:563–79.
[3] Blekhman II. Synchronization in science and technology. New York: ASME; 1988.
[4] Czolczynski K, Perlikowski P, Stefanski A, Kapitaniak T. Clustering of Huygens' clocks. Prog Theor Phys 2009;122:1027–33.
[5] Czolczynski K, Perlikowski P, Stefanski A, Kapitaniak T. Clustering and synchronization of Huygens' clocks. Physica A 2009;388:5013–23.
[6] Czolczynski K, Perlikowski P, Stefanski A, Kapitaniak T. Why two clocks synchronize: energy balance of the synchronized clocks. Chaos 2011;21:023129.
[7] Dilao R. Antiphase and in-phase synchronization of nonlinear oscillators: the Huygens's clocks system. Chaos 2009;19:023118.
[8] Fradkov AL, Andrievsky B. Synchronization and phase relations in the motion of two pendulum system. Int J Nonlinear Mech 2007;42:895.
[9] Huygens C. Letter to de Sluse. In: Oeuveres completes de Christian Huygens, (letters; No. 1333 of 24 February 1665, No. 1335 of 26 February 1665, No. 1345 of 6 March 1665), (Societe Hollandaise Des Sciences, Martinus Nijhoff, La Haye); 1893.
[10] Kapitaniak M, Czolczynski K, Perlikowski P, Stefanski A, Kapitaniak T. Synchronization of clocks. Phys Rep 2012;517:1–69.
[11] Kanunnikov AYu, Lamper RE. Synchronization of pendulum clocks suspended on an elastic beam. J Appl Mech Theor Phys 2003;44:748–52.
[12] Kumon M, Washizaki R, Sato J, Mizumoto RKI, Iwai Z. Controlled synchronization of two 1-DOF coupled oscillators. In: Proceedings of the 15th IFAC world congress. Barcelona; 2002.
[13] Pantaleone J. Synchronization of metronomes. Am J Phys 2002;70:992.
[14] Perlikowski P, Kapitaniak M, Czolczynski K, Stefanski A, Kapitaniak T. Chaos in coupled clocks. Int J Bifurcation Chaos 2012;22:1250288.
[15] Pikovsky A, Roesenblum M, Kurths J. Synchronization: an universal concept in nonlinear sciences. Cambridge: Cambridge University Press; 2001.
[16] Pogromsky AYu, Belykh VN, Nijmeijer H. Controlled synchronization of pendula. In: Proceedings of the 42nd IEEE conference on design and control. Hawaii: Maui; 2003. p. 4381–5.
[17] Senator M. Synchronization of two coupled escapement-driven pendulum clocks. J Sound Vib 2006;291:566–603.
[18] Strogatz SH. Sync: the emerging science of spontaneous order. London: Penguin Science; 2004.
[19] Ulrichs H, Mann A, Parlitz U. Synchronization and chaotic dynamics of coupled mechanical metronomes. Chaos 2009;19:043120.
[20] Pena Ramirez J, Fey RHB, Nijmeijer H. An experimental study on synchronization of nonlinear oscillators with Huygens' coupling. Nonlinear Theor Appl 2012;3(2):128–42.
[21] Pena Ramirez J, Fey RHB, Nijmeijer H. In-phase and anti-phase synchronization of oscillators with Huygens' coupling. Cybern Phys 2012;1(1):58–66.
[22] Fradkov A, Andrievsky B, Boykov K. Control of the coupled double pendulums system. Mechatronics 2005;15:1289–303.
[23] Strzalko J, Grabski J, Wojewoda J, Wiercigroch M, Kapitaniak T. Synchronous rotation of the set of double pendula: experimental observations. Chaos 2012;22:047503.
[24] Song B, Park JH, Wu Z-G, Zhang Y. Global synchronization of stochastic delayed complex networks. Nonlinear Dyn 2012;70:2389–99.
[25] Jeong SC, Ji DH, Park JH, Won SC. Adaptive synchronization for uncertain complex dynamical network using fuzzy disturbance observer. Nonlinear Dyn 2013;71:223–34.
[26] Zhang Liping, Jiang Haibo, Bi Qinsheng. Reliable impulsive lag synchronization for a class of nonlinear discrete chaotic systems. Nonlinear Dyn 2010;59:529–34.

7 Abstract, Doctoral Thesis and Main Objective in Polish

Streszczenie

Wyniki przedstawione w pracy dotyczą dynamiki oraz możliwości synchronizacyjnych (synchronicznego ruchu okresowego) układu składającego się z szeregu samowzbudnych wahadeł podwójnych podczepionych do belki. W skład pracy wchodzą trzy artykuły opublikowane w czasopismach z listy JCR.

W pierwszym artykule "Synchronization of two self-excited double pendula" oscylacje wahadeł zapewnione są przez tłumienie van der Pola napędzające górne wahadła. Dla tego układu wyprowadzono pięć ciągłych równań różniczkowych drugiego rzędu. Badania analityczne składały się z wyznaczenia na podstawie bilansu energii możliwych stanów synchronizacyjnych. Dla wahadeł identycznych wyznaczono cztery możliwe stany synchronizacyjne. Analizę numeryczną przeprowadzono przy pomocy programu do śledzenia orbit okresowych Auto07p. Umożliwia on śledzenie ewolucji rozwiązań okresowych w funkcji parametrów układu oraz określenie ich stateczności. W badaniach tych potwierdzono występowanie wszystkich stanów synchronizacyjnych uzyskanym metodą analityczną. Dalsze badania numeryczne dotyczyły analizy bifurkacyjnej uzyskanych rozwiązań okresowych przy zmianie częstości drgań własnych belki. Stwierdzono, że w badanym zakresie wartości parametru bifurkacyjnego dwa z czterech rozwiązań są zawsze stateczne, natomiast pozostałe dwa zmieniają swoją stateczność.

Następnym etapem badań było rozszerzenie analizy na dowolną liczbę wahadeł podwójnych. Rezultatem tych rozważań jest artykuł "Dynamics of n coupled double pendula suspended to the moving beam". Analityczne wyprowadzono warunek synchronizacji dla dowolnej liczy wahadeł podając równocześnie algorytm opierający się na hipotezach Goldbach'a pozwalający na obliczenie ilości rozwiązań. Ze względu na fakt, że liczba rozwiązań rośnie wykładniczo wraz ze zwiększającą się liczbą wahadeł zaprezentowano stany synchroniczne dla 3, 4 oraz 5 wahadeł podwójnych. Dla układu złożonego z 3 wahadeł podwójnych określono cztery możliwe stany synchronizacji. Układ 4 wahadeł podwójnych synchronizował się na cztery możliwe sposoby, natomiast dla układu złożonego z 5 wahadeł podwójnych określono sześć możliwych stanów synchronizacji. Analiza bifurkacyjna uzyskanych rozwiązań okresowych pokazała, że ich stateczność jest zależna od częstości drgań własnych belki.

W ostatnim artykule "Synchronization configurations of two coupled double pendula" analizowany model układu składa się z belki oraz dwóch wahadeł podwójnych podczepionych do niej. Ruch wahadeł wymuszany jest mechanizmem zegarowym umieszczonym pomiędzy górnym a dolnym wahadłem w każdym podwójnym wahadle. Zaproponowany model został opisany za pomocą nieciągłych równań różniczkowych drugiego rzędu. Uzyskany układ równań dał możliwość wyznaczenia wartości energii przekazywanych pomiędzy poszczególnymi elementami układu. Bilans energii pozwolił na analizę

stanów synchronicznych wahadeł podwójnych i wyznaczenie czterech takich konfiguracji. Następnie przeprowadzono badania numeryczne mające na celu potwierdzenie uzyskanych wyników analitycznych. Obliczenia wykonano dla wahadeł identycznych tzn. o jednakowych masach i długościach, oraz dla wahadeł nieidentycznych (zmieniano długość wahadeł). Dla wahadeł identycznych oraz nieidentycznych obliczono wykresy bifurkacyjne i wyznaczono obszary istnienia poszczególnych rodzajów synchronizacji przy zmianie częstości drgań własnych belki.

Teza i cel pracy.

Teza:

Odpowiedni dobór parametrów podwójnych wahadeł powoduje wzrost ich możliwości synchronizacyjnych.

Cel pracy:

Głównym celem pracy jest opis wpływu ruchu belki na możliwości synchronizacyjne podwójnych wahadeł przyczepionych do niej. Dla identycznych wahadeł zostaną przeanalizowane analitycznie występujące rozwiązania okresowe oraz numerycznie zbadane zostaną zakresy parametrów belki dla których są stateczne. Następnie analiza zostanie rozszerzona o numeryczne badania synchronizacji w ruchu okresowym przy nieidentycznych wahadłach (różniących się masami). W wyniku pracy powstanie katalog możliwych rodzajów synchronizacji w ruchu okresowym w przestrzeni parametrów układu dla n podwójnych wahadeł.